TEXAS Geosciences
The University of Texas at Austin
Jackson School of Geosciences

7th Annual
Jackson School of Geosciences
Student Research Symposium

February 3, 2018

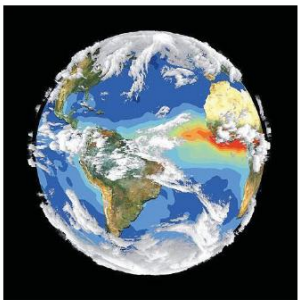


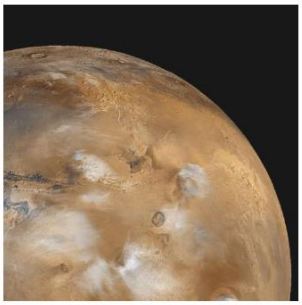

ConocoPhillips

Jackson School of Geosciences
GSEC
Graduate Student Executive Committee

Welcome to the 7th Annual
Jackson School Research Symposium!

It is with great pleasure we welcome you all to the 7th Annual Jackson School Research Symposium at UT-Austin! This symposium would not have been possible without the hard work of student volunteers, the support of faculty/research scientists, and generous support from ConocoPhillips. Thank you for taking part in supporting our students and growing research program within the Jackson School. Enjoy the posters!

Schedule of Presentations and Events

Breakfast, A.M. session poster set-up	8:30-9:00 a.m.
Early Career Graduate (ECG) posters	9:00-11:30 a.m.
Late Career Masters (LCM) posters	9:00-11:30 a.m.
Lunch, A.M. session poster take-down	11:30-12:30 p.m.
P.M. session poster set-up	12:30-1:00 p.m.
Undergraduate (U) posters	1:00-3:30 p.m.
Late Career PhD (LCPhD) posters	1:00-3:30 p.m.
Happy hour/judging	3:30 p.m.
Awards/closing	4:00 p.m.

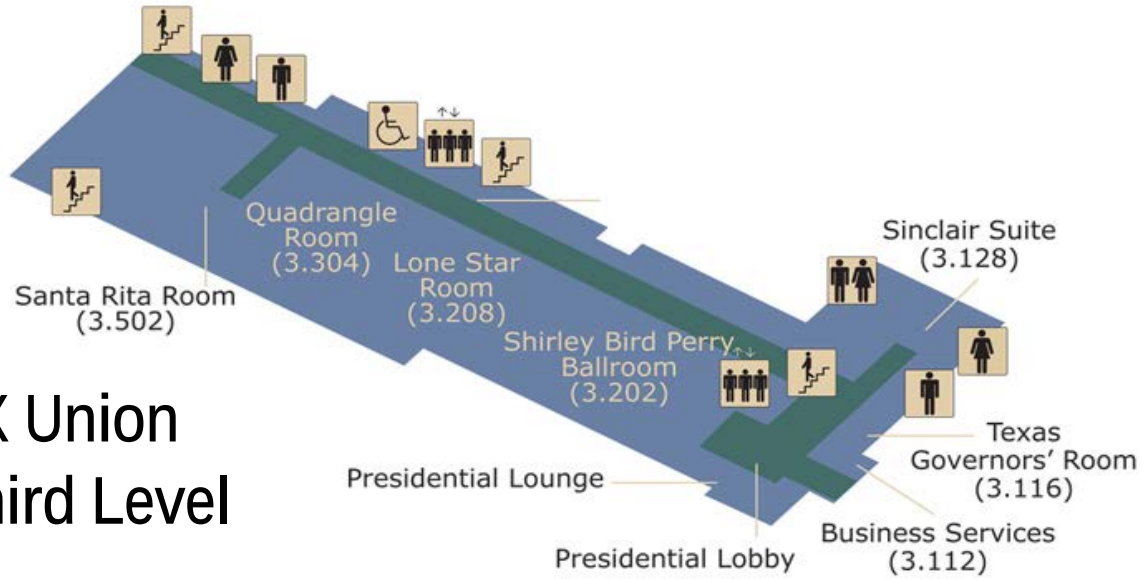

TX Union
Third Level

Shirley Bird Perry Ballroom (UNB 3.202)

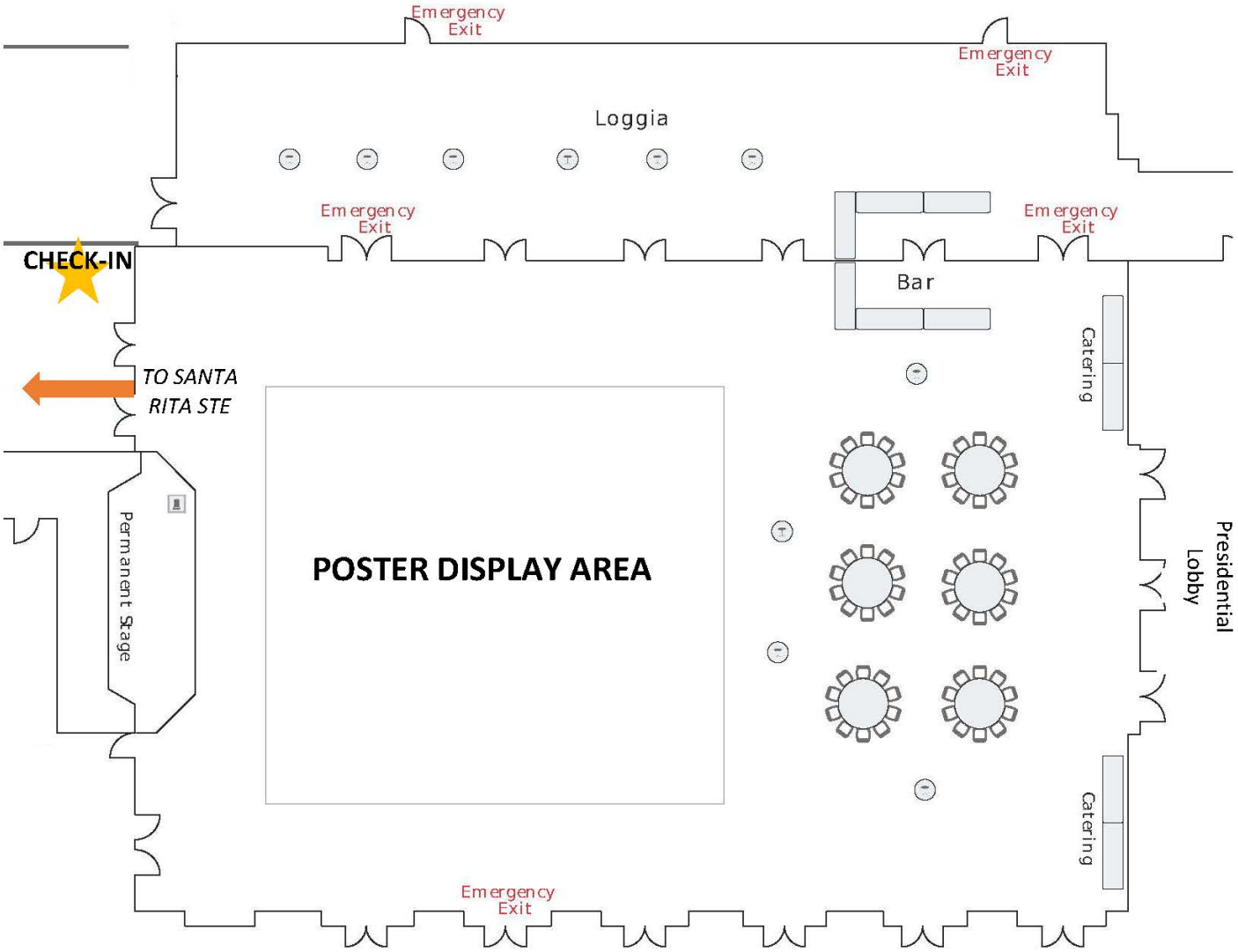

Table of Contents

Themes:

Climate, Carbon, and Geobiology (CCG)

Energy Geosciences (EG)

Marine Geosciences (MG)

Planetary Sciences (PS)

Solid Earth and Tectonic Processes (SETP)

Surface Processes and Hydrology (SPH)

Early Career Graduate Student (ECG)

Poster #	First Name	Last Name	Theme	Poster Title
ECG-1	Natchanan	Doungkaew	Other	Fracture Growth in Chemically Reactive Geologic Systems
ECG-2	Gabriel	Giacomone	Other	Initial basin floor fans architecture and facies analysis in an incipient back arc basin, Jurassic los Molles, la Jardinera area, Neuquén Basin Argentina
ECG-3	Abdulah	Eljalafi	CCG	Lacustrine Microbialite Architectural and Chemostratigraphic Trends: Green River Formation, Eastern Uinta Basin, Colorado and Utah
ECG-4	Sophie	Goliber	CCG	Development of automated methods for terminus picking of the Greenland ice sheet from Landsat imagery
ECG-5	Grace	Musser	CCG	Escaping the ghost of the forest: A new morphological dataset reveals a novel sister taxon for the adzebill of New Zealand (Aptornis).

ECG-6	Chijun	Sun	CCG	Mesoscale Convective System as a Dominant Control of the Isotopic Composition of Precipitation in the South-Central United States
ECG-7	Cody	Draper	EG	Wolfcampian Shelf-to-Basin Stratigraphic Framework of the Central Basin Platform and Midland Basin, Andrews County, Texas
ECG-8	Zhicheng	Geng	EG	Multi-scale Seislet transform
ECG-9	Eric	Goldfarb	EG	Changes in Ultrasonic Velocity from Fluid Substitution; Calculated with Laboratory Methods, Digital Rock Physics, and Biot Theory
ECG-10	Ben	Gremillion	EG	Improving Seismic Data Resolution Using Shaping Regularization with the Dip Moveout Correction
ECG-11	Ken	Ikeda	EG	Calculating Effective Elastic Properties of Berea Sandstone Using Segmentation-less Method without Targets
ECG-12	Eunsil	Jung	EG	Characteristics of Coarse-Grained Regressive-Transgressive Cyclic Sandstones of Jurassic Lajas Formation in Southern Neuquen Basin, Argentina
ECG-13	Harpreet	Kaur	EG	Seismic imaging in stratigraphic coordinates
ECG-14	Michael	McCann	EG	Establishing a Methodology to Measure the Static Elastic Properties of Fluids
ECG-15	Nam	Pham	EG	Automatic channel detection in seismic section using deep learning
ECG-16	Sebastian	Ramiro Ramirez	EG	Effect of Test Fluid in Steady-state Liquid Permeability Measurements of Siltstone Lithofacies in the Bone Spring Formation, Delaware Basin
ECG-17	Peter	Schemper	EG	Stratigraphy, sedimentology, and geochemistry of the East Texas Jurassic Smackover Carbonare Ramp Succession
ECG-18	Janaki	Vamaraju	EG	Enriched and hybrid galerkin finite element methods for seismic wave propagation in fractured media
ECG-19	Tiannong	Dong	EG	Spatial and temporal dependencies of structure II to structure I methane hydrate transformation in porous media under reservoir conditions

ECG-20	Dominik	Kardell	EG	The Evolution of Slow to Intermediate-Spreading Oceanic Crust in the South Atlantic: The Effects of Age, Sediment Thickness, and Spreading Rate on Upper Crustal Velocities
ECG-21	Kelly	Olsen	EG	Development of a shallow decollement along the south-central Chile margin from 2D seismic reflection data
ECG-22	Naoma	McCall	PS	Characterization of fractures in the Chicxulub peak ring: preliminary results from IODP Expedition 364
ECG-23	Brandon	Tober	PS	Radar reflectivity analysis of northern hemisphere boulder halos on Mars
ECG-24	Grace	Beaudoin	SETP	Halogen Cycling and Stable Isotope Geochemistry During Prograde Subduction Zone Metamorphism and Devolatilization
ECG-25	Clara	Brennan	SETP	Zircon 4He/3He Thermochronometry – Recovery of Helium-4 Concentration Profiles Across the Zircon Helium Partial Retention Zone and Implications for Thermal History Reconstruction
ECG-26	Kristina	Butler	SETP	Sediment routing and 3D stratigraphic architecture in the Patagonian foreland basin: Implications for Andean tectonics and flat-slab subduction
ECG-27	Zachary	Foster-Baril	SETP	Triassic and Jurassic Rift Basin Record of Provenance, Sediment Dispersal, and Extension during the Breakup of Pangea along the in the Proximal Eastern North American Margin, U.S.A.
ECG-28	Kunpeng	Liao	SETP	Impacts of Viscoelastic Rheology on Dynamic Topography
ECG-29	Chujie	Liu	SETP	Seismic Attenuation in the African LLSVP Estimated from PcS Phases
ECG-30	Evan	Ramos	SETP	A minimum constraint on amounts and rates of metamorphic decarbonation during arc magmatism
ECG-31	Benjamin	Rendall	SETP	Platform scale stratigraphic architecture of Pennsylvanian icehouse carbonates in the Sacramento Mountains, Otero County, NM
ECG-32	Catherine	Ross	SETP	U-Pb and (U-Th)/He Geo-Thermochronometry of the Chicxulub Impact Peak Ring

ECG-33	Brandon	Shuck	SETP	Constraints on Mantle Dynamics during Jurassic Rifting in the ENAM Area from Seismic and Petrological Modeling of the Oldest Oceanic Crust
ECG-34	Carolyn	Tewksbury-Christ	SETP	Rheological Properties and Heterogeneities Along the Down-Dip Extent of a Subduction Megathrust: Insights from the Condrey Mountain Schist, Northern California
ECG-35	Mert	Ugurhan	SETP	Timing and Characterization of the Cave Peak Porphyry Molybdenum Deposit, Culberson County, TX
ECG-36	Wanying	Wang	SETP	Asthenospheric Anisotropy Beneath the United States from Mantle Flow Models
ECG-37	Lakin	Beal	SHP	Isotopic and Geochemical Assessment of the Sensitivity of the Northern Guam Lens Aquifer to Intra- and Inter-Annual Variations in Hydroclimate
ECG-38	Yuqian	Gan	SHP	Continuous spectrum of sediment-density flow deposits observed along coarse-grained, medium-sized basin margin clinoforms, Jurassic Neuquén basin Argentina
ECG-39	Tyler	Meng	SHP	On the origin of the Crestone crater: low-latitude periglacial features in San Luis Valley, Colorado
ECG-40	Logan	Schmidt	SHP	Quantifying seasonal dynamic water storage in a fractured bedrock vadose zone with borehole Nuclear Magnetic Resonance
ECG-41	Paul	Southard	SHP	Impact of spring-associated riparian vegetation on channel morphology in ephemeral dryland channels: Henry Mountains, Utah, USA

Late Career Master's Student (LCMS)

Poster #	First Name	Last Name	Theme	Poster Title
LCMS-1	Henar	Rabadan Perucha	Other	Energy Transition in the Balearic Islands, Spain
LCMS-2	Graham	Soto-Kerans	Other	Late Paleozoic Provenance and Sediment Routing in the Southern Delaware Basin, West Texas
LCMS-3	Heather	Christensen	CCB	Soil gas dynamics and microbial activity in the unsaturated zone of a regulated river
LCMS-4	Sean	Bader	EG	Missing well log data interpolation and semiautomatic seismic well ties using data matching techniques
LCMS-5	Taylor	Canada	EG	Wolfcampian carbonate platform sequence stratigraphy of the Wylie Mountains, Van Horn, TX: Implications for a platform to basin Wolfcamp framework
LCMS-6	Landon	Lockhart	EG	Influence of shear and mean stress on pore pressure prediction at the Mad Dog Field, Gulf of Mexico
LCMS-7	Mario	Gutierrez	MG	Systematic Lithologic Calibration of Seismic Character of Neogene Mass-Transport Deposits in Mississippi Canyon of the Northern Gulf of Mexico, USA.
LCMS-8	Andrew	Parisi	PS	Geochronological Constraints on the Timing of Proposed Ordovician Meteorite Event Impact Structures in North America
LCMS-9	Scott	Eckley	SETP	3D Textural and Geochemical Analyses on Carbonado Diamond: Insights from Pores and the Minerals within Them
LCMS-10	Megan	Flansburg	SETP	Geo-Thermochronometric Insights on the Formation of the Ios Metamorphic Core Complex, Southern Cyclades, Greece
LCMS-11	Evelin	Gutiérrez	SETP	Provenance and geochronological insights into late Cretaceous-Paleogene foreland basin development in the Subandean zone and Oriente basin of Ecuador
LCMS-12	Eirini	Poulaki	SETP	Unravelling the Formation and Exhumation of the Cycladic Blueschist Unit and Basement in the Southern Aegean, Sikinos and Ios Islands, Greece
LCMS-13	Caroline	Hackett	SHP	Quantifying alluvium effects on karst aquifer recharge in the upper Nueces River, Texas
LCMS-14	Shawn	Lee	SHP	Critical Zone structure inferred from multiscale geophysical data across hillslopes at the Eel River CZO

Late Career Ph.D. Student (LPHD)

Poster #	First Name	Last Name	Theme	Poster Title
LPDH-1	Peter	Carlson	CCG	Hydrologic conditions and carbon cycling dynamics recorded in the carbon-isotope variations of a near-entrance speleothem
LPDH-2	Seungwon	Chung	CCG	The Impacts of Human-Driven Inputs on Terrestrial and Riverine Nitrogen Fluxes in the United States
LPDH-3	Maryia	Halubok	CCG	A Monte Carlo ray tracing model to improve simulations of solar-induced chlorophyll fluorescence radiative transfer
LPDH-4	Allison	Lawman	CCG	Reconstructing Tropical Southwest Pacific Climate Variability at Vanuatu using Geochemical Proxies from Corals
LPDH-5	Simon	Scarpetta	CCG	A new Miocene gerrhonotine from the Caliente Formation, California
LPDH-6	Lily	Serach	CCG	The Role of Priming in the Development of Stable and Radioactive Carbon Isotope Profiles of Soil Organic Matter
LPDH-7	Charles	Withnell	CCG	Implications of Modernizing our Perspective of Eastern North American Arvicoline Rodents in the Early and Middle Pleistocene
LPDH-8	Wen-Ying	Wu	CCG	Assessment of the Simulations of Global-scale River Flows from an Integrated Hydrological Modeling Framework
LPDH-9	Badr	Alulaiw	EG	Estimation of Pore Porosity and Fracture Parameters from 3D Seismic Data by Born Inversion
LPDH-10	Yaser	Alzayer	EG	Numerical Modeling of Differential Compaction Fracturing in Carbonate Systems
LPDH-11	Reetam	Biswas	EG	2D Full Waveform Inversion and Uncertainty Estimation using the Reversible Jump Hamiltonian Monte Carlo
LPDH-12	Reynaldy	Fifariz	EG	The UPSIDE POTENTIAL of the EARLY MIOCENE KUJUNG FORMATION CARBONATES, OFFSHORE EAST JAVA, INDONESIA
LPDH-13	Eric	Guiltinan	EG	?Making synthetic mudstone: Parametric resedimentation studies at high effective stress to determine controls on breakthrough pressure and permeability
LPDH-14	Dmitrii	Merzlikin	EG	Oriented anisotropy continuation using shifted hyperbola travel-time approximation
LPDH-15	Yunzhi	Shi	EG	Can deep learning help us classify salt body?

LPDH-16	Jennifer	Harding	MG	Detailed seismic velocity structure of the ultra-slow spread crust at the Mid-Cayman Spreading Center from travel-time tomography and synthetic seismograms
LPDH-17	Patrick	Meazell	MG	Sedimentological Characterization of a Deepwater Methane Hydrate Reservoir in Green Canyon 955, Northern Gulf of Mexico
LPDH-18	Benjamin	Smith	MG	Global versus Regional Carbon Isotope Signals: An Example from the Permian of West Texas and New Mexico
LPDH-19	Stefano	Nerozzi	PS	Ice caps under sand caps under an ice cap: revealing a record of climate change on Mars
LPDH-20	Eric	Petersen	PS	Mantle Morphology on Martian Debris-Covered Glaciers Reveals Deposition & Flow History
LPDH-21	Douglas	Barber	SETP	Integrating complimentary accessory phases (apatite, rutile, zircon) in isotopic and trace-elemental provenance studies: reconstructing the Proto-Zagros orogeny, NW Iran
LPDH-22	Rachel	Bernard	SETP	Plagioclase-dominated Seismic Anisotropy in the Eastern Mojave Lower Crust
LPDH-23	Tomas	Capaldi	SETP	Miocene to recent shortening along distal foreland uplifts and basin partitioning during flat-slab subduction in western Argentina
LPDH-24	Thomas	Etzel	SETP	Defining conditions of garnet growth across the central and southern Menderes Massif
LPDH-25	Sarah	George	SETP	Testing Models of Orogenic Development in Ecuador: Multi-proxy Provenance Analysis of the Hinterland Cuenca Basin
LPDH-26	Peter	Gold	SETP	Quaternary Slip History for the Agua Blanca Fault, northern Baja California, Mexico
LPDH-27	Cullen	Kortyna	SETP	Tectonomorphic Influence on Late Cretaceous-Paleogene Sediment Provenance and Dispersal Through West and South Texas From Detrital Zircon Geochronology
LPDH-28	Alissa	Kotowski	SETP	Length scales and types of heterogeneities along the deep subduction interface: Insights from an exhumed subduction complex on Syros Island, Greece
LPDH-29	Chelsea	Mackaman-Lofland	SETP	High Andean deformation, exhumation, and foreland basin deposition during Neogene changes in subduction zone geometry (32°S)
LPDH-30	Margaret	Odlum	SETP	Thermotectonic evolution of rifting to collision of the central to eastern Iberian-European margin using multi-mineral U-Pb and (U-Th)/He thermochronometery

LPDH-31	Pamela	Speciale	SETP	Rates of Olivine Grain Growth in 'Damp' Natural Dunites During Dynamic Recrystallization and Post-deformation Annealing
LPDH-32	Kelly	Thomson	SETP	Correlating Submarine Fan Complexes using Detrital Zircon Geochronometry
LPDH-33	Xinyue	Tong	SETP	A Plastic Formulation of Rate and State Dependent Friction: Emergence of Slip Transient and Earthquakes
LPDH-34	Charles	Abolt	SHP	Topographic Control on the Subsurface Heat Budget of Ice Wedge Polygons
LPDH-35	Benjamin	Cardenas	SHP	Coupling Aeolian Stratigraphic Architecture to Paleo-Boundary Conditions: The Scour-Fill Dominated Jurassic Page Sandstone
LPDH-36	Max	Daniller-Varghese	SHP	Influence of Waves and Tides on Delta-Front and Upper Slope Turbidity Currents and their Deposits: An Outcrop and Laboratory Study
LPDH-37	Stephen	Ferencz	SHP	Groundwater-Surface Water Interactions in a Dam-Regulated River: Hydrologic Processes and Water Quality Implications
LPDH-38	Lily	Jackson	SHP	Detrital zircon U-Pb geochronology of modern river sands in the Ecuadorian Andes: implications for tectonic history and sediment recycling
LPDH-39	Colin	McNeece	SHP	MATLAB geoChemistry: An open source geochemistry solver based on MRST
LPDH-40	Michael	O'connor	SHP	Groundwater Dynamics and Export from Active Layer Aquifers Overlying Permafrost
LPDH-41	Logan	West	SHP	Identification and preliminary characterization of the Lycium Member bed features in the Fish Creek-Vallecito Basin: Antidunes, cyclic steps, and more from a proto-Gulf of California deepwater supercritical fan
LPDH-42	Jinyu	Zhang	SHP	Weighing controls on shoreline and shelf-margin growth: Insights from Wilcox Group, Gulf of Mexico and numerical models

Undergraduate Student (U)

Poster #	First Name	Last Name	Theme	Poster Title
U-1	Elizabeth	Davis	Other	Pyroclastic Flows from Mount St. Helens: The Effects of Topography on Flow Behavior and Deposition on the Leeward Slope
U-2	Derry	Xu	Other	Isotopic compositions of meteoric water across an elevation gradient in Southern Peru
U-3	Jordan	Oefinger	CCB	Evidence of Possible Ocean Acidification at the Paleocene-Early Eocene Boundary Recorded in the Adriatic Carbonate Platform
U-4	Esben	Pedersen	CCB	The Control of Grain Size on Carbon Dioxide Dissolution into Water
U-5	Raeann	Garcia	EG	Cement Stratigraphy in Solution-Collapse Breccias, Lower Ordovician Knox Group, Tennessee-Kentucky
U-6	Sarah	Greer	EG	Migration deconvolution using non-stationary matching operators
U-7	Jesse	Gu	EG	Characterization of gas hydrate-bearing sediments from Green Canyon 955, Gulf of Mexico, using Raman spectroscopy
U-8	Jaime	Hirtz	SETP	Detrital Zircon Signal Migration in Eolian Systems: Investigating a Modern Foreland Dune Field in Argentina
U-9	Samantha	Robbins	SETP	Thermal Evolution of a Distal Hyperextended Margin - a Case Study of Zabargad Island, Red Sea
U-10	Ryan	Herring	SHP	Calculating the Volume of Late Quaternary Mississippi River Off Shelf Deposits
U-11	Sebastian	Munoz	SHP	Heat Transport in the Streambed of a Large Regulated River
U-12	Kindra	Nicholaides	SHP	Groundwater Model Using Variable Transmissivities Matches Observed Flows
U-13	Jacqueline	Rambo	SHP	Investigating fluvial pattern and delta-planform geometry based on varying intervals of flood and interflood

ECG

Fracture Growth in Chemically Reactive Geologic Systems

Natchanan Doungkaew
Doungkaew, N., Bureau of Economic Geology, The University of Texas at Austin, Austin, TX
Eichhubl, P., Bureau of Economic Geology, The University of Texas at Austin, Austin, TX

Fractures and faults control mechanical properties of the brittle crust and fluid flow in the subsurface. It is well known in engineering fracture mechanics that mechanisms of fracture propagation in chemically reactive environments are different from brittle failure under chemically inert conditions. How fracture growth is affected by chemical reactions under geologic subsurface conditions is not well understood. Understanding fracture formation in chemically reactive systems has implications for many fields in geosciences such as seismic and aseismic fault and fracture processes, migration of hydrocarbons, long term CO_2 storage, and geothermal energy production

I hypothesize that fractures that grow under high temperatures and in reactive environments should have 1) triangular shapes instead of the theoretical elliptical shape, and 2) lower width/height ratios compared to those formed at low temperatures without the presence of fluid. Those characteristics are caused by stress corrosions at fracture tips that resulted in faster growth in length compared to the growth in width, and the process is accelerated at high temperature. To test the hypothesis, I will compare shape and textural characteristics of natural fractures formed under different physiochemical conditions with fractures formed in the lab by constrained sintering. Field sites include Dixie Valley, NV (Boyer Ranch Fm) and Birch Creek Pluton, CA, (Campito Fm.) where the rocks have experienced chemical alterations and high temperatures in proximity to igneous intrusions, and the Orcutt Oil Field, CA (Sisquoc Fm) where fractures formed during in-situ combustion of hydrocarbons. The fracture characteristics include shapes, sizes, orientations, textural characteristics and compositions of fracture cement, shapes of fracture tips, locations of fracture tips relative to layer boundaries, and frequencies. Petrographic observations, fluid inclusion microthermometry, and SEM-CL imaging provide constraints on formation temperatures and pressures, fracture growth kinematics, and possible deformation mechanisms. I will conduct constrained sintering under controlled varying temperature and pressure on materials of varying mineral composition, grain size, and sorting to study the effects of host rock compositions on fracture formation.

First field observations show that fractures in the Boyer Ranch Fm have triangular shapes that deviated from the theoretical elliptical shapes. In addition, I have successfully created fractures in Longhorn white clay thin films coating ceramic substrates in unconfined sintering experiments using a muffle furnace. Microfractures with apertures of up to 0.15 mm form between 900?C and 1000?C, doubling in aperture between 1000°C and 1050?C. These fractures are interpreted to form in response to stresses resulting from constrained sintering and diffusive mass transfer during high-temperature alteration of the clay.

Keywords: fractures, reactive environment, constrained sintering, cold sintering, field study, fracture aperture, aperture profile, high temperature

ECG

INITIAL BASIN FLOOR FANS ARCHITECTURE AND FACIES ANALYSIS in an INCIPIENT BACK ARC BASIN, JURASSIC LOS MOLLES, LA JARDINERA AREA, NEUQUÉN BASIN ARGENTINA

Gabriel Giacomone
Giacomone, G., Jackson School of Geosciences, University of Texas at Austin, Austin, TX

The Jurassic deep water marine deposits of Los Molles Fm (Neuquén Basin, Argentina) have received much attention due to their characteristics as source rocks and the sandy deposits that act as reservoirs in many fields in the basin. Dark shales and intercalations of sandstones and conglomerates related to gravity flows characterize the section. These deposits represent deep-water marine settings that filled inherited topography associated with rift tectonics during the late Triassic and early Jurassic.
While many studies have focused on the upper part of the succession related to the slope and the upper basin floor fans, this project focuses on the initial deposits of the basin. The main objectives of my research will be to understand facies variability and architectural styles within the deposition of the first submarine fans and analyze these deposits from a reservoir point of view. Secondly and in a broader scenario, I will address the question of the control the inherited topography had on these deposits.
To achieve the proposed work, detail sections will be measured, photomosaic and satellite image interpretations will be carried out and outcrop samples will be taken to make thin sections and porosity-permeability tests.
It is expected that the initial fans might not have the best petrophysical properties but that the stacking and thickness would make them interesting as tight reservoirs in the subsurface. In addition, it is likely to find thickness variation of the deposits and a major control on the deposition of the fans due to inherited topography. The arrangement of architectural elements and petrophysical properties of the sandy facies will have major implications for reservoir development and exploration in this basin and in others with similar settings.

Keywords: Basin floor fans, turbidites, reservoir, deep water, Neuquen basin

CCG
ECG

Lacustrine Microbialite Architectural and Chemostratigraphic Trends: Green River Formation, Eastern Uinta Basin, Colorado and Utah

Abdulah Eljalafi
Eljalafi, A., Jackson School of Geosciences, The University of Texas at Austin, Austin, TX

Marginal lacustrine carbonates of the Green River Formation are well exposed in the eastern Uinta basin, where they are interbedded with fluvial and lacustrine sand and shale of the Douglas Creek Member. This study examines the stratigraphic architecture, lithofacies, and chemostratigraphy of the microbialite and other associated carbonate beds in the eastern Uinta basin, Colorado and Utah. Two facies associations occur within the carbonate units: Lacustrine Margin Carbonates, consisting of six packstone to rudstone lithofacies dominating littoral to upper sublittoral environments; and Lacustrine Microbial Carbonates, consisting of stromatolitic and thrombolitic lithofacies, dominating littoral to lower sublittoral zones. These are consistent with earlier work done by Swierenga et al., (2015) and Sarg et al., (2013) on similar beds in the surrounding area within the Uinta and Piceance basins respectively.
Multiple scales of carbonate cyclicity, indicated by excursions of $\delta^{18}O$ and $\delta^{13}C$ stable isotopes correlate to characteristic microbialite facies. Bed set scale cycles, on the order of 1 to 5 m, are characterized by deepening upward lithofacies that correlate to positive excursions of stable isotopes. Large scale trends, on the order of 10's to 100's of meters, are also observed in this study, and relate microbialite lithofacies to lake stage evolution developed by Tänavsuu-Milkeviciene & Sarg, (2012).
Lake stage 1 (fresh to mesosaline) corresponds to initial sparse microbialite deposition, with low diversity and relatively light $\delta^{18}O$ and $\delta^{13}C$ isotopic values that indicate initial fresh water conditions and relatively low paleo organic productivity. Lake stage 2 (transitional lake) corresponds to moderate microbialite diversity, larger biostromal and biohermal build ups, and heavier $\delta^{18}O$ and $\delta^{13}C$ isotopic values that characterize more saline conditions and higher paleo-organic productivity in the lake. Lake stage 3 (highly fluctuating lake) contains the highest microbialite diversity and marks the interval of heaviest $\delta^{18}O$ and $\delta^{13}C$ isotopic values; suggesting high paleo-organic productivity and the greatest lake restriction and highest salinity and alkalinity conditions. Lake stage 4 (rising lake) contains the last observed microbialite deposits, and marks the lowest microbialite diversity and a reversal in trend of $\delta^{18}O$ and $\delta^{13}C$ isotopic values; indicating freshening conditions and a decrease in paleo organic productivity.

Keywords: Microbialite, Carbonate, Chemostratigraphy

CCG
ECG

Development of automated methods for terminus picking of the Greenland ice sheet from Landsat imagery

Sophie Goliber
Goliber, S., Institute for Geophysics, The University of Texas at Austin, Austin, TX
Catania, G., Institute for Geophysics, The University of Texas at Austin, Austin, TX
Holt, J., Institute for Geophysics, The University of Texas at Austin, Austin, TX

Mass loss of the Greenland ice sheet from the past two decades can be attributed to in large part the speed-up and retreat of marine-terminating glaciers, and these changes are generally heterogeneous across the terminus of the ice sheet. A better understanding of the changes at the outlet glacier termini over seasonal/sub-seasonal timescales may reveal information on how glaciers adjust to climatic changes over a range of time scales. The NASA Landsat missions have provided a record of continuous, multispectral satellite imagery for 45 years with repeat observations every 16-18 days and with two Landsat satellites currently in orbit and one preparing for launch in 2020, a method to extract terminus position as data are collected would provide a way to continuously monitor the changes to the Greenland ice sheet in near real-time. Currently, all glacier termini are picked manually or semi-automatically, but this is labor intensive and places limits the detail of observations that can be made. Here we propose a technique to develop an automated image segmentation algorithm that will enable the identification of masks in individual Landsat scenes over glaciated terrain. Segmentation takes advantage of multiple differences between ice, water, snow, rock, and clouds (e.g. spectral, textural, geometrical, etc.) and allows the development of image masks classified by ground type. Using edge-detection algorithms we are able to extract out the curvilinear boundaries between ground types that enable terminus identification. Our plan is to examine a range of glacier termini from easier-to-detect termini (steep-cliffed, water/ice boundaries) to harder-to-detect termini (gently sloped, melange/ice boundaries) in order to develop a robust terminus picking tool. We will then compare our automatically-picked glacier termini with hand-picked termini to examine the robustness of the autopicker.

Keywords: Greenland, calving, landsat, glacier, ice

CCG
ECG

Escaping the ghost of the forest: A new morphological dataset reveals a novel sister taxon for the adzebill of New Zealand (Aptornis).

Grace Musser
Musser, G., The University of Texas at Austin, Austin, TX
Cracraft, J., The American Museum of Natural History, New York, NY

As focus on phylogenomic studies of faunas has increased, morphological studies have declined dramatically; however, recent genomic studies across several groups of animals have provided conflicting relationships, especially within short stem lineages arising around the K/Pg boundary. Within Neoaves, a group which comprises approximately 95% of all extant birds, these short internodes created by rapid evolutionary radiation around the K/Pg boundary result in conflicting topologies. Neoavian fossil taxa remain an understudied but critical key to resolving relationships among these stem lineages and providing insight into evolutionary changes in structure and function. One of the most controversial fossil taxa is the adzebill (*Aptornis*), an extinct terrestrial bird endemic to New Zealand that lived at least as far back as the early Miocene. Past morphological studies have placed adzebills as either a sister taxon to what the Kanak tribe calls “the ghost of the forest,” the flightless kagu of New Caledonia (*Rhynochetos jubatus*), or to the land- and waterfowl group Gallanseres; however, molecular studies reveal kagu and sunbittern (*Eurypyga helias*) to be sister taxa and posit that the adzebill is a rail (within Rallidae) or sister to Ralloidea (finfoots and rails). To better resolve the position of the adzebill we constructed a new and more comprehensive morphological dataset by identifying 370 discrete osteological characters for 37 extant and 2 fossil taxa, the latter comprising the South Island adzebill (*Aptornis defossor*) and the giant Chatham Island rail (*Diaphorapteryx hawkinsi*). We combined this dataset with 22 sequences of nuclear genomic data that were each 4,038 base pairs in length. Morphological results showed strong support for a kagu and sunbittern sister group (100% bootstrap support), and placed the adzebill as sister to trumpeters (*Psophia*) with poor support (<50% bootstrap support). Results from analysis of the combined data were similar, with kagu+sunbittern earning a 100% clade credibility value; however, adzebille+trumpeter also earned a 100% clade credibility value. Although the sister group containing kagu and sunbittern is consistent with recent genomic hypotheses, the relationship of the South Island adzebill and the black-winged trumpeter is novel and suggests the adzebill to be more closely related to Gruoidea (cranes, trumpeters and allies) than to the kagu, Ralloidea or Galloanseres. Better placement of taxa represented by fossils such as the adzebill will allow higher phylogenetic resolution at the base of the neoavian tree and aid in reconstructing phylogenetic relationships, phenotypic evolution and biogeographic history of taxa within Neoaves.

Keywords: evolution, avian morphology, combined data, systematics, biogeography

CCG
ECG

Mesoscale Convective System as a Dominant Control of the Isotopic Composition of Precipitation in the South-Central United States

Chijun Sun
Sun, C., The University of Texas at Austin, Austin, TX
Shanahan, T., The University of Texas at Austin, Austin, TX
Partin, J., The University of Texas at Austin, Austin, TX

The processes that control the isotopic composition of precipitation in the mid-latitudes are understudied compared to the high and low latitudes, but are critical for interpreting paleo records using isotope proxies. To better understand these processes, we investigated changes of isotopic composition of rainwater in central Texas using 20 months of event-based rainwater collection. We find that in both the event-based data and the monthly data from the Waco GNIP station, the dominant control on the isotopic composition of precipitation is the proportion that is derived from convective systems. This finding is consistent with previously reported data largely from tropical localities (Aggarwal et al. 2016), where large organized convective systems lead to high rainfall amounts and isotopically depleted precipitation. Although there are seasonal differences in the dominant rainfall types over the south-central US, with winter precipitation almost entirely stratiform, seasonality plays very little role in the net isotopic composition of precipitation because the total contribution during winter is small compared with spring, summer and fall. We also find that changes of source have little effect on the isotopic composition of rainfall, as the majority of the moisture is derived from the Gulf of Mexico with little influence of reevaporation or mixing. The majority of the warm season precipitation in the south-central US occurs in association with mesoscale convective systems (MCSs) and the development of these systems plays a critical role in the overall isotopic signature of precipitation. MCSs are characterized by a combination of intense, organized convection at their leading edges and trailing stratiform precipitation. Larger MCSs tend to contain higher proportions of stratiform rainfall and as a result, have isotopically depleted values. Proxy records from this region displaying more negative isotope values in the past should therefore be interpreted with caution as they could reflect either increases in cool versus warm season precipitation or changes in the intensity of warm season MCSs.

Keywords: Isotope, precipitation

EG
ECG

Wolfcampian Shelf-to-Basin Stratigraphic Framework of the Central Basin Platform and Midland Basin, Andrews County, Texas

Cody Draper
Draper, C., Department of Geological Sciences, The University of Texas at Austin, Austin, TX
Kerans, C., Department of Geological Sciences, The University of Texas at Austin, Austin, TX
Wahlman, G., Wahlman Geological Services, LLC, Austin, TX

The Lower Permian (Wolfcampian) is an exploration and production target on the Central Basin Platform, its eastern Slope, and in the Midland Basin. Shelf-to-basin stratigraphic frameworks can aid in understanding basinal trends by delineating the timing and mechanisms of sediment bypass and accumulation across the slope. However, efforts at correlating the stratigraphy between the platform, slope, and basin have been frustrated by ambiguous stratigraphic boundaries and the complexity of the slope. This project aims to understand the platform stratal architecture during peak icehouse as well as the link between sequence patterns and deposition on the slope and in the basin by utilizing high-resolution 3D seismic data, well-logs, core lithofacies data, and fusulinid biostratigraphic data from North Cowden, Midland Farms, and Mabee fields. Detailed facies and stratigraphic analysis of cores from the Wolfcamp platform and slope strata provide critical understanding of lithofacies, cyclicity, and larger sequence-scale facies organization. Fusulinid biostratigraphic data, provided by Dr. Greg Wahlman, are available to the project and are used to constrain the timing of sequence development and key phases of shelf-to-basin shedding of reservoir-quality allochthonous carbonates. Core facies include dolomites, and more typical Wolfcampian shelf margin to upper slope facies, such as subtidal crinoid and fusulinid wackestones to packstones, variously sorted skeletal grain dominated packstones, and higher energy ooid peloidal grainstones. As well, mixed siliciclastic and carbonate breccias associated with unconformities as well as soil horizons are present. Vertical facies changes are commonly abrupt. This shelf-to-slope core cross section is extended along both strike and dip using wireline log and seismic integration, leading to a well-constrained shelf-to-basin model that is much needed for the Wolfcampian. The developed stratigraphic model constrains the evolution and development of the eastern slope of the Central Basin Platform from the end of the Pennsylvanian through the Wolfcampian.

Keywords: Carbonate Slope, Shelf Margin, Midland Basin, Central Basin Platform, Wolfcamp

EG
ECG

Multi-scale Seislet transform

Zhicheng Geng
Fomel, S., Bureau of Economic Geology, The University of Texas at Austin, Austin, TX

The West China is rich in coal, oil and gas. However, most of the regions in West China are complicated in surface geological conditions, especially in areas such as mountainous regions and loessial regions. The sever curvature of surface and the dramatic changes in lithology pose great challenges on seismic data gathering and processing. All these challenges also have big impacts on the seismic data quality and reliability of interpretation results. As we know, seismic velocity is a critical factor in reflecting underground structure and lithology. If the velocity cannot be accurately determined, the quality of static correction, velocity analysis and the final imaging result cannot be ensured. As the difficulty of energy exploration increasing, the conventional seismic processing technology cannot satisfy the demand of refining modeling of near-surface layers. Methods with more accuracy for near-surface seismic velocity inversion begin to attract more and more attention.
The first-arrival traveltime tomography is currently a standard approach for imaging the near surface structures. But it cannot resolve complex situation such as hidden low-velocity layers. Early arrival waveform inversion is a robust approach for dealing with complex structures, but it may take significant computational efforts. Furthermore, we found that the results from waveform inversion may not allow fitting the first arrival traveltimes anymore because of nonuniqueness of the model solutions. Therefore, we can combine these inversion methods to construct the near surface velocity. First, we can obtain the high-quality inversion result containing low wavenumber information by using the first-arrival traveltime tomography, and then use the first-arrival waveform inversion to recover the high wavenumber component, so combined with inversion to obtain high quality inversion results.

Keywords: Seismic data processing, seislet

EG
ECG

Changes in Ultrasonic Velocity from Fluid Substitution; Calculated with Laboratory Methods, Digital Rock Physics, and Biot Theory

Eric Goldfarb
Goldfarb, E., The University of Texas at Austin
Ikeda, K., The University of Texas at Austin
Tisato, N., The University of Texas at Austin

Seismic and ultrasonic velocities of rocks are function of several variables including fluid saturation, and type. Understanding the effect of each variable on elastic waves can be valuable when using seismic methods for subsurface modeling. Fluid type and saturation are of specific interest to volcanology, water, and hydrocarbon exploration.

Often, laboratory testing is employed to understand the effects of fluids on elastic waves. However, laboratory testing is typically expensive and time consuming. It normally requires cutting rare samples into regular shapes. Fluid injection can potentially destroy specimens as removing the fluid after testing can prove difficult. On the other hand, theoretical modeling can predict the effect of fluids on elastic properties but it is often inaccurate. Alternatively, digital Rock Physics (DRP) can be used to investigate the effect of fluid substitution. DRP has the benefit of being non invasive, as it does not require regular sample shapes or fluid injection in the specimen.

Here, we compare the three methods for dry and wet sandstone to test the reliability of DRP. Ultrasonic velocities were obtained from laboratory testing. For comparison, we used a purely theoretical approach - i.e., effective medium theory, combined with dispersion theory - to estimate the wavespeeds at dry and wet conditions.

For DRP the dry sample was scanned with micro Computed Tomography (μCT), and a three dimensional (3D) array was recorded. We employed a segmentation-less method to convert each 3D array value to density, porosity, elastic moduli, and wavespeeds. Wave propagation was simulated numerically at similar frequency as the laboratory. Then, to simulate fluid substitution we numerically substitute air values for water and perform again the wave propagation experiment.

The results from DRP yielded similar velocities to the laboratory, and accurately predicted velocity change from fluid substitution. Theoretical modeling could not accurately predict velocity, and under-predicted the velocity change from fluid substitution. The mathematical approach proved to be no comparison for the laboratory measurement. DRP proved to be effective, and could be used in future with drill cuttings, perhaps to limit the use of expensive cores. DRP could also limit the requirement for physically testing fluid substitution.

Keywords: digital rock physics, ultrasonic velocity, fluid substitution, dispersion

EG
ECG

Improving Seismic Data Resolution Using Shaping Regularization with the Dip Moveout Correction

Ben Gremillion
Gremillion, B., Bureau of Economic Geology, The University of Texas at Austin, Austin, TX
Fomel, S., Bureau of Economic Geology, The University of Texas at Austin, Austin, TX

One of the major problems facing 3D seismic acquisition and processing is spatial aliasing, which results from irregular and incomplete coverage of a survey area. Aliased data can create artifacts in a final migrated image, making interpretation more difficult. Inversion has been previously proposed to address this issue. Shaping regularization, a form of inversion, is an iterative scheme that explicitly maps an estimated model to the space of acceptable models. Inversion of 2D data to zero-offset will be tested using the dip moveout (DMO) correction by finite-difference offset-continuation and shaping regularization. If initial results are promising, these methods can be applied to 3D data in future work.

Keywords: Inversion, Seismic Data Processing, Dip Moveout Correction

EG
ECG

Calculating Effective Elastic Properties of Berea Sandstone Using Segmentation-less Method without Targets

Ken Ikeda
Ikeda, K., Jackson School of Geosciences, The University of Texas at Austin, Austin, TX
Goldfarb, E., Jackson School of Geosciences, The University of Texas at Austin, Austin, TX
Tisato, N., Jackson School of Geosciences, The University of Texas at Austin, Austin, TX

Digital rock physics (DRP) allows performing common laboratory experiments on numerical models to estimate, for example, rock hydraulic permeability. The standard procedure of DRP involves turning a rock sample into a numerical array using X-ray micro-computed tomography (micro-CT). Each element of the array bears a value proportional to the X-ray attenuation of the rock at the element (voxel). However, the traditional DRP methodology, which includes segmentation, over-predicts rock moduli by significant amounts (e.g., ~30%). Recently, a new methodology – the segmentation-less approach – has been proposed leading to more accurate DRP estimate of elastic moduli. This new method is based on homogenization theory. Typically, the segmentation-less approach requires calibration points from known density objects, known as targets. However, not all micro-CT datasets have these reference points. Here, we introduce the method of pseudo-targets where we could apply segmentation-less on target-less CT images. Pseudo-targets are calibration points which are collected from the center of mineral grains within the sample CT image. We calculate the effective elastic properties of a Berea sandstone sample that was scanned at a resolution of 40 microns per voxel. We transform the CT images into density matrices with four calibration points: the whole rock, the center of quartz grains, the center of iron oxide grains, and the center of air-filled volumes. The first calibration point is obtained by assigning the density of the whole rock to the average of all CT-numbers in the dataset. Then, we locate the center of each phase by finding local extrema points in the dataset. The average CT-numbers of these center points are assigned the density equal to either pristine minerals (quartz and iron oxide) or air. Next, density matrices are transformed to porosity and moduli matrices by means of an effective medium theory. Finally, effective elastic properties are calculated using SOFI3D: the staggered-grid finite-difference elastic wave modelling software. The differences between simulated and measured P- and S-wave speed are -1% and -5%, respectively, which is more accurate than traditional DRP methods. Nevertheless, the presented methodology need to be further investigated and improved.

Keywords: Digital Rock Physics, Numerical Modelling

EG
ECG

Characteristics of Coarse-Grained Regressive-Transgressive Cyclic Sandstones of Jurassic Lajas Formation in Southern Neuquen Basin, Argentina

Eunsil Jung
Jung, E., Jackson School of Geosciences, The University of Texas at Austin, Austin, TX
Steel, R., Jackson School of Geosciences, The University of Texas at Austin, Austin, TX
Olariu, C., Jackson School of Geosciences, The University of Texas at Austin, Austin, TX

A Mid-Jurassic Lajas Formation outcrop analogs of the hydrocarbon-bearing southern Neuquen Basin, Argentina is a succession of repeated regressive-transgressive phases of deltas and estuarine deposits deposited across the shelf and the accumulated hundreds of meters thick as a topset succession of shelf-margin clinoforms. At the lowermost part of the Lajas Formation is underlain by Molles slope-deepwater mud and shelf edge delta which is characterized by distinctive and thick medium to coarse grained sand. Above the shelf edge delta, 10 to 20 m thick mud and a half meter of fine to medium sandstone are deposited and those are overlain by several sets of up to 10 m of white, well sorted, extremely cross-bedded sandstones. The lower boundary of this sandstone is sharp and conglomeratic, and had mud laminae. Single and compound dunes are well preserved in this white sand showing mainly NE and some of NW paleocurrent directions, and these white sand beds are extended a few kilometers over the study area. Those facies of the white sand beds and the existence of Turritella at the base of the packages can indicate the evidence of the revinement surface and overall transgression after the deposition of the shelf edge delta. Another important facies of Lajas Formation is medium-coarse sandstone with uni- or bi-directional cross-strata and parallel laminations with a small scale of (~10m) upward coarsening and thickening tendency which are interpreted as tidal dominated delta front. Also, sharp based and channelized coarse-grained sandstone beds contain abundant wood logs and cut down into parallel laminated or bi-directional cross-bedded sandstones. Evidence of significant wave influence is very rare. These strike-continuous and regression-transgression alternative cross-stratified sandstone bodies appear to have changes of relative sea-level providing understanding of migrating shoreline and shelf sediment transportation. This sand-rich T-R system is unusual as it contains relatively little mud and this character is interpreted to derive from strong tidal reworking of the river-driven sediment dispersal. Also, measured paleocurrents suggest that there may have been an anti-clockwise tidal gyre within this narrow southern end of the basin that may have tidally swept the shelf-edge coastlines. This outcrop analog study that shows the shoreline was dominated by fluvial-tidal processes can be directly applied to adjacent hydrocarbon fields in Neuquen Basin, and as a wider importance, can improve understanding of fluvial-tidal depositional systems in tectonic active settings.

Keywords: coarse-grained sandstones, regression-transgression, tidal deposits, Neuquen basin

EG
ECG

Seismic imaging in stratigraphic coordinates

Harpreet Kaur
Kaur, H., Bureau of Economic Geology,The University of Texas at Austin, Austin,TX
Fomel, S., Bureau of Economic Geology,The University of Texas at Austin, Austin,TX

Stratigraphic coordinates are a coordinate system aligned with the horizons in a seismic image. The vertical direction in stratigraphic coordinates corresponds to the direction normal to the major reflection boundaries. We are implementing low rank one step wave extrapolation for reverse time migration. We show that, by reformulating the wave propagation problem, it is possible to implement seismic migration directly in the stratigraphic coordinate system. The benefit of this approach is a closer connection between the output of imaging and reflectivity inversion, including the analysis of reflectivity versus angle.

Keywords: Low rank, stratigraphic coordinates

EG
ECG

Establishing a Methodology to Measure the Static Elastic Properties of Fluids

Michael McCann
McCann, M., Jackson School of Geosciences, The University of Texas at Austin, Austin, TX
Spikes, K., Jackson School of Geosciences, The University of Texas at Austin, Austin, TX
Tisato, N., Jackson School of Geosciences, The University of Texas at Austin, Austin, TX

Pore fluids significantly affect the elastic responses of rocks. Measuring the elastic properties of the pore fluids alone is required to understand how elastic properties of rocks will change when they are saturated with these pore fluids. The elastic properties of a material depend on the frequency of the wave propagating through the material. Methodologies and measurements of high-frequency elastic properties of fluids have been widely reported. What has not been established are methodologies for measuring the low-frequency (i.e. static) elastic properties of fluids in a laboratory setting.

Seismic experiments measure the low-frequency response of rocks because high frequencies attenuate during these large-scale experiments. These experiments, however, are expensive. Rock physics models can be used instead to predict the elastic properties of a fluid-saturated rock but require the elastic properties of the fluid alone. Using the static elastic properties rather than the already known high-frequency properties of pore fluids will provide more accurate values when calculating the static elastic properties of rocks saturated with pore fluids from rock physics models. The goal of this work is to establish a methodology to measure the bulk modulus and attenuation of various fluids at low-frequencies at various temperature and pressure conditions. Results should indicate noticeable differences in the low and high frequency values of moduli and attenuation.

Keywords: experimental rock physics

EG
ECG

Automatic channel detection in seismic section using deep learning

Nam Pham
Pham, N., Bureau of Economic Geology, The University of Texas at Austin, Austin, TX
Fomel, S., Bureau of Economic Geology, The University of Texas at Austin, Austin, TX

Channels are important geologic features in oil and gas exploration, because channel sands are excellent oil and gas reservoirs. Channels can often be mapped in on time or depth slices of 3D seismic images. In case of increasing number of channels to be interpreted and large seismic volume, manually mapping becomes more time-consuming, therefore automatic detection algorithms emerged naturally. There are different methods for automatic detection such as Steerable Pyramid (Mathewson and Hale 2008) and Directional structure-tensor-based coherence (Wu 2017). Deep learning can provide another approach to detect channels in seismic section.
Deep learning has been used widely in computer vision for object detection (Redmon 2016), image segmentation (Badrinarayanan 2016) and face recognition (Taigman 2016). As for 2D or 3D seismic application, deep learning has been used to map faults (Guitton 2017), salt dome (Waldeland 2017).
We propose to use deep learning to train on the interpreted channels in QCL released offshore Australia dataset using encoder-decoder architecture. Then the model will be tested to detect other channels in the dataset.

Keywords: channel structure, seismic, deep learning

EG
ECG

Effect of Test Fluid in Steady-state Liquid Permeability Measurements of Siltstone Lithofacies in the Bone Spring Formation, Delaware Basin

Sebastian Ramiro Ramirez
Ramiro-Ramirez, S., Institute for Geophysics
Bhandari, A., Institute for Geophysics
Flemings, P., Institute for Geophysics, Department of Geological Sciences
Polito, P., Department of Geological Sciences

We measured the horizontal effective permeability (kh,eff) of two (twin) siltstone core plugs from the Bone Spring formation using two different pore fluids: brine (120 kppm NaCl) and dodecane (C12H26). On average, kh,eff to dodecane was 30% higher than kh,eff to brine. We interpreted this permeability difference as the result of wettability behavior and initial fluid (brine and hydrocarbons) saturations in the core plug. We considered that our siltstone samples are water-wet, in which brine (i.e. the wetting phase) occupies small pores while hydrocarbons (i.e the non-wetting phase) occupy larger pores. Therefore, kh,eff to dodecane is higher because it is easier for this fluid to form a continuous phase in the porous media with the existing hydrocarbons present in the core plug. The kh,eff to each fluid was determined using the steady-state method. In this method, we generate a pore pressure differential between both ends of the core plug by setting a constant flow rate upstream and constant pressure downstream. At steady-state conditions, the corresponding pressure differential is used in Darcy's law to calculate the permeability. We repeat this process at different confining pressures to close any artificial microfracture that might be present in the sample, and to record the permeability-stress dependency of the rock. In this work, we hypothesize that the difference in permeability between brine and dodecane can be explained by the ease with which each liquid forms a continuous phase in the pore space. Dodecane (non-wetting phase) showed higher permeability because it occupies larger pores, and presumably mixed with hydrocarbons already present in the rock. We also showed that the steady-state liquid permeability method is suitable for permeability measurements to different fluids in microDarcy rocks.

Keywords: Petrophysics, Permeability, Unconventionals, Oil, Petroleum

EG
ECG

STRATIGRAPHY, SEDIMENTOLOGY, AND GEOCHEMISTRY OF THE EAST TEXAS UPPER JURASSIC SMACKOVER CARBONATE RAMP SUCCESSION

Peter Schemper
Loucks, R., Department of Geology, Jackson School of Geosciences, The University of Texas at Austin, Austin
Fu, Q., Department of Geology, Jackson School of Geosciences, The University of Texas at Austin, Austin

The Smackover Formation is a significant hydrocarbon producer in the northern Gulf of Mexico. Production within the Smackover comes from the often dolomitized oolitic grainstone facies present in the upper section. These upper Smackover reservoirs are sourced from organic rich Lower Smackover mudrocks (often referred to as the Brown Dense). A renewed understanding of the Smackover petroleum system, specifically the lower portion, will aid in continued exploration of age equivalent targets along the Gulf Coast and into Mexico. There remains a debate within the East Texas basin as to whether low-energy laminated mudrocks were deposited on the deep-water slope or in shallow-marine tidal-flats. This debate is significant because it affects our understanding of shoreline locations and relative sea-level oscillations for the given time period. Without a clear understanding of the depositional environments and sequence stratigraphy of the Lower Smackover, it would be difficult to assess its potential as an unconventional reservoir.

In this study, we analyze a core from the Travis Gas Unit #1, Van Zandt, TX, which has produced 13,639 MFCD of natural gas. The core is 550 ft long; this vertical section is composed of 95% Smackover Formation and also contains the lower section of the overlying Buckner Formation. The interval contains Smackover facies ranging from the contentious low-energy organic-rich laminated mudstones to skeletal and oolitic grainstones. The purpose of this research is to: (1) provide data to improve understanding of the Smackover regional sequence stratigraphy, (2) add to our understanding of conventional and unconventional reservoir potential in this section, and (3) characterize micro- to macropore networks in conventional reservoirs and nano- to micropores in unconventional reservoirs. In order to obtain a good constraint on facies types, oceanic conditions, and reservoir characteristics, we applied the following techniques to analyze the 550 ft. core: A description with binocular microscope, blue-dyed and blue-fluorescence dyed thin sections, x-ray diffraction analysis, XRF analysis, TOC, rebound hammer analysis for unconfined compressive strength, strontium, oxygen, and carbon Isotope analysis, and SEM analysis of Ar-ion milled samples for delineation of mineralogy, microtextures, and nano- to macropore networks.

Keywords: Carbonates, Sedimentology

EG
ECG

ENRICHED AND HYBRID GALERKIN FINITE ELEMENT METHODS FOR SEISMIC WAVE PROPAGATION IN FRACTURED MEDIA

Janaki Vamaraju
Vamaraju, J., Institute for Geophysics, John A. and Katherine G. Jackson School of Geosciences, The University of Texas at Austin, Austin, Texas, USA
Sen, M., Institute for Geophysics, John A. and Katherine G. Jackson School of Geosciences, The University of Texas at Austin, Austin, Texas, USA
De Basabe, J., Seismology Department, Earth Sciences Division, Centro de Investigacion Cientifica y de Educacion Superior de Ensenada, Mexico
Wheeler, M., Center for Subsurface Modeling, The Institute of Computational Engineering and Sciences, The University of Texas at Austin, Austin, Texas, USA.

Finite Element Methods (FEM) are becoming increasingly popular in modeling seismic wave propagation. These methods provide higher order accuracy, geometrical flexibility and adaptive gridding capabilities that are not easy to incorporate in traditional finite difference methods employed for generation of synthetic seismograms. Moreover, several studies have shown that Discontinuous Galerkin FEM (DGM) is a promising approach for modeling wave propagation in fractured media. It allows for discontinuities in the displacement field to simulate fractures or faults in a model. The approach is based on the interior-penalty formulation of DGM, and the fractures are simulated using the linear-slip model, which is incorporated into the weak formulation. On the other hand, the Spectral Element Method (SEM) can be used to simulate elastic wave propagation in non-fractured media. SEM uses continuous basis functions which do not allow for discontinuities in the displacement field. However, the computation cost of DGM is significantly larger than SEM due primarily to increase in the number of degrees of freedom. Here we propose Enriched Galerkin FEM (EGM) and Hybrid Galerkin FEM (HGM) for elastic wave propagation.

EGM uses the same bilinear form as DGM. The continuous Galerkin finite element spaces are enriched by discontinuous piecewise constants or bilinear functions. EGM satisfies local equilibrium while reducing the degrees of freedom in DGM formulations.

Hybrid Galerkin FEM (HGM) combines the salient features of DGM and SEM algorithms resulting in significant reduction in computational cost compared to a stand-alone DGM. We employ DGM in areas containing fractures and SEM in regions without fractures. The coupling between the domains at the interfaces is satisfied in the weak form through interface conditions. In this method, the degree of reduction in computation time depends primarily on the density of fractures in the medium.

Using realistic 2D/3D numerical examples, we show that our proposed methods outperform a stand-alone DGM with reduced computation cost and memory requirement while maintaining the same level of accuracy.

Keywords: finite element methods, seismic wave propagation, fractures, elastic

MG
ECG

Spatial and temporal dependencies of structure II to structure I methane hydrate transformation in porous media under reservoir conditions

Tiannong Dong
DONG, T., Institute for Geophysics and Department of Geological Sciences, The University of Texas at Austin, Austin, TX
Lin, J., Department of Geological Sciences, The University of Texas at Austin, Austin, TX
Flemings, P., Institute for Geophysics and Department of Geological Sciences, The University of Texas at Austin, Austin, TX
Gu, J., Department of Geological Sciences, The University of Texas at Austin, Austin, TX
Polito, P., Department of Geological Sciences, The University of Texas at Austin, Austin, TX
O'Connell, J., Institute for Geophysics, The University of Texas at Austin, Austin, TX

We used Raman spectroscopy to monitor methane hydrates transforming from structure II to structure I at the pore scale as a function of space and time. It is well documented that structure I hydrate is the thermodynamically stable phase for pure methane hydrate (<100 MPa, < ~20 °C), but due to kinetic limitation, initial methane hydrate formation produces a mixture of structure I and structure II hydrates. We observed that the structure transformation originated around the porous medium grains and over time slowly migrated into the pore space. We synthesized methane hydrates in spherical glass beads (210–297 μm in diameter) in a pressure cell with a sapphire window to integrate optical observations with Raman measurements. We injected CH_4 vapor into the cell and supplied only deionized water thereafter to maintain a constant pressure of 14.6 MPa at 3.5 °C, with 14.5 °C subcooling. We used Raman spectroscopy to map the methane hydrates in pore spaces at 5–25 μm resolution, in order to monitor the occupancy ratio of CH_4 in large cages to CH_4 in small cages, by their Raman peak intensity ratio, i.e., I(~2905 cm^{-1})/I(~2915 cm^{-1}). We identified 3 stages of hydrate formation at the pore scale: (1) after the initial hydrate formation, Raman mapping revealed that the occupancy ratio ranged from 0.5 to 3, indicating a mixture of structure I and II hydrates; (2) within ~1 week, we observed that all structure I hydrates occurred on the glass bead surfaces and structure II hydrates occupied the pore spaces; (3) over the following 2 weeks, structure II hydrates gradually recrystallized into structure I hydrates from glass bead surfaces towards the pore space. These results imply that (1) due to kinetics, the formation of methane hydrate in porous media is more complex than previously thought, and (2) the bulk physical and chemical properties of laboratory-synthesized methane hydrates in porous media may drift over time, as methane hydrates recrystallize from a metastable phase (structure II) to the thermodynamically stable phase (structure I).

Keywords: Methane hydrate, Pore scale, metastable

MG
ECG

The Evolution of Slow to Intermediate-Spreading Oceanic Crust in the South Atlantic: The Effects of Age, Sediment Thickness, and Spreading Rate on Upper Crustal Velocities

Dominik Kardell
Kardell, D., University of Texas Institute for Geophysics
Christeson, G., University of Texas Institute for Geophysics
Reece, B., Texas A&M University, Department of Geology and Geophysics
Arnulf, A., University of Texas Institute for Geophysics
Carlson, R., Texas A&M University, Department of Geology and Geophysics

The upper section of oceanic crust (layer 2A) commonly exhibits relatively low seismic velocities due to abundant pore and crack space created by the extrusive emplacement of magma and extensional faulting at the spreading ridge. Previous studies have shown that these velocities increase rapidly and cease to increase by crustal ages of 10-16 Myr. We use a recent multichannel seismic dataset collected with a 12.5 km streamer during the CREST cruise (Crustal Reflectivity Experiment Southern Transect) to build eleven 60-80 km-long tomographic velocity models. These two-dimensional models include both ridge-normal and ridge-parallel orientations and cover oceanic crust produced at slow to intermediate spreading rates. Crustal ages range between 0 and 70 m.y., spreading rates range between slow-spreading and intermediate-spreading, and sedimentary cover thickness ranges from 0 m close to the spreading center to ~500 m around 70 Ma.
Our results show a trend of increasing layer 2A velocities with age arguably throughout the entire length of the seismic transect. There is a rapid increase in velocities from ~2.8 km/s near the ridge to ~4.1 km/s around 7 Ma, and a slower increase to velocities around 4.9 km/s in ~52 m.y. old crust. This indicates an ongoing evolution of oceanic crust much older than predicted by previous studies. We observe more velocity heterogeneity for slow-spreading crust compared to intermediate-spreading crust and possibly a thinning of layer 2A with increasing age. While the sedimentation rate in the area of study is low overall, locally thick sedimentary cover thickness correlates poorly with elevated layer 2A velocities.

Keywords: Oceanic crust, layer 2A, slow spreading, seismic tomography

MG
ECG

Development of a shallow decollement along the south-central Chile margin from 2D seismic reflection data

Kelly Olsen
Bangs, N., University of Texas Institute for Geophysics
Arnulf, A., University of Texas Institute for Geophysics

In January and February, 2017, we acquired approximately 5,000 km of deep-penetrating 2D seismic reflection data along the Chile trench between 30 – 44 degrees S as a part of the 2017 Crustal Examination from Valdivia to Illapel to Characterize Huge Earthquakes (CEVICHE) project, on the R/V Langseth. We used a 6,600 in^3 airgun source to shoot every 50 m and recorded shots on a 15,100 m, 1212 channel streamer. This survey targeted the structure of this subduction zone across the slip regions of the 2015 Illapel (Mw 8.3), the 2010 Maule (Mw 8.8), and 1960 Valdivia (Mw 9.5) earthquakes. Two dip lines between 37.5°S and 39 degrees S, within the overlapping slip areas of the Maule and Valdivia earthquakes, show a range in the style of initial thrust faulting at the deformation front. At 37.5 degrees S, just south of the Arauco Peninsula, protothrusts at the deformation front are typical of many well-sedimented trench sections in subduction zones worldwide. Here we observe incipient landward-dipping thrusts consisting of ~15 faults with typical horizontal spacing of 750 m that can be seen to extend down through the entire 2.5 km thick sediment sequence to the top of the subducting ocean crust. Some form conjugate fault pairs, but all have small offsets of 10-50 m. These thrusts appear to sole into a proto-decollement located just above the top of the ocean crust; however, farther landward beneath the lower slope, a thick, ~ 2.5 km, sequence of layered sediment can be traced > 20 km into the subduction zone. The position of the primary decollement appears to be located near the top of the trench sediment sequence, well above the proto-decollement, allowing subduction of the entire trench sequence. A second line at 39 degrees S across the deformation front shows no frontal thrusts or apparent deformation within the 1.5 km thick section of trench sediment. All of the incoming sediment appears to be subducting beneath a stable decollement that we can image near the top of the trench sediment sequence. The decollement along the northern line may be currently stepping down and transitioning from minimal accretion, typical of this segment of the Chile margin, to accretion of the entire trench section. Alternatively, the initial deformation at the toe may cease and allow slip to shift upward to the shallow decollement and continue to subduct the entire trench sediment section.

Keywords: subduction, sediment, decollement, Chile

PS
ECG

Characterization of fractures in the Chicxulub peak ring: preliminary results from IODP Expedition 364

Naoma McCall
McCall, N., Institute for Geophysics, Jackson School of Geosciences, University of Texas at Austin, Austin, Texas
Gulick, S., Institute for Geophysics, Jackson School of Geosciences, University of Texas at Austin, Austin, Texas
Morgan, J., Department of Earth Science and Engineering, Imperial College London, SW7 2AZ, UK
Jones, L., Institute for Geophysics, Jackson School of Geosciences, University of Texas at Austin, Austin, Texas
Hall, B., Enthought, Inc, Austin, Texas

During Expedition 364, IODP/ICDP drilled the peak ring of the Chicxulub impact crater at Site M0077, recovering core from 505.7 to 1334.7 mbsf. The core has been imaged via X-ray Computer Tomography (CT) as a noninvasive method to create a 3-dimensional model of the core, providing information on the density and internal structure at a 0.3 mm resolution. Results from the expedition show that from 748 mbsf and deeper the peak ring is largely composed of uplifted and fractured granitic basement rocks originally sourced from approximately 8-10 km depth. Impact crater modeling suggests the peak ring was formed through dynamic collapse of a rebounding central peak within 10 minutes of impact, requiring the target rocks to temporarily behave as a viscous fluid. The newly recovered core provides a rare opportunity to investigate the cratering process, specifically how the granite was weakened, as well as the extent of the hydrothermal system created after the impact.

Based on the CT data, we identify four classes of fractures based on their CT facies deforming the granitoids: pervasive fine fractures, discrete fine fractures, discrete filled fractures, and discrete open fractures. Pervasive fine fractures were most commonly found proximal to dikes and impact melt rock. Discrete filled fractures often displayed a cataclastic texture. We present density trends for the different facies and compare these to petrophysical properties (density, NGR, resistivity). Fractured areas have a lower density than the surrounding granite, as do most filled fractures. This reduction suggests that fluid migrating through the peak ring in the wake of the impact either deposited lower density minerals within the fractures and/or altered the original fracture fill. The extent and duration of fluid flow recorded in these fractures will assist in the characterization of the post-impact hydrothermal system.

Future work includes combining information from CT images with thin sections and plug samples at similar depths, refinement of CT facies characterization, examining cross-cutting relationships to determine timing constraints of deformation processes, and measurement of the orientation of the fractures.

Keywords: Chicxulub, impact craters, CT

PS
ECG

RADAR REFLECTIVITY ANALYSIS OF NORTHERN HEMISPHERE BOULDER HALOS ON MARS

Brandon Tober
Tober, B., Institute for Geophysics, Jackson School of Geosciences, University of Texas at Austin,
Holt, J., Institute for Geophysics, Jackson School of Geosciences, University of Texas at Austin,
Levy, J., Department of Geology, Colgate Univesity
Grima, C., Institute for Geophysics, Jackson School of Geosciences, University of Texas at Austin,

Boulder halos are features composed of boulder-clasts distributed in circular or concentric patterns on a relatively muted topographic surrounding. These features have been documented extensively across the mid- to high-latitudes of Mars, with greatest abundance in the northern hemisphere between ~0-180° E. A study focused on the distribution and characteristics of these features at high latitudes on Mars proposes that boulder halos form by excavation of boulders from substrate at depth, beneath an overlying, ice-rich, non-boulder generating layer. Preferential distribution of these landforms implies that either surface processes support the preservation of these features in the northern hemisphere, or act to destroy them in the southern hemisphere.

Numerous studies have demonstrated the capacity for radar sounders to provide information on Mars' subsurface composition and structure. Here, we aim to analyze SHARAD data at both local- and regional-scales, in an effort to gain information on near-surface composition and structure from the radar response and surface echo strength of regions where boulder halos are prominent, and those where they are not. This study will primarily focus on Mars' northern hemisphere, due to the higher density and regional variability of boulder halos. Local-scale analysis of individual SHARAD tracks in areas where boulder halos are prominent will be focused in the northern plains between Utopia Planitia and Vastitas Borealis from ~55°-70°N and ~150°-180°E. Regional-scale analysis of surface echo power will be compared between this same region of high boulder halo density and the low boulder halo density region between ~55°-70°N and ~210°-270°E. A method of detecting the surface from SHARAD tracks will be developed so that regional measurements can be made on surface echo power. Information provided on the local-scale radar response to boulder halos, and regional-scale surface echo power may help to better understand the spatial distribution of boulder halos in Mars' northern hemisphere.

Keywords: Mars, Boulder Halos, Reflectivity, SHARAD

SETP
ECG

Halogen Cycling and Stable Isotope Geochemistry During Prograde Subduction Zone Metamorphism and Devolatilization

Grace Beaudoin
Beaudoin, G., The University of Texas at Austin, Austin, TX
Barnes, J., The University of Texas at Austin, Austin, TX
John, T., Freie Universität Berlin, Berlin, Germany

Halogens (F, Cl, Br, and I) are highly volatile elements commonly found in geologic fluids. In subduction zones, halogens are released from the down-going slab by dehydration reactions after being incorporated into the oceanic crust by seafloor hydrothermal alteration. The addition of halogens to slab-derived aqueous fluids can profoundly alter fluid properties, element transport capabilities, and phase stability. Halogen-bearing fluids have been shown to contribute to the suppression of slab-melting and the activation of dehydration reactions at shallower depths. Unfortunately, large uncertainties exist regarding the extent to which halogens devolatilize and fractionate during subduction.

In order to constrain global geochemical cycles and better predict fluid properties in modern convergent systems, this study will investigate the halogen chemistry of altered oceanic crust (AOC) that records progressive devolatilization during subduction. Metagabbro and metabasalt samples were collected from Alpine ophiolites that experienced variable pressure-temperature (P-T) conditions during Cretaceous subduction of the Tethys Ocean. Samples collected range from prehnite-pumpellyite to eclogite facies and will be used to reconstruct prograde volatile loss from the slab. Following the characterization of samples by detailed field and petrographic work, bulk and *in situ* geochemical analyses will be conducted to measure halogen concentrations, major and trace element concentrations, and chlorine stable isotope compositions ($\delta^{37}Cl$). Preliminary results show a decoupling of F and Cl during prograde metamorphism, largely controlled by mineral stability, and show no significant Cl-isotope fractionation. The results of this work will be used to extrapolate the composition of slab-derived fluids and residual material, enabling an improved understanding of phase equilibria and element transport during subduction, arc magma genesis, and the volatile budget of the mantle.

Keywords: halogen cycling, chlorine isotopes, subduction, devolatilization

SETP
ECG

Zircon 4He/3He Thermochronometry – Recovery of Helium-4 Concentration Profiles Across the Zircon Helium Partial Retention Zone and Implications for Thermal History Reconstruction

Clara Brennan
Brennan, C., The University of Texas at Austin, Austin, TX
Stockli, D., The University of Texas at Austin, Austin, TX

Low-temperature thermochronometry is a powerful tool used to constrain the timing and thermal evolution of a variety of geologic events, from meteorite impacts to volcanic eruptions to crustal exhumation. (U-Th)/He thermochronometry is particularly sensitive to reconstructing events in the upper crust and relies on the determination of age based on the accumulation and diffusive loss of radiogenic daughter product from the decay of U, Th, and Sm parent isotopes. (U-Th)/He data are commonly used to recover thermal histories in order to understand the geologic history of a mountain range or basin. The thermal sensitivity of a specific thermochronometric method is commonly depicted by a closure temperature. However, He closure does not occur at an abrupt temperature boundary, but is rather characterized by a Partial Retention Zone (PRZ) – a zone of only partial accumulation due to thermal-activated diffusive He loss. For zircon, the closure temperature is ~180°C, while the He PRZ has been shown to span a 190-140°C temperature interval. However, a single (U-Th)/He age, while often interpreted in the context of its closure temperatures, in reality can be the result of an infinite number of thermal histories. A significantly more powerful method to recover thermal histories is through the determination of spatial He diffusion gradients within a zircon grain.

This study explores single zircon $^{4}He/^{3}He$ thermochronometry for the recovery of thermal histories from exhumed and drilled crustal sections, respectively, to better understand the inversion of He diffusion profile topologies in zircon across the PRZ and the influence of parent nuclide zonation. $^{4}He/^{3}He$ thermochronometry is based on ^{4}He measurements against a homogenous ^{3}He background spallogenically produced by proton irradiation. This requires bombardment of the sample with an ~150 MeV proton beam to achieve an even distribution of spallogenic ^{3}He. The ^{3}He is created by inelastic fragmentation of stoichiometric major elements, such as oxygen – a mechanism similar to the production of ^{3}He used in cosmogenic nuclide dating of geomorphologic features. The uniform synthetic ^{3}He distribution allows ^{4}He concentration profile measurements and fractional loss step-heating experiments, as ^{4}He can be normalized by the ^{3}He. Additionally, the step heating allows for the possibility of calculating ^{4}He and ^{3}He diffusion kinetics.

$^{4}He/^{3}He$ step heating experiments are performed in ultra-high vacuum by diode laser heating of the sample and noble gas mass-spectrometry using a Thermo Helix Split Flight Tube (SFT) magnetic-sector mass-spectrometer. Subsequently, zircon U and Th zonations are measured by LA-ICP-MS depth profiling. The measured $^{4}He/^{3}He$ fractional loss data and the 1D U and Th zonation data can be inverted using Monte Carlo inverse modeling (HeFTy) to determine the time-temperature evolution of samples across the zircon He PRZ. The results are then compared to the multi-sample data from the same crustal sections for benchmarking.

Keywords: thermochronometry, 4He/3He thermochronometry, partial retention zone, PRZ, Wassuk Range

SETP
ECG

Sediment routing and 3D stratigraphic architecture in the Patagonian foreland basin: Implications for Andean tectonics and flat-slab subduction

Kristina Butler
Butler, K., Jackson School of Geosciences, The University of Texas at Austin, Austin, TX

The Patagonian foreland basin of southern Argentina is broken by large basement blocks related to phases of thick-skinned shortening, potentially triggered by flat-slab subduction. These structures are analogous to thick-skinned Laramide uplifts of western North America and the Sierras Pampeanas of central Argentina. Two separate contractional phases are currently recognized (Late Cretaceous-Paleocene and Miocene), with a possible intervening enigmatic Paleogene extensional phase. An integrated understanding of the cratonward migration of thick-skinned shortening into the foreland and the resultant stratigraphic response remains elusive. The Paso del Sapo-Lefipan-Salamanca succession (500 m thick) offers a continuous stratigraphic record from the Andean foothills to the modern Atlantic Ocean, over the critical transition from Late Cretaceous shortening into a period of possible Paleogene extension. To date, no researchers have attempted a regional approach to assess the partitioning of the Patagonian foreland by thick-skinned deformation. Additionally, the depositional systems and sediment routing patterns of the Upper Cretaceous-Paleogene succession are incompletely described. I propose a high-resolution analysis of the stratigraphic architecture and sediment routing evolution of the Upper Cretaceous–Paleogene succession of the Patagonian foreland. I will use a regional multi-disciplinary approach, including a 3D network of cm-scale measured sections, provenance analyses (detrital zircon geochronology, paleocurrent measurements, and sandstone petrography), 2D seismic and core interpretation, and drone assisted photography/photogrammetry. I believe this interval may reveal asynchronous cratonward migration of early Andean deformation. The proposed locality provides a unique opportunity to understand the partitioning of foreland basins by thick-skinned deformation and the associated stratigraphic consequences on a continental scale, which encompasses sedimentary processes from source to sink.

Keywords: thick-skinned shortening, flat-slab subduction, source-to-sink, 3D stratigraphic architecture, Patagonia

SETP
ECG

Triassic and Jurassic Rift Basin Record of Provenance, Sediment Dispersal, and Extension during the Breakup of Pangea along the in the Proximal Eastern North American Margin, U.S.A.

Zachary Foster-Baril
Foster-Baril, Z., The Department of Geological Sciences, The University of Texas at Austin, Austin, TX
Stockli, D., The Department of Geological Sciences, The University of Texas at Austin, Austin, TX

Triassic and Jurassic sedimentary rocks along the proximal portion of the Eastern North American Margin (ENAM) provide a record of rifting, continental breakup, and the geometric development of the ENAM. The proximal margin rift basins, from South Carolina to Connecticut, provide an ideal location to study the early tectonostratigraphic evolution of this magma-rich continental margin. Syn-rift basins provide a rich record of siliclastic and volcanic strata deposited during progressive rifting leading to the breakup of Pangea and opening of the Central Atlantic. The Newark Supergroup encompasses the syn-rift strata in each of the individual basins and consists of alluvial, fluvial, and lacustrine lithofacies. The deposition of syn-rift strata occurred in a series of half grabens with footwalls dipping predominately to the east. The basin bounding faults likely formed along preexisting fault boundaries active during the Appalachian Orogeny. Syn-rift sedimentation began in the Late Triassic and ended shortly after the Central Atlantic Magmatic Province (CAMP) eruptive event based on sparse palynomorph and Ar/Ar geochronology. While researchers consider the ENAM a magma-rich rifted margin due to the syn-rift CAMP basaltic magmatism, the well-persevered stratigraphic record shows syn-rift deposition pre-dates CAMP volcanism by 20-30 Myr. Therefore, questions remain on the magnitude of crustal extension and thinning and the ENAM rift margin geometry prior to the CAMP volcanism and magmatic break-up. While previous works focused on the individual basin stratigraphies and basin-bounding fault systems, no integrated regional tectonic model or holistic modern analysis of these early syn-rift basins in the context of lithospheric extension and break-up exist.

We propose a systematic reconstruction of the tectonic and stratigraphic history to determine the spatial and temporal trends in basin formation during progressive rifting and lithospheric thinning using: 1) fluvial and lacustrine stratigraphy to reconstruct ancient basin morphology and depositional systems; 2) detrital zircon U-Pb-He double dating to determine sediment sources, sediment dispersal, and depositional ages; and 3) bedrock thermochronometry to determine exhumation histories of the rocks in the footwall of normal faults, bounding these rift basins. The combination of these data will provide high-resolution tectonostratigraphic and thermal history datasets to test proposed geodynamic models and reconstruct the structural, stratigraphic, and thermal evolution of continental breakup along the US ENAM. These data will allow for a better understanding of the magnitude of rifting and crustal thinning in the proximal portion of the ENAM and the overall rift asymmetry prior to CAMP volcanism. Particularly, the sparse provenance data from ENAM rift basins and the detrital record from the W USA suggest a prominent and coherent early rift shoulder uplift and drainage divide, indicative of a very asymmetric early ENAM rift. Similar rifted margins in the north-central Atlantic, including Nova Scotia and Morocco, provide considerable hydrocarbon potential. Hence, improving the fundamental understanding of the early structural and depositional evolution provides insights on hydrocarbon potential of the little explored ENAM.

Keywords: Eastern North American Margin, rift, detrital zircon double dating, tectonostratigraphy

SETP
ECG

Impacts of Viscoelastic Rheology on Dynamic Topography

Kunpeng Liao
Liao, K., Institute for Geophysics and Department of Geological Science, The University of Texas at Austin, Austin, TX
Becker, T., Institute for Geophysics and Department of Geological Science, The University of Texas at Austin, Austin, TX

Conventional numerical models of mantle convection typically employ purely viscous or viscoplastic rheologies. This is justified for the mantle because its relaxation time (order of thousands of years) is usually much smaller than the time scale of mantle convection (order of millions of years). This time scale difference allows the influence of elasticity to be ignored. However, the cold lithosphere has a larger viscosity than the asthenospheric mantle, which implies a longer stress relaxation time. This allows elastic behaviors that can be important for lithospheric deformation and stress distribution. Here, we investigate the effects of viscoelastic rheology on surface topography and stress state in a lithosphere – plume interaction model using numerical and analytical approaches. Results show that viscoelastic responses will create higher, narrower topography and smaller stress in the lithosphere than in the case of purely viscous rheology. Unlike the free slip boundary condition used in traditional numerical models, we apply a realistic, Earth-like stress free condition on the surface, which can avoid overestimation generated by a free slip approximation. This is particularly important in thick, high viscosity lithosphere due to the absence of plate bending resistance and no slip effects at the base of the lithospheric mantle.

Keywords: Dynamics of lithosphere and mantle, Viscoelastic rheology, Numerical solutions and analysis

SETP
ECG

Seismic Attenuation in the African LLSVP Estimated from PcS Phases

Chujie Liu
Liu, C., University of Texas at Austin
Grand, S., University of Texas at Austin

Seismic tomography has shown that the lowermost mantle beneath the south central Pacific and southern Africa are marked by broad regions with ~3% slower shear velocity than normal. The structures have come to be known as large-low-shear-velocity provinces (LLSVPs). The cause of the seismic anomalies associated with the LLSVPs is of great interest to geophysicists as they are related to the chemical, thermal, and dynamic structure of the mantle. Some have interpreted the heterogeneity in the LLSVPs to be caused by purely thermal effects while others believe the LLSVPs are chemically distinct from normal mantle. Seismic velocity variations alone cannot distinguish the thermal from chemical interpretations. Anelastic structure, however, can help discriminate among models of the LLSVPs as intrinsic attenuation is much more sensitive to temperature than to chemical variations. In this study, we use PcS seismic waves, from an earthquake located in the Scotia Arc, recorded by 50 broadband seismometers deployed in Southern Africa during the Kaapvaal experiment (1997-1999) to estimate Q in the African LLSVP. With increasing epicentral distances, the upward leg PcS waves in lower mantle sweep from normal mantle into the African LLSVP. We divided the PcS data into a group that sampled the LLSVP and another group that passed through normal lower mantle. We determined Δt^* between these two groups by stacking spectra and using the spectral ratio method. The waves passing through the LLSVP are noticeably more attenuated than those outside. Taking Q values outside the LLSVP from different published 1D Q models (e.g. PREM [Dziewonski and Anderson, 1981]; QLM9 [Lawrence and Wysession, 2006a]; QHR12 [Hwang and Ritsema, 2011]), we estimate the corresponding average shear wave Q in the African LLSVP to be 127, 115, and 118, far lower than any published average Earth Q models for the lower mantle. Using a range of activation energies (E*), from 200 - 500 kJ/mol (Matas and Bukowinski, 2007), we estimate the temperature anomaly within the African LLSVP to be 250 -800 K. Uncertainty is primarily due to uncertainties in the activation energy.

Keywords: attenuation, body wave, LLSVP

SETP
ECG

A minimum constraint on amounts and rates of metamorphic decarbonation during arc magmatism

Evan Ramos
Ramos, E., Department of Geological Sciences, The University of Texas at Austin, Austin, TX
Barnes, J., Department of Geological Sciences, The University of Texas at Austin, Austin, TX
Hesse, M., Department of Geological Sciences, The University of Texas at Austin, Austin, TX

Recent studies have highlighted metamorphic CO_2 production as a potentially significant source of atmospheric carbon over geologic timescales (e.g. Lee et al., 2013; Nabelek et al., 2014; Lee and Lackey, 2015; Kelemen and Manning, 2015). However, the quantification of amounts and fluxes of metamorphic CO_2 production during arc magmatism remains elusive. As such, we present results from simple two-dimensional models of fluid-rock interaction as a proxy for metamorphic decarbonation.

Of the three fluxes of metamorphic CO_2 to the atmosphere in arc systems, – skarnification, host rock assimilation, and thermal decomposition – this study focuses on the quantification of a minimum flux by skarnification. Contact metamorphosed and metasomatized carbonates are primary sources of CO_2 during skarnification and as carbonates are silicified, their oxygen isotope compositions limit towards igneous signatures. In our fluid-rock interaction model, we track how the $\delta^{18}O$ values of carbonates change in response to hydrothermal fluid flow and heat transport induced by a magmatic intrusion. The condition for decarbonation is met when the carbonate $\delta^{18}O$ value matches that of an end-member igneous rock. Introducing any thermodynamic modeling of mineral reactions to the existing model would induce more decarbonation and thus this model represents a minimum constraint.

Over a variable set of parameters, we find that the most important factors that affect metamorphic decarbonation are host rock permeability and the size of the intrusion. Both of these variables have direct relationships with decarbonation amounts and rates; the more permeable the host rock and/or the larger the intrusion, the more frequent the condition for decarbonation is met. Importantly, our modeled decarbonation rates match previous estimates when host rocks have uniform permeability; more work needs to be done to ground-truth this condition. Nevertheless, this study presents a viable way forward in the assessment of metamorphic CO_2 fluxes during arc magmatism and its effect on the evolution of Earth's long-term climate.

Keywords: arc magmatism, carbon, oxygen isotopes, numerical modeling, fluid-rock interactions

SETP
ECG

PLATFORM SCALE STRATIGRAPHIC ARCHITECTURE OF PENNSYLVANIAN ICEHOUSE CARBONATES IN THE SACRAMENTO MOUNTAINS, OTERO COUNTY, NM

Benjamin Rendall
RENDALL, B., Bureau of Economic Geology, The University of Texas at Austin, Austin, TX
BACHTEL, S., Bachtel Geoscience Pontificators, Bend, OR
KERANS, C., Jackson School of Geosciences, The University of Texas at Austin, Austin, TX

The Sacramento Mountains escarpment in Otero county, NM contains well-exposed Paleozoic (Ordovician-Permian) carbonate strata, much of which is temporally equivalent to producing subsurface intervals in the Permian Basin. Of particular interest are world class, continuous exposures of later Paleozoic rocks that record the shift from a “transitional” climate during the Mississippian to full “icehouse” conditions in the Pennsylvanian. The Mississippian-Pennsylvanian boundary also represents a time of a changing tectonic regime from an extensional to compressional setting, which in turn corresponds to a shift from clean carbonate deposition to a mixed carbonate-siliciclastic system. This regional structural change was also likely the cause for the shift in basin position from a southern location during the Mississippian a western location during the early Pennsylvanian. Associated changes in cycle development and reservoir-scale stratigraphic architecture provide a first order control on distribution of hydrocarbon play elements in comparable subsurface settings. In the Sacramento Mountains, continuous north-south trending cliff bands are dissected by east-west trending canyons and drainages that, together, provide three-dimensional control through the entire Mississippian-Pennsylvanian section.

Previous work has shown that Mississippian strata was deposited on a southward-dipping ramp that became progressively steepened through time. Mississippian carbonates are largely middle-to-outer ramp crinoidal grainstones and packstones that pass downdip into mudstones and debris flows. The Mississippian section also contains many famous examples of deeper water Waulsortian mounds that predictably change geometry with respect to their position on the ramp. Pennsylvanian strata in the Sacramentos has been studied in detailed windows, primarily with respect to the abundant phylloid algae bioherms and mixed-carbonate siliciclastic cycles that are the result of reciprocal sedimentation during times of high amplitude, high frequency sea level fluctuations. Deeper-water deposits in the Pennsylvanian have been sparsely reported and their relationship to platform equivalents has not been well-demonstrated, however, large-scale slope folds have been observed in the Desmoinesian aged carbonates in Dog Canyon, possibly indicating proximity to a steepened margin. While the regional stratigraphic architecture of the Mississippian has been documented, the evolution of the of the Pennsylvanian carbonate platform remains poorly understood.

This project will use detailed field mapping aided by measured sections, aerial and panoramic drone photography, digital outcrop modelling, and carbon-oxygen isotope data to document the reservoir-scale stratigraphic evolution from a Mississippian ramp to a steep margined platform in the Pennsylvanian. Facies mapping and outcrop modelling should help refine predictive concepts in transitional and icehouse settings and enhance subsurface correlation of reservoir intervals.

Keywords: Sacramento Mountains, Pennsylvanian, Icehouse, Carbonates

SETP
ECG

U-Pb and (U-Th)/He Geo-Thermochronometry of the Chicxulub Impact Peak Ring

Catherine Ross
Ross, C., DSG, UTIG
Stockli, D., DSG
Gulick, S., UTIG
Rasmussen, C., UTIG
Robbins, S., DSG

The Chicxulub impact crater is the best-preserved large impact crater on the Earth and is the only terrestrial crater with an unequivocal peak ring. The ~200 km crater formed when a 12-km wide asteroid hit the Yucatan Peninsula, resulting in catastrophic events such as a ~M10-11 earthquake, tsunami, seiches, wildfires, worldwide ejecta, sub-marine mass-wasting, and significant climatic effects. The Chicxulub impact coincides temporally with the K-Pg boundary and mass extinction of 75% of life – subsequently allowing for evolution and the age of the mammals. Recently, the International Ocean Discovery Program/International Continental Drilling Project Expedition 364 drilled into the peak ring to explore how rocks weaken through time during large impacts, allowing for the collapse and formation of relatively wide, flat craters. Apatite U-Pb and zircon/apatite (U-Th)/He thermochronometry will be used to quantify the thermal evolution during and after the impact experienced by the upper and lower peak ring samples from the expedition drill cores. The overarching goal is to examine the thermal history of the suevites and shocked granitoids of the peak ring. Thermal events associated with impacts include three stages: the first and second comprise catastrophic thermal events directly related to the impact, referred to as the contact/compression and excavation stages. The third phase involves post-event hydrothermal mineral alteration or metamorphism. We intend to reconstruct the thermal history of the Chicxulub peak ring through the third stage with temperatures ranging from 500-40°C. Furthermore, the Yucatan granitic basement – the impact target crust - has not been thoroughly investigated regarding crystallization ages and plate tectonic context. Preliminary zircon U-Pb LA-ICP-MS dating of granite samples have yielded a continuous range of concordant zircon U-Pb ages between ~300 and ~340 Ma – an unusual age cluster for Gondwanan Yucatan/Maya block. In the Carboniferous, NW Gondwana collided with the Laurentia, forming a collisional belt stretching from the Ozark-Ouachita region to the Marathon Mountains area of west Texas. The Yucatan granites may either represent part of the magmatic arc related to southward subduction of the Rheic Ocean as recorded in the Delicias Basin or formed by syn-collisional magmatism in response to slab break-off. More importantly, however, the initial zircon U-Pb geochronology is important because the age is uncommon in the region and thus can be used as a unique age signature/tracer in detrital zircon provenance studies tracking Chicxulub-related tsunami and ejecta deposits in the circum-Gulf of Mexico.

Keywords: Chicxulub impact crater, Yucatan basement, geochronology, Gulf of Mexico, thermochronometry

SETP
ECG

Constraints on Mantle Dynamics during Jurassic Rifting in the ENAM Area from Seismic and Petrological Modeling of the Oldest Oceanic Crust

Brandon Shuck
Shuck, B., Institute for Geophysics, The University of Texas at Austin
Van Avendonk, H., Institute for Geophysics, The University of Texas at Austin

The thickness and seismic velocity structure of the oceanic crust that first formed after continental breakup can help us understand the nature and dynamics of the asthenospheric mantle beneath the rift zone. Variations in the structure of the oldest oceanic crust can be explained by differences in the composition of the mantle melt source (i.e. primitive vs depleted), mantle potential temperature, magma differentiation, and the final pressure of melting. Previous studies have shown how these conditions affect mantle melting processes and crystallization in crust at a new mid-ocean ridge.
To examine the relationship between mantle melting, continental breakup, and the formation of new oceanic crust, we first use the high-quality seismic refraction and reflection data of oceanic crust from the Eastern North American Margin Community Seismic Experiment. In particular, we focus on the Blake Spur Magnetic Anomaly (BSMA), which lies approximately 300 km offshore Cape Hatteras, North Carolina, and is thought to represent the initial stages of seafloor spreading in the Central Atlantic. The oceanic crust along the BSMA is 8.2-9.9 km thick, and we observe *Vp* from 6.1-7.3 km/s and *Vs* from 3.5-4.2 km/s increasing vertically from the upper to lower crust. With these constraints, we seek to investigate the mantle melting conditions that led to BSMA crustal formation. To achieve this, we implement MELTS, a software package capable of modeling phase proportions during melting and crystallization. With the aid of MELTS, our study is carried out in three successive modeling stages: 1) adiabatic decompression melting of rising mantle, 2) extraction of mantle melts to shallower depths where they crystallize and form crust, and 3) calculation of seismic velocities from the modal abundances of mineral phases and their chemical compositions.
We find that a mantle potential temperature around 1400°C is consistent with the BSMA crustal thickness. Additionally, models that allow melt to fractionally crystallize throughout the crust display greater compositional variations, and can explain the significant vertical seismic velocity gradient that is observed in the BSMA lower crust.

Keywords: rifting, Pangea, passive margin, seismic, tomography

SETP
ECG

Rheological Properties and Heterogeneities Along the Down-Dip Extent of a Subduction Megathrust: Insights from the Condrey Mountain Schist, Northern California

Carolyn Tewksbury-Christ
Tewksbury-Christle, C., Department of Geological Sciences, The University of Texas at Austin, Austin, TX
Behr, W., Department of Geological Sciences, The University of Texas at Austin, Austin, TX
Helper, M., Department of Geological Sciences, The University of Texas at Austin, Austin, TX

Episodic tremor and slow slip (ETS) is commonly observed in warm subduction zones down-dip of a locked megathrust. Proposed mechanisms for ETS involve some form of rheological heterogeneity along the subduction interface. Observations from exhumed subduction-related rocks allow us to investigate the constitutive laws that govern the interface, as well as the types and distributions of rheological heterogeneities that develop and/or persist in the tremor source region. The Late Jurassic to Early Cretaceous Condrey Mountain Schist (CMS), Klamath Mountains, northern California, provides insight into interface rheology along the down-dip extent (350-450°C, 5-8 kbar) of a subduction megathrust. The CMS consists of greenschist and blueschist facies metasediments (including graphitic mica schists), metabasalts, and metaserpentinites, all pervasively deformed under prograde metamorphic conditions with minimal retrogressive overprint. A transect of peak metamorphic temperatures determined using graphite crystallinity shows a constant, but small, inverted thermal gradient with increasing structural depth, suggesting equilibration of temperature discontinuities during underplating. Despite the lack of thermal contrasts, rheological heterogeneities are preserved in the form of km-scale cryptic thrusts that separate lithological packages deforming by different mechanisms. Graphitic mica schists exhibit pervasive cleavage-microlithon fabrics indicative of deformation by quartz dissolution-precipitation creep. Blueschist-facies oceanic crustal sequences juxtaposed against the graphitic mica schists show coeval deformation, but are deformed primarily by dislocation creep in amphibole. These observations suggest that the subduction megathrust likely transitions down-dip into a viscous (rather than frictional) interface shear zone, but that original lithological heterogeneities persist in the form of non-Newtonian vs. Newtonian viscous patches.

Keywords: rheology, subduction interface, Episodic Tremor and Slow Slip, graphite, Na-amphibole

SETP
ECG

Timing and Characterization of the Cave Peak Porphyry Molybdenum Deposit, Culberson County, TX

Mert Ugurhan
Kyle, J., Jackson School of Geosciences ,The University of Texas at Austin, Austin, TX
Elliott, B., Bureau of Economic Geology, The University of Texas at Austin, Austin, TX
Stockli, D., Jackson School of Geosciences, The University of Texas at Austin, Austin, TX

The Cave Peak molybdenum deposit is a breccia-hosted porphyry system, located on the eastern flank of the Sierra Diablo Mountains in western Texas. The Cave Peak intrusive system consists of an outer rhyolite breccia mass with a complex intrusive core that was overprinted by multiple hydrothermal events. Molybdenite is the primary Mo-bearing mineral and occurs as stockwork veinlets and fine disseminations throughout the deposit. At least three spatially and temporally different Mo zones were identified by earlier exploration activities. Enrichments of Sn, W. and Nb are also present. The Marble Canyon Stock is a compositionally zoned unmineralized pluton 1.5 km southwest of Cave Peak; previous studies have suggested a genetic link between the two plutons. Petrographic studies and whole-rock geochemistry were conducted on sub-surface core samples to understand the 3D nature of Cave Peak system. Al_2O_3, Fe_2O_3, K_2O, Na_2O, MgO, CaO, Ti_2O, P_2O_5 are linearly correlated with silica on Harker diagrams at Cave Peak and Marble Canyon Stock. Trace elements plots from Rb, U, Th and Mo concentrations are also showing linear trends implying the relationship between Cave Peak and Marble Canyon Stock.
Quartz syenite and monzonite from the Marble Canyon Stock reveal zircon crystallization ages of 36.2 ± 0.15 Ma (n=40) and 36.1 ± 0.09 Ma (n=34), respectively. These new U-Pb ages are consistent with existing K-Ar ages and display the co-temporal relationship. The youngest major intrusion at Cave Peak, an alkali feldspar granite porphyry, yielded a crystallization age of 34.8 ± 0.4 Ma (n=40). Re-Os geochronology of molybdenite from the upper and lower Mo zones is in progress to constrain the time relationships between the distinct hydrothermal events. Mo isotope analyses will be conducted on sub-surface samples from different depths of Cave Peak porphyry Mo and Red Hills porphyry Cu-Mo systems. The objective is to understand Mo isotope signatures of different tectonic environments.

Keywords: Porphyry Mo System, Molybdenite, Whole-Rock Geochemistry, Zircon, U-Pb Geochronology

SETP
ECG

Asthenospheric Anisotropy Beneath the United States from Mantle Flow Models

Wanying Wang
Wang, W., Department of Geological Sciences & Institute of Geophysics, Jackson School of Geosciences, The University of Texas at Austin, Austin, TX
Becker, T., Department of Geological Sciences & Institute of Geophysics, Jackson School of Geosciences, The University of Texas at Austin, Austin, TX

The asthenospheric olivine aggregates are suggested to align with the maximum shear of mantle flow. The fast propagation orientations, which are the polarization directions of the faster quasi-S waves resulted from shear wave splitting (SWS) phenomenon, are parallel to the fast axes of the upper mantle olivine aggregates. In this study, we use mantle flow models with inputs inferred from seismic and mineral physics studies to simulate the shear beneath the lithosphere and predict the asthenospheric anisotropy. When comparing the fast propagation orientations from shear wave splitting measurements with absolute plate motions, the overall small angular misfit beneath the US suggests the dominant effect of the shear caused by the lithosphere. Beneath the regions with large angular misfit, active mantle flow and lithospheric thickness variations might contribute to the misfit beneath eastern Basin and Range, southern Rocky Mountains, and mid-Atlantic offshore; frozen-in lithospheric anisotropy and edge effect near the cratonic root might contribute to the misfit beneath the Appalachian Mountains. We compare the predicted anisotropies with the SWS observed fast propagation orientations, and investigate the effect of density driven flow combines with lateral viscosity variations on predicted anisotropy. The results suggest that a strong and wide cratonic keel that extends to the east of New England, a weak oceanic asthenosphere and a continuous strong lithosphere through the central US to offshore Atlantic are needed in the lateral viscosity structure input for the flow model to reduce misfit. Density driven upwelling and local lithospheric thinning slightly improve the fit beneath the Basin and Range.

Keywords: Seismic anisotropy, geodynamics, mantle flow, asthenosphere, lithosphere

SHP
ECG

Isotopic and Geochemical Assessment of the Sensitivity of the Northern Guam Lens Aquifer to Intra- and Inter-Annual Variations in Hydroclimate

Lakin Beal
Beal, L., Jackson School of Geosciences, The University of Texas at Austin, Austin, TX
Wong, C., Jackson School of Geosciences, The University of Texas at Austin, Austin, TX
Banner, J., Jackson School of Geosciences, The University of Texas at Austin, Austin, TX
Gingerich, S., U.S. Geological Survey
Jocson, J., Department of Geoscience, University of Guam
Jenson, J., Department of Geoscience, University of Guam

Characterizing the sensitivity of groundwater systems to changes in climate is critical, especially in karst terrains where the link between the surface and subsurface is strong. The Northern Guam Lens Aquifer (NGLA) is the major source of freshwater supporting human populations in the northern part of the island, including U.S. military operations that may expand in the future. To better understand the vulnerability of the freshwater lens to variability in hydroclimate, we assess spatial and temporal variability of isotopic and geochemical compositions of vadose and phreatic groundwater sampled from cave drip sites and production wells from 2008-2015, an interval that spans El Niño and La Niña events. Our results indicate that groundwater compositions are dominantly controlled by mixing of fresh-water with seawater and water-rock interaction. Contrasting variability between rainfall and groundwater $\delta^{18}O$ values document a recharge bias toward the wet season. Intra- and inter-annual variations in Na concentrations and $\delta^{18}O$ values in dripwater and groundwater sampled from wells reflect sensitivity of recharge to seasonal variations in rainfall amount and increasing annual rainfall amounts over the study interval. Our results are consistent with the existing conceptual model of the NGLA system, demonstrating the presence of both conduit and diffuse flow pathways and spatial variability in the extent to which the freshwater lens interacts with underlying seawater. The sensitivity of the freshwater lens, as demonstrated by our results, points to the vulnerability of groundwater resources to changes in recharge associated with climate change and land use change and increases in population.

Keywords: Vadose Zone, Phreatic Zone, Tropical, Groundwater Geochemistry, Groundwater Isotopes

SHP
ECG

CONTINUOUS SPECTRUM OF SEDIMENT-DENSITY FLOW DEPOSITS OBSERVED ALONG COARSE-GRAINED, MEDIUM-SIZED BASIN MARGIN CLINOFORMS, JURASSIC NEUQUE?N BASIN, ARGENTINA

Yuqian Gan
Gan, Y., Jackson School of Geosciences, The University of Texas at Austin, Austin, TX
Steel, R., Jackson School of Geosciences, The University of Texas at Austin, Austin, TX
Olariu, C., Jackson School of Geosciences, The University of Texas at Austin, Austin, TX
Carvajal, C., Monterey Bay Aquarium Research Institute, Moss Landing, CA
De Almeida Jr., F., Instituto de Geocie?ncias, Universidade Estadual de Campinas, Brazil

Sedimentary density flow transformations and associated deposits are key elements in basin margin construction, however, while basin margin clinoforms are usually visible in seismic sections, detailed analysis of sedimentary facies and stratigraphic architecture of sediment density flows is only available from outcrops. Cliniforms (300 m high) from the southern Jurassic Neuque?n Basin, Argentina (La Jardinera area) show a well-exposed shelf to deepwater succession from the fluvial and shelfal areas to the upper slope, lower slope and basin floor, and provide a unique opportunity to study both seismic scale clinoforms and millimeter-scale sediment density flow transformation deposits that have accumulated on and bypassed the clinoform. Upper-slope conglomerate and coarse-grained sandstone facies are found in incised canyons kilometers long and a hundred meters thick, showing the characteristics of sandy debrites and high-density turbidites with poor sorting and occasional inverse grading. Lowerslope channels are one order of magnitude smaller than the upper-slope canyons, and are filled with amalgamated, tabular bedded, fine to medium-grained, normally-graded low-density turbidity deposits. Pebble-sized conglomeratic debrite and coarse-grained high-density turbidite sandstone re-occur in the basin floor fan deposits, and in ‘channel-lobe transition zone’. The described facies of sediment density flow deposits and deepwater element architecture strongly point to multiple flow transformations across the shelf margin, and various mechanisms controlling sediment bypass and basin margin evolution. The sediment delivered to the slope channels was supplied by a periodically flooding, gravel-sand mixed river-delta system across a narrow (< 40 km) shelf. The river derived coarse-grained sediments delivered to the shelf break became sandy debrites and high-density turbidites within upper slope canyons, possibly due to the high sediment-concentration during river flooding and/or shelf margin collapse after deposition at the shelf edge. The low-density turbidite forming the lower-slope channel fills may be the result of the transformation of upper-slope coarse-grained sediment density flows into low density turbidites due to (1) gradual deposition and increasing ambient water entrainment, or (2) reworking by turbidity currents of unconsolidated coarse-grained deposits on the upper slope. Either way, the two flow transition mechanisms partition coarse grains to the upper slope channels and finer grains to the lower slope, and both mechanisms contribute to construction of the shelf margin slope. In contrast, the presence of conglomerate and coarse- grained sandstone facies on the basin floor suggests high rates of sediment bypass of the slope and deposition due to gradient reduction and flow deceleration, thus building the bottomset of the basin margin clinoform. Some of the coarse-grained deposits in the channel-lobe transition zone are associated with significant soft sediment deformation (e.g. meter-scale flames) of the underlying sandy substrate; similar facies elsewhere have been linked to hydraulic jump in turbidity currents signaling another flow transformation triggered by gradient decrease on the basin floor. Thus clinoforms of the La Jardinera area of southern Neuque?n Basin provide key facies resolution to characterize a broad spectrum of sediment density flow deposits, and thus discern possible flow transformations involved in the construction of shelf margins and infilling of basins.

Keywords: sediment density flow, clinoform, slope channel

SHP
ECG

ON THE ORIGIN OF THE CRESTONE CRATER: LOW-LATITUDE PERIGLACIAL FEATURES IN SAN LUIS VALLEY, COLORADO

Tyler Meng
Schwans, E., Colorado School of Mines Geophysics Department
Meng, T., Colorado School of Mines Geophysics Department
Prudhomme, K., Colorado School of Mines Geophysics Department
Morgan, M., Colorado Geological Survey at Colorado School of Mines

Located just within the northern boundary of the Great Sand Dunes National Park is the Crestone Crater, an elliptical feature consisting of a raised rim surrounding a central depression. The elongate Crater has an approximate diameter of 100 meters and reaches a depth of 10 meters at its center relative to its rim. Its origin is largely unknown and has perplexed regional geologists and residents of Crestone, Colorado for more than 80 years. This project used on-site and remote geophysical methods to characterize the processes that led to the geomorphologic surface expression observed today. Formation hypotheses examined encompass extraterrestrial, eolian, and periglacial processes. Field methods utilized include a gravity survey and further analysis of gravity data collected by a previous student investigation of the Crater. Additionally, a recent LiDAR dataset spanning the San Luis Valley was employed to remotely analyze the main feature, similar features in the area, and surrounding eolian and alluvial surfaces. An extraterrestrial origin was deemed unlikely due to the non-unique gravity signature of the Crater, and its topographic similarity to other terrestrial depressions identified in the valley. Furthermore, the expression of known eolian features in the valley indicates that eolian processes alone would not produce such a prominent feature in the level of vegetation observed. Proximal glacial deposits in the Sangre de Cristo range show that windblown sand in which these features are clustered is adjacent to areas of past glaciation, and thus would have been affected by freeze-thaw cycles. It was concluded with a high degree of certainty that Crestone Crater and similar features nearby are relic collapsed hydraulic pingos formed during Pleistocene periglacial activity, providing further insight into periglacial features at low latitudes while demonstrating the value of LiDAR analysis of small geologic features on a regional scale.

Keywords: periglacial

SHP
ECG

Quantifying seasonal dynamic water storage in a fractured bedrock vadose zone with borehole Nuclear Magnetic Resonance

Logan Schmidt
Schmidt, L., The University of Texas at Austin, Austin, TX
Minton, B., The University of Texas at Austin, Austin, TX
Kerans, S., The University of Texas at Austin, Austin, TX
Rempe, D., The University of Texas at Austin, Austin, TX
Hiedari, Z., The University of Texas at Austin, Austin, TX

In many uplands landscapes, water is transiently stored in the weathered and fractured bedrock that underlies soils. The timing and spatial pattern of this “rock moisture” has strong implications for ecological and biogeochemical processes that influence global cycling of water and solutes. However, available technologies for direct monitoring of rock moisture are limited. Here, we quantify temporal and spatial changes in rock moisture at the field scale across thick (up to 20 m) fractured vadose zone profiles using a novel narrow diameter borehole nuclear magnetic resonance system (BNMR). Successive BNMR surveys were performed using the Vista Clara Inc. Dart system in a network of boreholes within two steep, intensively hydrologically monitored hillslopes associated with the Eel River Critical Zone Observatory (ERCZO) in Northern California. BNMR data showed agreement with estimates of the temporal and spatial pattern of rock moisture depletion over the dry season via downhole neutron and gamma density surveys, as well as permanently installed continuous time domain reflectometry. Observable shifts in the BNMR-derived T2 distribution over time provide a direct measure of changes in the amount of water held within different pore sizes (large vs. small) in fractured rock. Analysis of both BNMR and laboratory-scale NMR (using a 2MHz benchtop NMR spectrometer) measurements of ERCZO core samples at variable saturation suggest that rock moisture changes associated with summer depletion occur within both large (fracture) and small (matrix) pore sizes. Collectively, our multi-method field- and laboratory- scale measurements highlight the potential for BNMR to improve quantification of rock moisture storage for better understanding of the biogeochemical and ecohydrological implications of rock moisture circulation in the Critical Zone.

Keywords: hydrology, geophysics, well logging, vadose zone

SHP
ECG

Impact of spring-associated riparian vegetation on channel morphology in ephemeral dryland channels: Henry Mountains, Utah, USA

Paul Southard
Southard, P., Department of Geosciences, The University of Texas at Austin, Austin, TX
Johnson, J., Department of Geosciences, The University of Texas at Austin, Austin, TX
Matheny, A., Department of Geosciences, The University of Texas at Austin, Austin, TX
Rempe, D., Department of Geosciences, The University of Texas at Austin, Austin, TX

Riparian vegetation has been shown to have an important effect on channel morphology and in-channel sediment distribution via its influence on hydraulics and sediment dynamics. In order to isolate the impact vegetation has on channel morphology, single channels that are variably vegetated along their length are desirable for study, because it can be assumed that flow conditions and long-term sediment flux experience minimal change between major tributaries. Dryland channels with ephemeral runoff that are dotted with small low-discharge springs provide an excellent natural laboratory to effectively distinguish riparian vegetation as a variable and examine how it affects channel evolution. Field observations from Henry Mountains, Utah, USA from October, 2017 document channel morphology styles in spring-fed reaches that are distinct from those in sparsely-vegetated dry reaches. The presence of dense vegetation, notably grassy mats and reeds, seems to produce more uniform cross-sectional shape with narrow, deeply incised channels supported by intense rooting on banks, and a longitudinal profile that is characterized by frequent vegetation-supported, non-bedrock knickpoints. Analysis of two NCALM lidar datasets for this region, along with USGS 10 meter DEM's, provides an opportunity to gauge how suitable data with this resolution and capture method is for this study, magnitudes of distinct morphological characteristics, and whether there is a clear correlation between magnitude and quantitative metrics of vegetation density from LiDAR and remote sensing.

Keywords: Riparian, morphology, vegetation, LiDAR, knickpoints

LCMS

Energy Transition in the Balearic Islands, Spain

Henar Rabadan Perucha
Rabadan, H., Energy and Earth Resources program, The University of Texas at Austin, Austin, TX

Island, a piece of land surrounded by water, too remote to be supplied, too beautiful to be exploited. Islands distributed worldwide suffer the same global pressures as any other territory but are aggravated by their own particular constraints. The supply of energy to islands is no exception. Thus, for the purpose of my research, I will focus on energy resource evaluation and scenario analysis to facilitate the supply of energy to islands while preserving the islands' pristine nature. Although this methodology can be applied to any region worldwide, I will analyze the case of the Balearic Islands.

The extreme dependence on fossil fuels to satisfy the electricity demand of this archipelago, mainly 50% oil, 22% coal, and 19% natural gas, have devastating repercussions on energy security (93.5% coal, 99.7% oil, and 99.8% natural gas imported). Moreover, this also slows down the region's recovery from the 2008 economic crisis. Lastly, pollution and climate change are growing concerns among the population since this archipelago is a natural reserve.

In terms of legislation, European Union directives establish energy and climate change goals to its Member States for 2020 and 2030. These directives define targets of energy consumption supplied by renewable energies, transportation fueled by renewable resources, greenhouse gas emissions, and energy efficiency levels. In order to reach these goals, the Spanish government created the Plan de Energi?as Renovables, which reflects European percentages as minimum values and facilitates the integration of renewables in all the Comunidades Autonomas (counties). From the regional point of view, Plan Director Sectorial Energe?tico de las Islas Baleares has been modified to provide the needed urban planning directions for the development of renewable energy sources on these islands.

In order to (1) meet this regulation regionally, (2) increase the quality of life in this territory, and (3) soften the growing global energy demand, the goal of my research is to consider all the current and potential energy resources in the Balearic archipelago (including resources proposed by the EU, the national and regional governments, and the author recommendations). In the next step, I will evaluate their technical viability

and related environmental and legislative limitations. Once the viable energy resources are determined, different combinations of these technologies will be analyzed from the economic, social, and environmental perspectives. My conclusions will focus on the comparison of the different scenarios and how they would benefit the population of the Balearic Islands and the world.

References

Red Ele?ctrica de Espan?a 2016. El sistema ele?ctrico espan?ol Informe 2016. Red Ele?ctrica de Espan?a publications.

European Union 2009. Official Journal of the European Union, European Directive 2009/28/EC.

Instituto para la Diversificacio?n y Ahorro de la Energi?a 2011. Plan de Energi?as Renovables 2011-2020. Madrid: Gobierno de Espan?a publications.

Gobierno de las Islas Baleares 2015. Plan Director Sectorial Energe?tico de las Illes Balears. Palma: Boleti?n Oficial de las Islas Baleares.

Keywords: Energy transition, Balearic Islands, Spain, Renewables

LCMS

Late Paleozoic Provenance and Sediment Routing in the Southern Delaware Basin, West Texas

Graham Soto-Kerans
Soto-Kerans, G., Bureau of Economic Geology, The University of Texas at Austin, Austin, TX
Stockli, D., Department of Geological Sciences, Jackson School of Geosciences, The University of Texas at Austin, Austin, TX
Covault, J., Bureau of Economic Geology, The University of Texas at Austin, Austin, TX
Janson, X., Bureau of Economic Geology, The University of Texas at Austin, Austin, TX
Stockli, L., Department of Geological Sciences, Jackson School of Geosciences, The University of Texas at Austin, Austin, TX

Classic sediment provenance studies, including petrography or heavy minerals analysis, of foreland basin deposits has long been employed to constrain sediment sourcing and supply. More recently, the advent of isotopic provenance data, especially detrital zircon (DZ) U-Pb, has started to provide critical and detailed process-oriented insights into the dynamic and temporal linkages between basin formation, hinterland tectonics and unroofing, sediment routing, drainage reorganization, and basin subsidence as well as the basin fill history. However, due to complications, such as multi-cycle sediment recycling, stratal cannibalization or ambiguous hinterland source DZ signatures, successful provenance interpretations in collisional tectonics settings require meticulous inspection and differentiation of data arrays. Integration of DZ U-Pb ages with depositional systems analysis and petrography can contribute to a more comprehensive understanding of sediment provenance and the dynamic hinterland-basin linkages. The late Paleozoic Permian Basin in west Texas is a prolific hydrocarbon basin. Its tectonic formation and basin fill evolution remain controversial, but are overall associated with the Ouachita-Marathon orogeny along the SW US margin of Laurentia. Given the potential spatial and temporal complexities in basin evolution and the applied implications for hydrocarbon exploration make the Permian basin an extremely interesting candidate for a regional foreland basin case study.

This study presents 1983 new DZ U-Pb ages from eleven turbiditic and conglomeratic sandstones from a stratigraphic section in the southern Delaware Basin, spanning Mississippian to Guadalupian strata and the entire time interval from pre-, syn-, to post-collisional deposition. This stratigraphic section captures the evolution of the southern Delaware Basin from Mississippian flysch deposition, syn-orogenic Wolfcamp aggradation in the Marathon foredeep through shelf-margin flooding and backstepping during the Leonardian and subsequent strong progradation of the following Guadalupian section. Complexities in provenance have hindered tectonostratigraphic interpretations of the southern margin of the Permian Basin. Depth-profile LA-ICP-MS of individual zircon grains to recover core-rim age domains was employed to further resolve ambiguities in detrital provenance, effectively enhancing probable and possible source terranes These new results show a dramatic change in DZ U-Pb age signature from the Mississippian Tesnus Formation that is dominated by Grenville ages and completely lacks Neoproterozoic ages to increasing Paleozoic and Neoproterozoic age modes during the late Pennsylvanian and into the Guadalupian. This trend indicates tectonostratigraphic evolution of the Marathon fold and thrust belt (FTB) and progressive unroofing of Neoproterozoic volcanics from the inverted distal Laurentian margin, early Paleozoic passive-margin strata and accreted Peri-Gondwanan terranes followed by unroofing and tapping of Gondwanan source terranes deeper in the hinterland during post-orogenic times. Core-rim U-Pb age relationships fall into eight clusters, corresponding to distinct provinces of Laurentian, Peri-Gondwanan, Grenville, Pan-African, and Amazonian sediment source areas. These clusters convincingly corroborate a dominant southern source for sediment input into the southern Delaware Basin during the Mississippian to Guadalupian. These combined observations suggest that presence of proximal high-relief areas, generated by the Ouachita-Marathon orogeny, dominated the sediment fill history of the Mississippian to Guadalupian southern Delaware Basin and that axial input along the Alleghenian-Ouchita foredeep was likely minimal. This study dictates new constraints on sediment provenance in the southern Delaware Basin, and exhibits a possible analogue for sediment dispersal confinement, tectonostratigraphic reconstruction of complex collisional packages, and unroofing patterns in a

foreland basin system.

Keywords: provenance, sediment routing, permian basin, detrital zircon, geochronology

CCG
LCMS

Soil gas dynamics and microbial activity in the unsaturated zone of a regulated river

Heather Christensen
Christensen, H., Geological Sciences, The University of Texas at Austin, Austin, TX
Ferencz, S., Geological Sciences, The University of Texas at Austin, Austin, TX
Cardenas, M., Geological Sciences, The University of Texas at Austin, Austin, TX
Neilson, B., Utah Water Research Laboratory, Civil and Environmental Engineering, Utah State University, Logan, Utah
Bennett, P., Geological Sciences, The University of Texas at Austin, Austin, TX

Over 60% of the world's rivers are dammed, and are therefore regulated. In some river systems, river regulation is the dominant factor governing fluid exchange and soil gas dynamics in the hyporheic region and overlying unsaturated zone of the river banks. Where this is the case, it is important to understand the effects that an artificially-induced change in river stage can have on the chemical, plant, and microbial components of the unsaturated zone. Daily releases from an upstream dam cause rapid stage fluctuations in the Lower Colorado River east of Austin, Texas. For this study, we utilized an array of water and gas wells along a transect perpendicular to the river to investigate the biogeochemical process occurring in this mixing zone. The gas wells were installed at several depths up to 1 meter, and facilitated the continuous monitoring of soil gases as the pulse percolated through the river bank. Water samples collected from the screened wells penetrated to depths below the water table and were analyzed for nutrients, carbon, and major ions. Additionally, two soil cores were taken at different distances from the river and analyzed for soil moisture and grain size. These cores were also analyzed for microbial activity using the total heterotroph count method and the acetylene inhibition technique, a sensitive method of measuring denitrifying activity. The results provide a detailed picture of soil gas flux and biogeochemical processes in the bank environment in a regulated river. Previous work found that meter-scale changes in river stage propagate through the bank as significant fluctuations to the water table. We propose that these conditions create an area in the subsurface that is subjected to daily cycles of saturation and drying, supporting enhanced microbial oxidation of soil organic matter. Measured soil CO_2 exhibited periodic variations with the fluctuating water table, with most peak values occurring during water table drawdown. Along the transect CO_2 concentrations increased with increasing depth down to the water table, and decreased with increasing distance away from the river.

Keywords: Water table fluctuations, Soil gas, Microbial respiration

EG
LCMS

Missing well log data interpolation and semiautomatic seismic well ties using data matching techniques

Sean Bader
Bader, S., Bureau of Economic Geology, The University of Texas at Austin
Wu, X., Bureau of Economic Geology, The University of Texas at Austin
Fomel, S., Bureau of Economic Geology, The University of Texas at Austin

Relating well log data, measured in depth, to seismic data, measured in time, involves estimating well log impedance and a time to depth relationship using available sonic and density logs. When sonic and density logs are available, the seismic to well tie typically involves a subjective, labor-intense, workflow that depends on the interpreter's experience and intuition. The problem is worsened when sonic and density logs are not available as it is challenging to incorporate wells into integrated reservoir studies that cannot be tied to seismic. We propose an approach that estimates missing well log information, automatically ties wells to seismic data and generates a global log property volume using data matching techniques. We first use local similarity to align all logs to constant geologic time and interpolate missing well log information. Local similarity is then used to tie available wells with seismic data. Log data from each well is interpolated along the local seismic structure to generate global log property volumes. The accuracy of seismic well ties is tested using blind well tests. We apply this workflow to a 3D seismic dataset with 26 wells and achieve consistent and verifiably accurate seismic well ties.

Keywords: well log, seismic, well tie, interpolation, data integration

EG
LCMS

Wolfcampian carbonate platform sequence stratigraphy of the Wylie Mountains, Van Horn, TX: Implications for a platform to basin Wolfcamp framework

Taylor Canada
Canada, T., University of Texas at Austin
Kerans, C., University of Texas at Austin
Zahm, C., BEG, University of Texas at Austin

The Wolfcamp unconventional play in the Permian Basin is currently one of the most active drilling targets in North America. Despite this interest, the Wolfcampian strata in the Delaware Basin lack a detailed platform-to-basin sequence stratigraphic model. In recent years, access to Wolfcampian age carbonate platforms in West Texas has been restricted, though a nearly complete platform record in the Wylie Mountains near Van Horn, TX has recently become available for study. This study documents the development of the Hueco Wolfcampian carbonate platform on the western margin of the Delaware Basin and syntectonic controls on deposition during the waning stages of the Marathon-Ouachita orogeny. Eleven measured sections and two 3D drone models have been used to characterize the sequence development of the Hueco Formation using the framework established by Fitchen (1995) and Playton and Kerans (2002) in the Sierra Diablo Mountains 20 miles northwest of the study area.

The Wolfcampian Hueco Group includes the siliciclastic Pow Wow Formation at the base and 300 meters of platform interior carbonates. The Hueco Formation carbonates are comprised of three upward shallowing sequences with fossiliferous skeletal and peloidal assemblages capped by dolomitic algal laminite capped cycles. These sequences roughly correlate with the platform margin and slope deposits in the Sierra Diablo Mountains with some variability due to local structural features and variable degrees of erosion at the Wolfcamp-Leonard unconformity. The Wolfcamp-Leonard unconformity in the Wylie Mountains is marked by an influx of conglomerates and siltstones associated with a drop in sea level at the end of Wolfcampian time. This clastic pulse, as well as the Pow Wow Formation clastics at the base of the Hueco, may have clastic basinal equivalents that can be used to tie the platform sequence stratigraphy to the subsurface Wolfcamp with log and core data. Linking the Wolfcampian platforms to their basinal equivalents may assist in predicting the composition and frequency of siliciclastic and detrital carbonate influx to the basin with implications for improved reservoir quality in those intervals.

Keywords: Carbonates, Sedimentology, Outcrop, Wolfcamp

EG
LCMS

Influence of shear and mean stress on pore pressure prediction at the Mad Dog Field, Gulf of Mexico

Landon Lockhart
Flemings, P., The University of Texas at Austin, Austin, TX
Nikolinakou, M., The University of Texas at Austin, Austin, TX
Heidari, M., The University of Texas at Austin, Austin, TX

We present a new method to predict pore pressure that couples velocity with the full stress tensor and quantify the amount of pressure induced by both non-uniaxial vs. uniaxial mean and deviatoric (shear) stresses. We evaluate our results against the mean effective stress (MES) and the traditional vertical effective stress (VES) approaches at the Mad Dog Field, Gulf of Mexico, which is associated with a large salt body. Because of loading from the salt, stresses are not uniaxial; the fraction of horizontal to vertical stress (K_0), which is constant in uniaxial basins, changes around the salt body. This leads to either an elevation or a reduction in mean and/or shear stress relative to the far field where wells are typically calibrated. Both the MES and the traditional VES approaches can only account for mean and shear stresses that are proportional to the vertical stress (through K_0). In contrast, we couple velocities with geomechanical modeling and develop a workflow that predicts pore pressure for any stress state. Our workflow closely predicts the measured pressures below salt, whereas the traditional method under-predicts pressures up to 1.5 ppg. We show that accounting for the mean stress drives this improvement. We also closely predict pressure in front of the salt where shear is elevated; in contrast, the traditional method under-predicts by as much as 1.4 ppg. Overall, our methodology and results predict pressures that more closely match the observed, and show that pore pressure is driven by a combination of mean stress and shear stress. Furthermore, the impact of our study extends beyond salt bodies; our methodology can improve pressure prediction in geological environments where the stress state is not uniaxial, such as anticlines, synclines, continental margins or thrust belts.

Keywords: Pore pressure prediction, geomechanics

MG
LCMS

Systematic Lithologic Calibration of Seismic Character of Neogene Mass-Transport Deposits in Mississippi Canyon of the Northern Gulf of Mexico, USA.

Mario Gutierrez
Gutierrez, M., Institute For Geophysics, The University of Texas at Austin, Austin, TX
Snedden, J., Institute For Geophysics, The University of Texas at Austin, Austin, TX

Few publications have attempted detailed lithologic calibration of Mass Transport Deposits, usually as a byproduct of mud log descriptions. While the principal motivation for further understanding these slope failure deposits are driven by the economics of deep-water hydrocarbon exploration, the geohazard-related risks of storm-wave loading, and the shallow gas, also provide a driving concern for these deposits. Such risks can be mitigated and prevented by in-depth analysis of slope stability and failure. The Mississippi Canyon of the Northern Gulf of Mexico is one of the few basins to contain enough available density of seismic and well data to provide a well-constrained lithologic characterization throughout a MTD–rich continental margin.

The proposed hypothesis evaluates: 1) the differences between attached and detached MTDs in the Neogene Northern Gulf of Mexico through seismic characterization and well log analysis, 2) variations of MTD dimensions and map geometries in relation to depositional age throughout the northeastern and northcentral Gulf of Mexico, and 3) the differentiation between sand-prone and shale-prone MTD's in relation to associated depositional mechanisms. This study will attempt lithologic calibration of MTDs in Pleistocene –Miocene strata of the study area through integration of seismic observations (focused in supra-salt basins, which have the highest seismic data quality) and lithologic related information extracted from logs, mud logs (cuttings), and available core data to further constrain the distribution of MTD types, lithology, and geometries.

Initial interpretations reflect a variance of seismic character responses to the presence of sandstone and shale (constrained by wells) throughout different regions and salt tectonic domains of the MTD geobodies. Further analysis will relate different seismic facies throughout MTDs to improve the understanding of seismic character and related lithologic facies throughout the deposits, in addition to also constraining the potential reservoir quality and seal integrity uncertainties of selected MTDs. Additionally, this approach can stand as an analog to other similar areas with much less well control, such as the southern Gulf of Mexico.

Keywords: deepwater, Gulf of Mexico, Mass Transport Deposit, Seismic

PS
LCMS

Geochronological Constraints on the Timing of Proposed Ordovician Meteorite Event Impact Structures in North America

Andrew Parisi
Parisi, A., Jackson School of Geosciences, The University of Texas at Austin
Catlos, E., Jackson School of Geosciences, The University of Texas at Austin

The Earth experienced a drastic increase in the number of meteorite impacts following the breakup of the L-Chondrite Parent Body in the Mid-Ordovician. This bombardment, the Ordovician Meteorite Event (OME), has been confirmed from impact structures or meteoritic debris in Sweden, Russia and China. Yet despite the long lasting and global nature of this event, no OME evidence has been confirmed in the Western Hemisphere.

In North America, there are a series of impact structures which are speculated to have formed during the OME. These structures have been tentatively dated to the mid-Ordovician. The ages of these structures have been constrained based on stratigraphic and biostratigraphic evidence, but accurate, absolute, ages have proven difficult to determine.

This project will attempt to determine the formation age of two of those impact structures. The Ames Astrobleme (OK, USA) and Slate Islands Archipelago (ON, Canada) were chosen due to previous work and the ease of accessing impact generated material. The Ames Astrobleme is a buried complex impact structure centered on the town of Ames, Oklahoma; numerous core samples have been extracted from the structure due to its oil producing nature. The Slate Islands are an archipelago near Terrace Bay, Ontario, and are thought to be the eroded central uplift peak of ancient asteroid crater. Impact related material (suevites, melt glass and brecciated target rock) were collected from each impact site on two separate occasions.

To determine the age of the craters, shock metamorphosed minerals were dated via thermochronological techniques. Shocked zircon crystals were separated from whole rock samples and dated via U/Pb analysis at the Jackson School of Geosciences. When plotted on a concordia diagram, the data reveals the cooling history of the target rocks and the most recent heating event. However, in the case of both impact structures, the data is providing unexpected conclusions. The current data suggests the rocks underwent heating events outside the established stratigraphic age of the structures, which also do not correspond to any known regional tectonic activity. Continuing work is being performed to determine the source of these discrepancies.

Keywords: Asteroid Impact, Geochronology, Ordovician

SETP
LCMS

3D Textural and Geochemical Analyses on Carbonado Diamond: Insights from Pores and the Minerals within Them

Scott Eckley
Eckley, S., Department of Geological Sciences, Jackson School of Geosciences, The University of Texas at Austin
Ketcham, R., Department of Geological Sciences, Jackson School of Geosciences, The University of Texas at Austin

Carbonado is an enigmatic variety of polycrystalline diamond found only in placer deposits and Proterozoic metaconglomerates in Brazil and the Central African Republic with unknown primary origin. These highly porous black nodules possess a narrow range of isotopically light carbon ($\delta^{13}C$ -31 to -24 ‰), a primarily crustal inclusion suite unusually enriched in REEs and actinides filling the pore spaces, a crystallization age from 2.6 to 3.8 Ga, and other atypical features which have led to a variety of formation theories from extra-solar to deep mantle.

We have completed the first multi-sample 3D textural analysis on nine carbonados using high resolution X-ray CT (XCT) and bulk-sample geochemical work. We have documented a variety of textures in both pore structure and mineralogy within pores. All pore textures feature a preferred orientation. Spatial coherence in pore fillings in some specimens suggest that secondary minerals formed by in-situ breakdown of primary inclusion phases. This, combined with the presence of pseudomorphs, support the hypothesis that elements comprising the secondary minerals within the pore spaces are actually primary.

To provide further context for our observed pore fabrics, we also analyzed a framesite, a less porous polycrystalline diamond found in kimberlites thought to crystallize shortly before eruption. Both diamond varieties have bladed/elongated pores forming a foliation with a moderate lineation. The similarity in fabrics suggests a similar process could have formed both carbonados and framesites.

Step-leaching and ICP analysis on three African and two Brazilian samples was performed to measure incompatible element concentrations. Periodic XCT imaging allowed us to trace leaching progress and effectiveness. Not only is the modern-day inclusion suite highly enriched in REE (Average ΣREE = 2,359 ppm), but its REE pattern matches that of kimberlite. This suggests a genetic origin may exist between carbonado and kimberlite.

These data can shed light on the origin and constrain the age of carbonado, which may have far-reaching implications on the timing, origin, and mobility of light-carbon fluids in the mantle, early Earth's redox conditions, and the nature of a crystallization environment that can concentrate highly incompatible elements.

Keywords: Carbonado Diamond, X-ray Computed Tomography, ICP-MS, Mantle Geochemistry

SETP
LCMS

Geo-Thermochronometric Insights on the Formation of the Ios Metamorphic Core Complex, Southern Cyclades, Greece

Megan Flansburg
Flansburg, M., The University of Texas at Austin, Austin, TX
Poulaki, E., The University of Texas at Austin, Austin, TX
Stockli, D., The University of Texas at Austin, Austin, TX
Soukis, K., National and Kapodistrian University of Athens, Athens, Greece

The North Cycladic, West Cycladic, and Naxos-Paros Detachment Systems accommodated large-scale Oligo-Miocene exhumation in the backarc of the retreating Hellenic subduction zone. While bivergent detachment faults in the northern and western Cyclades are either contained within the Cycladic Blueschist Unit (CBU) or at the CBU-Upper Unit interface, the sheared contact between the CBU and the underlying Cycladic Basement in the southern Cyclades (Ios) has been debated for over 30 years, largely due to the ambiguous coexistence of both top-to-the-N and top-to-the-S shear sense indicators and a lack of robust timing information. Reliable chronostratigraphic and thermal history constraints allow us to ascertain the nature of the CBU/Basement contact. Zircon U-Pb dating for the granitic Basement core of Ios gave Carboniferous-Permian age and shows that surrounding Basement metasedimentary units can be divided into two groups based on detrital zircon signatures and provides insights on Carboniferous-Permian paleogeography. An older group of metasedimentary rocks have maximum depositional ages (MDAs) ranging from ~580 Ma to 354 Ma and predate the intrusions, and late Permian Basement paragneisses are younger than the intrusions and likely originally deposited unconformably on the older units. Samples from the CBU in northern Ios yielded MDAs ranging from Mid-Jurassic to Late Cretaceous and occur in repeated section due to thrusting and subduction accretion. MDA data from mapped CBU at the southern end of Ios yielded Ordovician to Permian ages, calling into question their assignment as CBU, while also revealing older over younger relationships. Zircon (U-Th)/He ages for the Basement and the CBU on Ios are ~9-14 Ma, young down-dip both north and south of the metamorphic dome, and do not exhibit any differential cooling across their contact--suggesting that they were juxtaposed prior to Miocene detachment faulting and exhumed in response to non-exposed top-to-the-N and top-to-the-S detachment faulting in north and south Ios, respectively. This is supported by the fact that both units experienced Eocene subduction metamorphism as evidenced by 60-45 Ma metamorphic zircon rims. Interestingly, apatite U-Pb ages for the Cycladic Basement are ~290-300 Ma, and therefore were not reset during Eocene subduction, suggesting subduction temperatures could not have exceeded ~400°C.

Keywords: detachment faulting, metamorphic core complex, Cyclades, Aegean Sea, Hellenic Subduction Zone, geochronometry, low-temperature thermochronometry

SETP
LCMS

PROVENANCE AND GEOCHRONOLOGICAL INSIGHTS INTO LATE CRETACEOUS-PALEOGENE FORELAND BASIN DEVELOPMENT IN THE SUBANDEAN ZONE AND ORIENTE BASIN OF ECUADOR

Evelin Gutiérrez
Gutierrez, E., Department of Geological Sciences and Institute for Geophysics, Jackson School of Geosciences, University of Texas at Austin, Austin, TX 78712
Horton, B., Department of Geological Sciences and Institute for Geophysics, Jackson School of Geosciences, University of Texas at Austin, Austin, TX 78712
Vallejo, C., Departamento de Geología, Escuela Politécnica Nacional, Ladrón de Guevara E11-253, Quito, 170605, Ecuador
Jackson, L., Department of Geological Sciences and Institute for Geophysics, Jackson School of Geosciences, University of Texas at Austin, Austin, TX 78712

The tectonic history of the Oriente foreland basin and adjacent Subandean Zone of Ecuador during contractional mountain building in the northern Andes can be revealed through integrated stratigraphic, geochronological, structural, and provenance analyses of clastic sediments deposited during orogenesis. We present new maximum depositional ages and a comprehensive provenance analysis for key stratigraphic units deposited in the western (proximal) Oriente Basin. Detrital zircon U-Pb ages were obtained from Upper Cretaceous and Cenozoic clastic formations from exposures in the Subandean Zone.
The sampled stratigraphic intervals span critical timeframes during orogenesis in the Ecuadorian Andes. Cenozoic formations have poorly defined chronostratigraphic relationships and are therefore a primary target of this study. In addition, the newly acquired U-Pb age spectra allow clear identification of the various sediment source regions that fed the system during distinct depositional phases.
Maximum depositional ages (MDA) were obtained for five samples from three formations: the Tena (MDA=69.6 Ma), Chalcana (MDA=29.3 Ma), and Arajuno (MDA= 17.1, 14.2, 12.8 Ma) Formations, placing them in the Maastrichtian, early Oligocene, and early-middle Miocene, respectively. Detrital zircon U-Pb ages identify clear signatures of at least four different sources: craton (1600-1300 Ma, 1250-900 Ma), Eastern Cordillera fold-thrust belt (600-450 Ma, 250-145 Ma), Western Cordillera magmatic arc (<88 Ma), and recycling of cratonic material from the Eastern Cordillera.
The U-Pb age spectra of the Upper Cretaceous-Paleogene type sections allow us to recognize variations in the contribution of each recognized source over time. We identify recycled material with two dominant peak ages (1250-900 Ma and 600-450 Ma), material derived from the adjacent uplifted orogen or recycled from foredeep sediments incorporated into the deforming wedge. Finally, an apparent unroofing event is inferred from a 250-145 Ma age peak in the Plio-Pleistocene Mesa-Mera Formation revealing the persistent shortening deformation influencing the structural configuration and sediment dispersal patterns of the Oriente Basin and Subandean Zone.

Keywords: Foreland, Geochronology, Provenance, Ecuador

SETP
LCMS

Unravelling the Formation and Exhumation of the Cycladic Blueschist Unit and Basement in the Southern Aegean, Sikinos and Ios Islands, Greece

Eirini Poulaki
Poulaki, E., Department of Geological Sciences, The University of Texas at Austin, Austin, TX
Flansburg, M., Department of Geological Sciences, The University of Texas at Austin, Austin, TX
Stockli, D., Department of Geological Sciences, The University of Texas at Austin, Austin, TX
Soukis, K., National and Kapodistrian University of Athens

The Cycladic Islands of Greece expose an assemblage of HP/LT metamorphic rocks that record both processes related to subduction and back-arc metamorphic core complex formation in the wake of the Hellenic subduction zone retreat. Sikinos and Ios Islands are located in the southern Cyclades and expose both the Cycladic Blueschist Unit (CBU) - greenschist-facies marbles and schists with preserved blueschist-facies - and the tectonically underlying Cycladic Basement (CB) - felsic plutonic rocks and metasedimentary country rocks known as the Carapace. Both units experienced Eocene subduction under eclogite/blueschist facies conditions and Miocene large-magnitude back-arc extension under greenschist facies conditions. The contact between the two units has been described as an extensional shear zone or a subduction-related thrust that was reactivated as an extensional top-to-the-N detachment.
This study presents new (1) zircon U-Pb and trace elements data to determine detrital provenance and maximum depositional ages (MDAs) of the CBU intervals, constrain protolith ages for the CB and Carapace, and quantify the timing of HP-LT metamorphism, (2) zircon (U-Th)/He cooling ages to elucidate the cooling and exhumation history of the CBU and CB in Sikinos and the nature of the contact between the two units.

Zircon U/Pb indicate that the CBU exhibits a spread of detrital zircon U-Pb ages with age modes at Triassic, Permian Carboniferous, Silurian and Proterozoic. The MDAs from Ios reveal an older over younger relationship, which can be explained by thrusting and subsequent repetition of the sequence, whereas on Sikinos there is a progression from older to younger ages. Interestingly, metamorphic rims at ~50 Ma in both CBU and Basement indicate that the two units were already juxtaposed before peak HP/LT metamorphism. Notably, zircon metamorphic rims of ~26 Ma have not been reported in the CBU of the southern Cyclades prior to this study. These rims appear to be restricted a zone along the CBU-Basement contact, suggesting fluid flow as a possible explanation. Zircon (U-Th)/He ages from CB and CBU trend from old to young towards the stretching lineation (N-S), hence the Basement and CBU were likely exhumed together (~9 to 12 Ma) due to a low-angle normal fault located north of the island.

Keywords: Greece, Blueschist, Metamorphic Core Complex, Geochronology, Thermochronology

SHP
LCMS

Quantifying alluvium effects on karst aquifer recharge in the upper Nueces River, Texas

Caroline Hackett
Hackett, C., Jackson School of Geosciences, The University of Texas at Austin, Austin, TX
Gary, M., Jackson School of Geosciences, The University of Texas at Austin, Austin, TX
Rempe, D., Jackson School of Geosciences, The University of Texas at Austin, Austin, TX

The Edwards and Trinity aquifers are crucial resources in south-central Texas, with the former serving as the primary water source for over 2 million people in the greater San Antonio area. The Nueces River basin is the largest contributor of recharge to the Edwards Aquifer, and recent studies suggest that areas in the Edwards Contributing Zone supply autogenic and allogenic recharge, with inter-aquifer flow possible. Alluvium mantled over the karstic Glen Rose limestone in the upper Nueces floodplain provides significant storage of river underflow and shallow groundwater, which become an important source of river discharge in low flow conditions and thus recharge to the Edwards and Trinity aquifers. To quantify the role of transient floodplain storage on recharge, we study Candelaria Creek, a spring-fed gaining stream and major tributary to the Nueces. Candelaria Creek flows around 30 cfs year-round (contributing up to 70% of river flow during drought conditions), while Nueces River discharge decreases by 50-80% upstream of the creek confluence. Fluorescent dye tracer testing suggests subsurface velocities greater than 300 m/day through alluvial gravel deposits or karst conduits between the Nueces and Candelaria. Analyses of radon and strontium concentrations and conductivity permit us to constrain the velocities and residence times of springflow, streamflow, and regional groundwater. Geophysical surveys across the study site, including electrical resistivity, ground penetrating radar, and electromagnetic surveys, allow us to quantify alluvium thickness and thus the potential volume of dynamic floodplain water storage. We upscale our intensive local observations to compute a regional water balance under drought and flood conditions using distributed climate, groundwater, and streamflow measurements at the regional scale. Ultimately we quantify the role of alluvium in buffering discrete infiltration into karst features and promoting diffuse recharge.

Keywords: karst, surface water-groundwater interactions, recharge, Edwards Aquifer, alluvium

SHP
LCMS

Critical Zone structure inferred from multiscale geophysical data across hillslopes at the Eel River CZO

Shawn Lee
Lee, S., The University of Texas at Austin
Rempe, D., The University of Texas at Austin
Holbrook, S., Virginia Polytechnic Institute and State University
Schmidt, L., The University of Texas at Austin
Hahm, J., University of California, Berkeley
Dietrich, W., University of California, Berkeley

Except for boreholes and road cut, landslide, and quarry exposures, the subsurface structure of the critical zone (CZ) of weathered bedrock is relatively invisible and unmapped, yet this structure controls the short and long term fluxes of water and solutes. Non-invasive geophysical methods such as seismic refraction are widely applied to image the structure of the CZ at the hillslope scale. However, interpretations of such data are often limited due to heterogeneity and anisotropy contributed from fracturing, moisture content, and mineralogy on the seismic signal. We develop a quantitative framework for using seismic refraction data from intersecting geophysical surveys and hydrologic data obtained at the Eel River Critical Zone Observatory (ERCZO) in Northern California to help quantify the nature of subsurface structure across multiple hillslopes of varying topography in the area. To enhance our understanding of modeled velocity gradients and boundaries in relation to lithological properties, we compare layered refraction and tomography results with borehole logs of nuclear magnetic resonance (NMR), gamma and neutron density, standard penetration testing, and observation drilling logs. We then use these relations to develop a method of probabilistic lithology determination. Together, our sensitivity analyses and multi-method data comparison provide insight into the interpretation of seismic refraction and borehole logs for the quantification of CZ structure and hydrologic dynamics.

Keywords: Critical Zone, CZO, refraction, seismic, geophysics, borehole

CCG
LCPHD

Hydrologic conditions and carbon cycling dynamics recorded in the carbon-isotope variations of a near-entrance speleothem

Peter Carlson
Carlson, P., The University of Texas at Austin, Austin, TX
Banner, J., The University of Texas at Austin, Austin, TX
Breecker, D., The University of Texas at Austin, Austin, TX

Near-entrance speleothems have traditionally been avoided for stable-isotope paleoclimate reconstructions, due to concerns about kinetic isotope effects, but the typically high growth rates of speleothems in such well-ventilated cave environments can allow for precise dating of high-resolution speleothem records. At Westcave Preserve in central Texas, we use seasonal variations in speleothem calcite $\delta^{18}O$ values and [Mg] to develop a seasonally-resolved age model for a near-entrance, 20^{th}-century speleothem (WC-3). Combining this age-model with radiocarbon measurements of WC-3 and the 20^{th}-century atmospheric bomb pulse record, we determined the relative size and turnover times of three carbon pools that best reproduce the ^{14}C pulse recorded in the stalagmite. We present this 3-pool model of epikarst carbon cycling here, along with a record of $\delta^{13}C$ in WC-3 calcite. The carbon-cycling model informs our interpretations of speleothem $\delta^{13}C$, allowing us to account for decade-to-century-scale trends in atmospheric carbon as well as the effects of pCO_2-dependency of carbon isotope fractionation in plant material on stalagmite $\delta^{13}C$. We have removed these effects, and compared the resulting residual $\delta^{13}C$ record to local instrumental records (NCDC and daily onsite precipitation records). We find that the 36-month running Palmer Drought Severity Index (PDSI) explains 25% of the variation of a 3-year mean of residual $\delta^{13}C$. For most of the record, troughs in 36-month PDSI (dry periods) correspond to maxima in the running mean of residual $\delta^{13}C$. Multiple processes can explain the correspondence between aridity and higher $\delta^{13}C$. These include: 1) increases in drip intervals allowing for more degassing of CO_2 before the water reaches the stalagmite; 2) decreases in carbon isotope fractionation between plant matter and atmospheric CO_2 during periods of water stress; and 3) decreases in belowground pCO_2 and resultant increases in drip water pH pushing DIC speciation away from isotopically negative carbonic acid. We also find that the timing of higher-resolution $\delta^{13}C$ peaks varies throughout the record, with carbon isotope maxima recorded semiannually to biannually. The controls on $\delta^{13}C$ variations at this scale are likely complicated, depending on seasonal-scale variations in epikarst aridity or water residence time, the timing and magnitude of precipitation events, or local wind speed and direction.

Keywords: speleothems, paleoclimate, carbon isotopes, oxygen isotopes, trace elements,

CCG
LCPHD

The Impacts of Human-Driven Inputs on Terrestrial and Riverine Nitrogen Fluxes in the United States

Seungwon Chung
Chung, S., Department of Geological Sciences, The John A. and Katherine G. Jackson School of Geosciences, The University of Texas at Austin, Austin, TX
Yang, Z., Department of Geological Sciences, The John A. and Katherine G. Jackson School of Geosciences, The University of Texas at Austin, Austin, TX

Nitrogen (N) is important to support the demands for food and energy production of the global population, primarily through agriculture and burning fossil-fuels. Excessive reactive N in terrestrial and freshwater systems, led by human activities, is causing wide-ranging environmental problems, such as harmful algal blooms, coastal dead zones and biodiversity loss. This underscores the need to find a favorable balance of reactive N between human demands and environmental threats. Previous studies presented the quantitative descriptions of N cycling based on various approaches and data, but large uncertainties of modeled N fluxes imply that our knowledge of sources, fates and exchanges of N within and between terrestrial and freshwater ecosystems is still deficient.

This poster presents a N cycle modeling framework for integrating a terrestrial ecosystem model (i.e., Noah-MP with terrestrial C and N dynamics, called Noah-MP-CN) with a vector-based streamflow routing model (i.e. the Routing Application for Parallel computation of Discharge, RAPID) to simulate landscape and riverine N fluxes. We concentrate on the N cycling from land to the river mouth, i.e., using a state-of-the-art land surface model under the atmospheric effects to simulate terrestrial N dynamics, and connecting a routing model to describe N transport from soil to streams. We also focus on human perturbations on N cycling, as described by Net Anthropogenic Nitrogen Inputs (NANI) data for the continental U.S. in a consistent and complex manner.

The feasibility of integrating the terrestrial N dynamics with the routing model for water flow and N will be demonstrated through the operation of the developed model with 36-year atmospheric forcing and NANI. This model will be demonstrated by comparing the modeled N budgets against past studies. Riverine N fluxes will be evaluated using the observed data for nitrate concentration and streamflow. Energy, hydrology and carbon cycles will also help to range the uncertainties of this model. For example, model output for evapotranspiration, runoff and net primary production will be evaluated based on field and remote-sensing observed data. This approach will help to describe the impacts on the surface water and energy balances of using the advanced N modeling.

Keywords: Nitrogen, Riverine Flux

CCG
LCPHD

A Monte Carlo ray tracing model to improve simulations of solar-induced chlorophyll fluorescence radiative transfer

Maryia Halubok
Halubok, M., JSG, The University of Texas at Austin
Gu, L., Climate Change Science Institute, Oak Ridge National Laboratory
Yang, L., JSG, The University of Texas at Austin

A model of light transport in a three-dimensional vegetation canopy is being designed and evaluated. The model employs Monte Carlo ray tracing technique which offers simple yet rigorous approach of quantifying the photon transport in a plant canopy. This method involves simulation of a chain of scattering and absorption events incurred by a photon on its path from the light source. Implementation of weighting mechanism helps avoid 'all-or-nothing' type of interaction between a photon packet and a canopy element, i.e. at each interaction a photon packet is split into three parts, namely, reflected, transmitted and absorbed, instead of assuming complete absorption, reflection or transmission.
The performance of the model is being evaluated through comparison against established plant canopy reflectance models. This photon transport model is to be coupled to a leaf level solar-induced chlorophyll fluorescence (SIF) model with the aim of further advancing of accuracy of the modeled SIF, which, in its turn, has a potential of improving our predictive capability of terrestrial carbon uptake.

Keywords: solar-induced chlorophyll fluorescence, Monte Carlo model, photon transport

CCG
LCPHD

Reconstructing Tropical Southwest Pacific Climate Variability at Vanuatu using Geochemical Proxies from Corals

Allison Lawman
Lawman, A., Institute for Geophysics, The University of Texas at Austin, Austin, TX
Quinn, T., Institute for Geophysics, The University of Texas at Austin, Austin, TX
Partin, J., Institute for Geophysics, The University of Texas at Austin, Austin, TX
Taylor, F., Institute for Geophysics, The University of Texas at Austin, Austin, TX
Thirumalai, K., Department of Earth, Environmental and Planetary Sciences, Brown University, Providence, RI
Wu, C., Department of Geosciences, National Taiwan University, Taipei, Taiwan
Shen, C., Department of Geosciences, National Taiwan University, Taipei, Taiwan

The Medieval Climate Anomaly (MCA: 950-1250 CE) is identified as a period during the last 2 millennia with Northern Hemisphere surface temperatures similar to the present. However, our understanding of tropical climate variability during the MCA is poorly constrained due to a lack of sub-annually resolved proxy records. We investigate interannual (2-8 year) variability during the MCA using geochemical records developed from well preserved *Porites lutea* fossilized corals from the tropical southwest Pacific (Tasmaloum, Vanuatu; 15.6°S, 166.9°E). An absolute U-Th date of 1127.1 ± 2.7 CE indicates that the selected fossil coral lived during the MCA. We use paired coral Sr/Ca measurements to reconstruct sea surface temperature (SST). Modern temperature variability on interannual timescales at Vanuatu is associated with the El Niño-Southern Oscillation (ENSO) in the tropical Pacific. To quantify the magnitude of variability in tropical SST records, we use histograms and probability density functions of monthly SST and SST anomaly data. To provide context for the fossil coral record and demonstrate our data analysis technique, our analysis also incorporates two modern coral records from Sabine Bank (15.9°S, 166.0°E) and Malo Channel (15.7°S, 167.2°E), Vanuatu for comparison. Based on ~100 years of fossil coral Sr/Ca-SST and replicated modern coral Sr/Ca-SST, we find that interannual variability at Vanuatu during the MCA (1046-1145 CE) is of similar magnitude to an interval with less ENSO activity observed during the 20th century (1920-1939 CE).

Keywords: paleoclimatology, paleoceanography, tropical climate variability

CCG
LCPHD

A new Miocene gerrhonotine from the Caliente Formation, California

Simon Scarpetta
Scarpetta, S., Jackson School of Geosciences, University of Texas at Austin, Austin, TX

Gerrhonotinae (i.e., alligator lizards) is an extant lizard clade with a rich Cenozoic fossil record in the Americas and a diverse assemblage of species still inhabiting regions of North and Central America. There are 55 extant species in six genera, but because many extant species are rare in museum collections there is currently a lack of published skeletal data, hindering accurate identification of fossils. Here, I describe a new gerrhonotine lizard known from a partial skull from the University of California Museum of Paleontology (UCMP). The UCMP specimen is from the Caliente formation in southern California and is 11.5-12.5 Ma old (Miocene, Clarendonian North American land mammal age). I used x-ray computed tomography (CT) scans to visualize the specimen and elucidate cranial anatomy that is inaccessible from the physical specimen alone. The new taxon is unique among gerrhonotines in that it possesses cephalic osteoderms with tall, sail-like keels, which is a trait previously unobserved in gerrhonotines. To place the fossil phylogenetically and taxonomically, I conducted phylogenetic analyses of Gerrhonotinae using both molecular and morphological data. These analyses incorporate morphological characters that are new to the literature as well as novel osteological CT data for many species. Preliminary analysis indicates that the specimen represents a new taxon. Additionally, I describe two other lizard fossils found in the same assemblage to help provide a paleoecological interpretation of the habitat of the fossil gerrhonotine.

Keywords: Gerrhonotinae, phylogenetics, fossils, computed tomography, paleoecology

LCPHD-6

CCG
LCPHD

The Role of Priming in the Development of Stable and Radioactive Carbon Isotope Profiles of Soil Organic Matter

Lily Serach
Serach, L., Department of Geological Sciences, The University of Texas at Austin, Austin, TX
Breecker, D., Department of Geological Sciences, The University of Texas at Austin, Austin, TX

The stability of soil carbon (C) is one of the largest sources of uncertainty in global C cycle models and is central to identifying potential feedbacks to a warming climate. The role that more stable soil organic matter (SOM) pools could have in these feedbacks is highly uncertain. Stable C isotope ($\delta^{13}C$) and radiocarbon (^{14}C) SOM profiles are used to understand the processes involved in soil C stabilization. In this study, we use a 1-dimensional, 3 pool soil C model to simulate the development of SOM $\delta^{13}C$ and ^{14}C profiles in a well-drained forest soil. Under the simplest model scenario where decomposition rate constants for each SOM pool remain fixed, model runs exhibit a buildup of slowly degrading C in the shallow subsurface (0-5cm) where fresh, labile C typically dominates in natural soils. Additionally, magnitudes of trends in SOM $\delta^{13}C$ and ^{14}C profiles were inconsistent with those observed in natural profiles, suggesting a deficiency in this version of the model. We hypothesize that the observed disparity between modeled and natural profiles is due to the absence of priming in the model. Priming effects presume a change in decomposition rate constants for recalcitrant C pools upon the addition of labile C to the soil. As such, priming effects were simulated in the model by making decomposition rate constants a function of labile C input (e.g., root C and leaf litter). The incorporation of priming into the model yields larger, more realistic shifts in SOM $\delta^{13}C$ profiles and trends in ^{14}C profiles that vary based on the sensitivity of recalcitrant pools to labile C addition. So far, the results from this study support the hypothesis that SOM $\delta^{13}C$ and ^{14}C profiles cannot be explained without priming. These results highlight the importance of priming to our understanding of the persistence of stable C in the soil and our ability to use SOM $\delta^{13}C$ and ^{14}C trends as a means to quantify C stability.

Keywords: Soil organic matter, carbon, radiocarbon

CCG
LCPHD

Implications of Modernizing our Perspective of Eastern North American Arvicoline Rodents in the Early and Middle Pleistocene

Charles Withnell
Withnell, C., The University of Texas at Austin, Austin, TX

The fields of vertebrate paleontology and evolutionary biology have undergone a tremendous amount of change since the Modern Synthesis. Changes in how we identify fossils, apomorphy (derived characteristics) based identifications, changes in how we name fossils (e.g., no chronotaxa, problematic biogeography, recognition of intraspecies variation), and the shift to 'tree thinking' have changed the way the fossil record is conceptualized and understood. However, Quaternary paleontology and one group in particular, arvicoline rodents, have been largely immune to these changes.

Arvicoline rodents (voles, lemmings, and muskrats) have been the backbone of North American mammalian biochronology for the Pliocene-Pleistocene since the 1940s. Recent research confirmed that arvicoline rodents can be troublesome biochronologic taxa based on three reasons that have large implications for their utility in Pliocene-Pleistocene biochronology. (1) New data on temporal and spatial distributions raised questions about the utility of some taxa as biochronologic tools (e.g., *Microtus paroperarius*, *Allophaiomys pliocaenicus*, *Lemmiscus curatus*). (2) The shift to monophyly as an organizing principle has important consequences and implications for how we think about the diversification of arvicoline rodents and the taxonomic hierarchy of the group. (3) Alterations to prior evolutionary models, results from phylogenetic hypotheses, and the general introduction of 'tree thinking' to arvicoline rodents have changed the way we conceptualize the group and the utility of arvicolines for biochronology.

Here I am going to begin to address these issues and explore the consequences of modernizing how we identify, name, and contextualize arvicoline rodents by giving preliminary results from three sites of my dissertation: Cumberland Cave Maryland, Port Kennedy Pennsylvania, and Conard Fissure Arkansas.

Keywords: Arvicoline rodents, biochronology, Pleistocene, vertebrate paleontology

CCG
LCPHD

Assessment of the Simulations of Global-scale River Flows from an Integrated Hydrological Modeling Framework

Wen-Ying Wu
Wu, W., Department of Geological Sciences, The University of Texas at Austin, Austin, TX
Yang, Z., Department of Geological Sciences, The University of Texas at Austin, Austin, TX
Lin, P., Department of Geological Sciences, The University of Texas at Austin, Austin, TX
Maidment, D., Center for Research in Water Resources, The University of Texas at Austin, Austin, TX

Gauged streamflow data provide an integrated measure of hydrologic processes over the entire watershed. However, current understanding of large-scale river flows is limited because of insufficient gauged observations. Therefore, an integrated hydrological modeling framework is needed to take advantage of gridded meteorological forcing, land surface modeling, channeled flow modeling, ground observations, and satellite remote sensing. Launched in August 2016, the National Water Model successfully incorporates weather forecasts to predict river flows for more than 2.7 million rivers across the continental United States, which transfers a “synoptic weather map” to a “synoptic river flow map” operationally. In this study, we apply a similar framework to a high-resolution global river network database, which was developed from a hierarchical Dominant River Tracing (DRT) algorithm, and runoff output from the Global Land Data Assimilation System (GLDAS) to a vector-based river routing model (The Routing Application for Parallel Computation of Discharge, RAPID) to produce river flows from 2001 to 2016 using Message Passing Interface (MPI) on TACC's Stampede system. In this simulation, global river discharges for more than 177,000 rivers are computed every 30 minutes and outputed every 3 hours. The modeling framework’s performance is evaluated with various observations including river flows at more than 400 gauge stations globally. Although the model exhibits an overall good performance, there are mean biases in available water storage, evapotranspiration and runoff. The time delay from cross-correlation between modeled and observed flows shows that land cover characteristics and river geometry parameters should be considered as they affect flow travel time on land and within channels, respectively. The low spatial correlation in cold regions during spring indicates the inadequate treatment of snowmelt and soil freeze–thaw processes in the land surface model. Directions for future research will be outlined and discussed.

Keywords: water cycle, climate, runoff, streamflow

EG
LCPHD

Estimation of Pore Porosity and Fracture Parameters from 3D Seismic Data by Born Inversion

Badr Alulaiw
Alulaiw, A., Jackson School of Geosciences, The University of Texas at Austin, Austin, TX
Sen, M., Institute for Geophysics, The University of Texas at Austin, Austin, TX

The presence of natural fractures plays an important role in enhancing the permeability in many reservoirs. Thus, estimating the fracture parameters is crucial for hydrocarbon exploration and production. For a fractured reservoir with vertical and rotationally invariant fractures, the linear slip model characterizes the reservoir using four parameters: two elastic parameters describing the isotropic host rock and two fracture parameters - normal ΔN and tangential ΔT fracture weaknesses. This model, however, ignores the effect of pore porosity on the anisotropy and hence the fracture parameters may be inaccurate. In this work, we estimate the fracture parameters as well as pore porosity using an expression for stiffness tensor for a porous fractured medium. We use the ray-Born approximation to compute the seismic response of a laterally varying porous reservoir. We use a global optimization method for inversion of reservoir properties.

Using synthetic examples, we compare the inversion results from both unconstrained and constrained simultaneous (PP and PSV components) seismic inversion as well as constrained inversion using only the PP component. We show the importance of including a constraint to circumvent the trade-off between ΔN and porosity. Unlike the unconstrained inversion, the estimated values from the constrained inversion are acceptable. We also observe that the simultaneous constrained inversion is more robust than using the PP component alone.

Keywords: Fracture Characterization, Inversion, Global Optimization, Anisotropy, Porosity

LCPHD-10

EG
LCPHD

Numerical Modeling of Differential Compaction Fracturing in Carbonate Systems

Yaser Alzayer
Alzayer, Y., Department of Geological Sciences, The University of Texas at Austin, Austin, TX
Zahm, C., Bureau of Economic Geology, The University of Texas at Austin, Austin, TX
Kerans, C., Department of Geological Sciences, The University of Texas at Austin, Austin, TX

Differential compaction has been proposed by many as a mechanism for syndepositional deformation in carbonate systems. However, outcrop and core observations typically include multiple deformation events that overprint the early fractures creating challenges for isolating features that are only relevant to differential compaction. Therefore, we employ finite-discrete element models to investigate and quantify factors only relevant to differential compaction fracturing. Models are used to (1) quantify the amount of differential compaction required to develop early fractures within carbonate mound complexes, (2) predict location of fracturing related to differential compaction, and (3) determine the effect of layer-parallel slip on fracturing.

Results show that cm-scale differential subsidence in response to differential compaction over carbonate mounds is sufficient to generate fractures. Two sets of forced folds are formed in response to differential compaction. The first overlie the mound crest-to-flank transition and the second correspond to mound flank-to-inter-mound area transition. Differential compaction fractures are concentrated at the hinges of these folds. Increasing the coefficient of sliding friction (μ) does not influence the spatial distribution and intensity of fractures, however, it controls fracture aperture. Fracture apertures are widest at mechanical boundaries when incorporating layer-parallel slip. High μ values correspond with lower magnitudes of layer-parallel slip and subsequently lower fracture apertures than models with low μ values. When no slip is allowed (i.e., not specifying a mechanical boundary between different lithologies) the fracture intensity increased significantly. Fracture apertures are widest at the center of fractures rather than at mechanical boundaries. The higher fracture intensity is due to the lack of strain being accommodated by layer-parallel slip. This type of model may reflect conditions where lithology changes are gradual and mechanical boundaries are not well developed.

The presented results suggest that fracturing by differential compaction can be easily developed and therefore may be generally underestimated in carbonate systems. The location of fracturing caused by differential compaction in carbonate systems is controlled by the geometry of the rigid antecedent topography. Layer-parallel slip is often overlooked as a mechanism to dissipate stress because evidence for it is not easily observed in outcrops. The models presented offer a unique insight into the effects layer-parallel slip has on fracture aperture as well as fracture intensity in absence of well-defined mechanical layering. The presented models offer a way to validate that differential compaction is a mechanism for early fracture development in carbonate systems and highlights the utility of such models as predictive tool for fracturing. This work has implications on fluid flow in carbonate aquifers and hydrocarbon reservoirs where early fracture systems influence diagenesis, subsequent deformation, and migration pathways.

Keywords: Fractures, carbonates, numerical modeling, differential compaction

EG
LCPHD

2D Full Waveform Inversion and Uncertainty Estimation using the Reversible Jump Hamiltonian Monte Carlo

Reetam Biswas
Biswas, R., Institute for Geophysics, The University of Texas at Austin, Austin, TX
Sen, M., Institute for Geophysics, The University of Texas at Austin, Austin, TX

Seismic data are used to generate high resolution subsurface images, which require detailed velocity models. Full Waveform Inversion (FWI), has recently gathered immense popularity in inverting for the elastic wave velocities from the seismic data. FWI is a non-linear and non-unique inverse problem that uses complete time and amplitude information for estimating the elastic properties. Typically FWI is performed using local optimization methods in which the subsurface model is described by using a large number of grids. The number of model parameters is determined a priori. In addition, the convergence of the algorithm to the globally optimum answer is largely dictated by the choice of a starting model. Here, we apply a trans-dimensional approach, which is based on a Bayesian framework to solve the waveform inversion problem. In our approach, the number of model parameters is also treated as a variable, which we hope to estimate. We use Voronoi cells and represent our 2D velocity model using certain nuclei points and employ a recently developed method called the Reversible Jump Hamiltonian Monte Carlo (RJHMC). RJHMC is an effective tool for model exploration and uncertainty quantification. It combines the reversible jump MCMC with the gradient based Hamiltonian Monte Carlo (HMC). We solve our forward problem using time-domain finite difference method while adjoint method is used to compute the gradient vector required at the HMC stage. We demonstrate our algorithm with noisy synthetic data for the well known Marmousi model. Convergence of the chain is attained in about 3000 iterations; marginal posterior density plots of velocity models demonstrate uncertainty in the obtained velocity models.

Keywords: FWI, Transdimensional, Inversion

LCPHD-12

EG
LCPHD

The UPSIDE POTENTIAL of the EARLY MIOCENE KUJUNG FORMATION CARBONATES, OFFSHORE EAST JAVA, INDONESIA

Reynaldy Fifariz
Fifariz, R., Bureau of Economic Geology, The University of Texas at Austin, Austin, TX
Janson, X., Bureau of Economic Geology, The University of Texas at Austin, Austin, TX
Kerans, C., Department of Geological Sciences, The University of Texas at Austin, Austin, TX
Setiawan, M., Pertamina Hulu Energi – West Madura Offshore (PHE-WMO), Indonesia
Thoha, S., Pertamina Hulu Energi – West Madura Offshore (PHE-WMO), Indonesia

Cenozoic carbonates are proven prolific hydrocarbons reservoir in the SE Asia region. In the offshore East Java area, Indonesia, hydrocarbon productions are mainly coming from the Oligocene-Miocene Kujung Formation carbonates especially the Early Miocene Kujung-1 carbonate buildups. This study aims to investigate the upside potential based on existing indicators from well data of hydrocarbon accumulation in the area surrounding the carbonate buildups.

Based on seismic and well data, we interpret the Kujung-1 interval as isolated carbonate buildups complex that can be subdivided into three areas: buildup-core, buildup-flank, and inter-buildups. Hydrocarbon productions have been mainly coming from the buildup-core area that is characterized by massive carbonates of reefal facies with less than 5% shale content. Distinctively, wells from KE-X3, KE-X4, and KE-X8 field area that penetrated the buildup-flank and inter-buildups area show alternation of carbonate and shale beds. We interpret this alternation as a result of episodic carbonates sedimentation and possible re-sedimentation during periods of a relatively decreasing accommodation outside the buildup-core area. In contrast, shales were deposited during periods of a relatively increasing accommodation under lower energy condition in the buildup-flank and inter-buildups area.

Based on petrophysical calculations of well-logs data, we interpret an interval of up to 120 feet thick near the top of this carbonates-shales alternation as an upside potential for hydrocarbon reservoir in the KE-X8 field area. The calculation results show that the carbonate beds in the buildup-flank and inter-buildups area can act as reservoir for hydrocarbon accumulation that is possibly trapped stratigraphically. Within this upside potential interval, the calculated porosity ranges from 15-21 % with the highest permeability from core analysis measured at 42.6 millidarcy. Subsequently, we utilized acoustic impedance inversion and static reservoir modeling to map the carbonate reservoir distribution. Preliminary hydrocarbon resources and reserves calculations yielded encouraging results for this interval to be developed as part of an integrated fields development strategy.

Keywords: Carbonates, Buildups, Miocene, Upside Potential, Reservoir

LCPHD-13

EG
LCPHD

?Making synthetic mudstone: Parametric resedimentation studies at high effective stress to determine controls on breakthrough pressure and permeability

Eric Guiltinan
Guiltinan, E., Department of Geological Sciences, University of Texas at Austin, Austin, TX
Espinoza, N., Petroleum and Geosystems Engineering, University of Texas at Austin, Austin TX
Cockrell, L., Department of Geological Sciences, University of Texas at Austin, Austin, TX
Cardenas, M., Department of Geological Sciences, University of Texas at Austin, Austin, TX

The geologic sequestration of CO2 is widely considered a potential solution for decreasing anthropogenic atmospheric CO2 emissions. As CO2 rises buoyantly within a reservoir it pools beneath a caprock and a pressure is exerted upon the pores of the caprock proportionally to the height of the pool. The breakthrough pressure is the point at which CO2 begins to flow freely across the caprock. Understanding the mineralogical and grain size controls on breakthrough pressure is important for screening the security of CO2 sequestration sites. However, breakthrough pressure and permeability measurements on caprocks are difficult to conduct in a systematic manner given the variability in and heterogeneity of naturally occurring mudstones and shales causing significant noise and scatter in the literature. Recent work has even revealed the ability for CO2 to pass through thin shale beds at relatively low pressures.
To broaden the understanding of shale breakthrough and permeability, we developed an approach that allows for the creation of resedimented mudstones at high effective stresses. Resedimented samples also include calcium carbonate cement. Using this technique, we explore the controls on entry pressure, breakthrough pressure, and permeability of synthetic mudstones. Understanding the effect of mineralogy and grain size on the permeability and breakthrough pressure of mudstones at reservoir stresses will help in the selection and uncertainty quantification of secure CO2 storage sites.

Keywords: Percolation Threshold, Breakthrough Pressure, CO2 Sequestration, Resedimentation, Mudrocks

EG
LCPHD

Oriented anisotropy continuation using shifted hyperbola travel-time approximation

Dmitrii Merzlikin
Merzlikin, D., Bureau of Economic Geology, The University of Texas at Austin, Austin, TX
Fomel, S., Bureau of Economic Geology, The University of Texas at Austin, Austin, TX
Sripanich, Y., Bureau of Economic Geology, The University of Texas at Austin, Austin, TX

Velocity continuation is a process of continuous image propagation in velocity. It allows one to generate an image corresponding to a certain migration velocity without returning to the original data. We extend the theory of velocity continuation to account for non-hyperbolic shape of travel-time curves in anisotropic media using shifted-hyperbola approximation. Corresponding image propagation process becomes two-dimensional, where propagation parameters are the normal moveout velocity and the anisotropy parameter. Continuity of image transformation with respect to migration parameters leads to superior computational efficiency of the proposed approach with respect to conventional migration velocity analysis techniques in anisotropic media. Synthetic data examples demonstrate the validity of the method.

Keywords: Diffraction imaging, velocity analysis, seismic anisotropy

EG
LCPHD

Can deep learning help us classify salt body?

Yunzhi Shi
Shi, Y., Bureau of Economic Geology, The University of Texas at Austin, Austin, TX
Wu, X., Bureau of Economic Geology, The University of Texas at Austin, Austin, TX
Fomel, S., Bureau of Economic Geology, The University of Texas at Austin, Austin, TX

Salt boundary interpretation is important for salt tectonics and velocity-model building in seismic migration. Interpreting salt boundaries often involves computing a salt attribute image and picking salt boundaries from the attribute image. Although automatic methods have been proposed for computing salt attributes and extracting salt boundaries, the salt interpretation remains a human-intensive and time-consuming task. In practice, a salt body can be complicated by factors including poor imaging, discontinuous structures, and rapidly varying geometries.

In this study, we investigate to apply the recent developments in computer vision research to the salt body classification problem. Considering it as an image segmentation, we design a deep learning neural network inspired by SegNet to achieve highly-adaptive automation of salt boundary interpretation problem in order to minimize the manual effort in this process.

Keywords: Interpretation, salt, deep learning

LCPHD-16

MG
LCPHD

Detailed seismic velocity structure of the ultra-slow spread crust at the Mid-Cayman Spreading Center from travel-time tomography and synthetic seismograms

Jennifer Harding
van Avendonk, H., University of Texas Institute for Geophysics, Austin, TX
Hayman, N., University of Texas Institute for Geophysics, Austin, TX
Grevemeyer, I., GEOMAR Helmholz Centre for Ocean Research, Kiel, Germany
Peirce, C., Durham University, Durham, England

The Mid-Cayman Spreading Center (MCSC), an ultraslow-spreading center in the Caribbean Sea, has formed highly variable oceanic crust. Seafloor dredges have recovered extrusive basalts in the axial deeps as well as gabbro on bathymetric highs and exhumed mantle peridotite along the only ~110 km MCSC. Wide-angle refraction data were collected with active-source ocean bottom seismometers in April, 2015, along lines parallel and across the MCSC. Travel-time tomography produces relatively smooth 2-D tomographic models of compressional wave velocity. These velocity models reveal large along- and across-axis variations in seismic velocity, indicating possible changes in crustal thickness, composition, faulting, and magmatism. It is difficult, however, to differentiate between competing interpretations of seismic velocity using these tomographic models alone. For example, in some areas the seismic velocities may be explained by either thin igneous crust or exhumed, serpentinized mantle. Distinguishing between these two interpretations is important as we explore the relationships between magmatism, faulting, and hydrothermal venting at ultraslow-spreading centers. We therefore improved our constraints on the shallow seismic velocity structure of the MCSC by modeling the amplitude of seismic refractions in the wide-angle data set. Synthetic seismograms were calculated with a finite-difference method for a range of models with different vertical velocity gradients. Small-scale features in the velocity models, such as steep velocity gradients and Moho boundaries, were explored systematically to best fit the real data. With this approach, we have improved our understanding of the compressional velocity structure of the MCSC along with the geological interpretations that are consistent with three seismic refraction profiles. Line P01 shows a variation in the thinness of lower seismic velocities along the axis, indicating two segment centers, while across-axis lines P02 and P03 show variations in igneous crustal thickness and exhumed mantle in some areas.

Keywords: marine geophysics, mid-ocean ridges, oceanic crust, seismology

LCPHD-17

MG
LCPHD

Sedimentological Characterization of a Deepwater Methane Hydrate Reservoir in Green Canyon 955, Northern Gulf of Mexico

Patrick Meazell
Meazell, K., Institute for Geophysics, The University of Texas at Austin, Austin, TX
Flemings, P., Department of Geological Sciences & Institute for Geophysics, The University of Texas at Austin, Austin, TX
Santra, M., Institute for Geophysics, The University of Texas at Austin, Austin, TX

Grain size is a controlling factor of hydrate saturation within a Pleistocene channel-levee system investigated by the UT-GOM2-1 expedition within the deepwater northern Gulf of Mexico. Laser diffraction and settling experiments conducted on sediments from 413-440 meters below the seafloor reveal the presence of two interbedded lithologic units, identified as a silty sand and a clayey silt, according Shepard's classification system. The sand-rich lithofacies has low density and high p-wave velocity, suggesting a high degree of hydrate saturation. Conversely, the clay and silt dominated lithofacies is characterized by a higher density and low p-wave velocity, suggesting low hydrate saturation. The sand-rich lithofacies is well-sorted and displays abundant ripple lamination, indicative of deposition within a high-energy environment. The clayey-silt is poorly-sorted and lacks sedimentary structures. The two lithofacies are interbedded throughout the reservoir unit; however, the relative abundance of the sand-rich lithofacies increases with depth, suggesting a potential decrease in flow energy or sediment flux over time, resulting in the most favorable reservoir properties near the base of the unit.

Keywords: sedimentology, hydrate, stratigraphy, submarine channels, Gulf of Mexico

MG
LCPHD

Global versus Regional Carbon Isotope Signals: An Example from the Permian of West Texas and New Mexico

Benjamin Smith
Smith, B., Department of Geological Sciences, The University of Texas at Austin
Kerans, C., Department of Geological Sciences, The University of Texas at Austin

Carbon isotope excursions in marine carbonates often record changes in the global carbon cycle through geologic time. However, apparent $\delta^{13}C$ excursions may also reflect the influence of regional oceanographic effects, especially in restricted or epieric settings. Proper interpretation of the carbon isotope record relies on an accurate assessment as to the regional or global nature of these disturbances. If excursions are the result of global carbon cycle changes, then they can often be used as global chronostratigraphic markers related to periods of rapid environmental change (e.g. mass extinction). If instead these excursions are the result of regional processes, they may provide useful record of changes in local basin water chemistry. The potential effect of these regional changes in oceanographic conditions must be critically evaluated before an excursion is deemed suitable for global correlation.
The Guadalupian/Lopingian (Permain) boundary and its associated mass extinction event have received considerable attention in the recent literature. Unlike the larger end-Permian extinction, the $\delta^{13}C$ excursion associated with the end-Guadalupian extinction is not present globally. This study examines variations in trace element and stable isotope geochemistry from the Delaware Basin of West Texas and New Mexico. Interpretation of geochemical data within a pre-existing shelf-to-basin stratigraphic framework suggests a link between basin water chemistry and sea level changes during the entirety of the Guadalupian. In light of this potential control, severe restriction of the basin near the Guadalupian/Lopingian boundary should be considered a possible control on the local carbon isotope record. This work provides an example of how chemostratigraphy and sedimentology can be used to interpret regional versus global oceanographic effects in the carbonate record.

Keywords: carbon isotopes, chemostratigraphy, carbon cycle,

PS
LCPHD

Ice caps under sand caps under an ice cap: revealing a record of climate change on Mars

Stefano Nerozzi
Nerozzi, S., Institute for Geophysics, The University of Texas at Austin, Austin, TX
Holt, J., The University of Arizona, Tucson, AZ

The cavi unit is an aeolian deposit of sand and water ice making up a large fraction of Planum Boreum in the north polar region of Mars. On the basis of crater counting and stratigraphy, previous studies determined an age of 10-100 Ma for this unit, meaning that its strata potentially recorded regional and global climate conditions and processes in the recent martian past (i.e. middle-late Amazonian). Prior studies involving imagery, spectrometry and radar sounding determined that the cavi unit is composed of a mixture of water ice and lithic materials (e.g. basalt, gypsum). However, there is still no consensus on its precise composition, and it remains unclear which fraction, sand or water ice, dominates. Precise constrains on composition are needed to determine the importance of the cavi unit as a water and sediment reservoir, reconstruct its accumulation history and understand the regional and global processes that shaped it to its observable morphology.
Radar profiles acquired by the Shallow Radar reveal a deep reflector within Planum Boreum that we associate with the basal contact of the cavi unit with the surrounding lowlands. We use an inversion technique to determine the dielectric constant of this unit and, in turn, the bulk composition of this unit with the aid of a ternary diagram based on a mixing power law.
Our exercise reveal that the bulk dielectric constant of the cavi unit has substantial spatial variability. In particular, the cavi unit in Olympia Planum has a bulk dielectric constant equivalent to a mixture of 60% basaltic sand and 40% water ice, which corresponds to the higher end of typical aeolian sand porosities assuming that ice occupies the intergranular pore space. In contrast, the rest of the unit has a dominant ice fraction of 70-85%, exceeding by far the maximum observed porosity of aeolian sand deposits of 50%. We note that compared to Olympia Planum, the cavi unit main lobe is crossed by several internal reflectors that suggest the presence of a similar number of significant changes in composition. Based on this qualitative observation, and the trend of decreasing dielectric constant with increasing thickness and latitude, we hypothesize that the central cavi unit is made of alternating sand and water ice layers. Water ice accumulation models specifically tuned for Mars' north pole predict substantial water ice accumulation at high latitudes during periods of low spin axis obliquity followed by complete sublimation during high obliquity periods. We hypothesize that some of this ice has been preserved by aeolian sand sheets, which prevented complete ice sublimation. Such sand mantles have been observed on top of water ice in Planum Boreum, and occurrences of sand sheets can be observed within the overlying ice cap in visible outcrops and radar profiles. Therefore, we find that the record of past ice caps accumulation was not completely lost by sublimation, but preserved within sand sheets. The high water ice fraction makes the cavi unit an important water ice reservoir, potentially the third largest on Mars after the two polar caps.

Keywords: Mars, water, ice, radar, polar, cap

PS
LCPHD

Mantle Morphology on Martian Debris-Covered Glaciers Reveals Deposition & Flow History

Eric Petersen
Petersen, E., UTIG
Holt, J., UTIG
Levy, J., Colgate University

Debris-covered glaciers are common in the mid-latitudes of Mars where they are found at the base of mesa-like massifs, in the depths of canyons, and in the basins of impact craters. The Shallow Radar Sounder (SHARAD) on Mars Reconnaissance Orbiter (MRO) has been used to sound through many of these glaciers and image the basal contact between a relatively pure water ice core and underlying bedrock; the thickness of the surface debris layer has been constrained to the order of 1-10 m thick (Holt et al., 2008; Plaut et al., 2009).

The surfaces of Martian debris-covered glaciers exhibit a range of morphologies including pits-and-buttes, thermal contraction crack polygons, and raised moraine-like features (Mangold, 2003). We have shown in previous work that varied roughness of pits-and-buttes terrain can have a strong effect on SHARAD sounding of glaciers (Petersen et. al, 2017), with sufficiently high roughness rendering the detection of the basal contact unfeasible due to coherent signal loss.

In this study we seek to understand the cause of varied roughness of the surface debris mantle through geomorphic observation. We used images from the High Resolution Imaging Science Experiment (HiRISE, also on MRO) with a 25-50 cm/px resolution. We also used stereo images from HiRISE to produce Digital Terrain Models (DTMs) at 1 m/px resolution using the Ames Stereo Pipeline.

We found that high roughness pits-and-buttes (>5 meters relief) generally exhibit an orientation sub-perpendicular to the glacial flow direction. In one location with observed butte relief up to ~10 meters we observed layering of light and dark bands of material (average thickness 2.0 ± 0.2 m) which were continuous across neighboring buttes within an area at least ~300 m x 200 m. Pits and buttes are observed to grade into raised moraine-like features, with the tops of the buttes flush with the top of the moraine-like features.

We interpret these results to indicate that the material making up the raised moraine-like features is the same as that which makes up the buttes, the buttes being produced by differential erosion of said material. The periodic layering, pitted morphology, and results of previous mapping work (i.e. Baker and Head, 2015) suggest that this material is a layered ice-rich mantle deposited during periods of high obliquity subsequent to the formation of the debris-covered glaciers. We propose that the flow-perpendicular orientation of pits-and-buttes is produced by mantle crevassing driven by glacier flow, followed by differential ice sublimation. In this model the depth of incision into the mantle and the roughness height of buttes is controlled by the flow history of the underlying debris-covered glacier. This is supported by the observation that glaciers exhibiting high roughness mantles also have steeper surface slopes (>2 degrees as opposed to ~1 degree) suggesting a more vigorous flow history.

This work demonstrates a connection between glacial processes, morphology, and geophysics for Martian debris-covered glaciers while advancing new observations into the structure of the glacial surface mantle.

Keywords: mars, debris-covered glaciers, geophysics, geomorphology, planetary science

SETP
LCPHD

Integrating complimentary accessory phases (apatite, rutile, zircon) in isotopic and trace-elemental provenance studies: reconstructing the Proto-Zagros orogeny, NW Iran

Douglas Barber
Barber, D., Dept. of Geological Sciences, Jackson School of Geosciences, The University of Texas at Austin, Austin, TX
Stockli, D., Dept. of Geological Sciences, Jackson School of Geosciences, The University of Texas at Austin, Austin, TX
Galster, F., Dept. of Geological Sciences, Jackson School of Geosciences, The University of Texas at Austin, Austin, TX
Horton, B., Dept. of Geological Sciences, Jackson School of Geosciences, The University of Texas at Austin, Austin, TX

Detrital zircon (DZ) U-Pb geochronology is a powerful provenance tool but has recognized limitations in particular geologic settings due to variable zircon fertility among different rock types, the potential of non-unique source terrane ages, or complex recycling and mixing. However, integration of multiple analytical techniques and accessory phases can significantly improve resolution and amplify uniqueness of provenance signals and allow for a more detailed source characterization by utilizing multiple criteria such as crystallization age, cooling history, and petrogenic and geodynamic environment. In this study, U-Pb, trace-element, and (U-Th)/He analyses were applied to detrital zircon, rutile, and apatite from the Proto-Zagros foreland basin, which formed as a result of Cretaceous ophiolite obduction onto Arabia and was subsequently overprinted in the Arabia-Eurasia collision. These new integrated provenance results are used to test competing paleogeographic models and delineate the timing and nature of Protozagros unroofing. They reveal that Lower Cretaceous siliciclastic deposits in northern Arabia were strictly sourced from the Arabian-Nubian shield and East African orogenic belt. Maastrichtian-Paleocene strata record a major provenance shift; DZ trace-elements indicate major sediment influx from Triassic oceanic crust, whereas other proxies document arrival of detritus with diverse metamorphic and igneous signatures from the Eurasian continent, inverted Arabian rift margin, and a Cretaceous island arc. DZ thermochronometry constrains the major cooling and exhumation phase of these source units as late Campanian-Maastrichtian. Based on these new results, we present a reconstruction of the tectonic elements associated with the Proto-Zagros collision and discuss how the incorporation of accessory phase trace-element analysis dramatically changes the paleogeographic interpretation compared to a traditional detrital zircon U-Pb dataset. Overall, the integration of complimentary detrital accessory phases and analytical techniques in the Proto-Zagros significantly enhances provenance reconstructions beyond traditional zircon U-Pb data and provides multiple criteria to assess the tectonic evolution of source terranes that have been eroded or overprinted by later events.

Keywords: foreland basin provenance; detrital zircon-apatite-rutile, U-Pb geochronology, trace-element geochemistry, Zagros

SETP
LCPHD

Plagioclase-dominated Seismic Anisotropy in the Eastern Mojave Lower Crust

Rachel Bernard
Bernard, R., Department of Geological Sciences, The University of Texas at Austin, Austin, TX
Behr, W., Department of Geological Sciences, The University of Texas at Austin, Austin, TX

Observations of seismic anisotropy have the ability to provide important information on deformation and structures within the lithosphere. While the mechanisms controlling seismic anisotropy in the upper mantle are fairly well understood (i.e., olivine "lattice preferred orientation" or LPO), less is known about the minerals and structures controlling regional lower crustal anisotropy. We use lower crustal xenoliths from young cinder cones in the eastern Mojave/western Basin and Range to investigate mineral LPOs and their effect on seismic anisotropy. Lower crustal gabbros were collected from two areas roughly 80 km apart — the Cima and Deadman Lake Volcanic Fields. Lower crustal fabrics measured using EBSD are dominated by LPOs in plagioclase associated with both plastic deformation and magmatic flow. In all fabric types, plagioclase LPOs produce seismic fast axes oriented perpendicular to the foliation plane. This is in contrast to mantle peridotite xenoliths from the same locations, which preserve olivine LPOs with fast axes aligned parallel to the foliation plane. The orthogonal orientations of mantle and lower crustal fast axes relative to foliation implies that even where fabric development in both layers is coeval and kinematically compatible, their measured anisotropies can be perpendicular to each other, therefore appearing anti-correlated when measured seismically. Furthermore, our observation of plagioclase-dominated LPO and negligible concentrations of mica is at odds with the common assumption that lower crustal anisotropy is dominated by micaceous minerals, whose slow axes reliably align parallel to lineation or flow. In contrast, our data show that for plagioclase, fast axes align perpendicular to flow and the slow axes are variably aligned within the foliation plane. Therefore, for a crustal section dominated by plagioclase LPO with assumed horizontal foliation, there would be a vertical rather than a horizontal axis of symmetry, resulting in a lack of azimuthal anisotropy and minimal shear wave splitting for vertically propagating waves. Crustal seismic studies in this type of setting may only be able to identify crustal flow planes, but not flow directions. These findings may be generally applicable to regions of significant mafic volcanism and lower crustal magmatic underplating.

Keywords: crust, seismic, anisotropy, lattice, microstructures

LCPHD-23

SETP
LCPHD

Miocene to recent shortening along distal foreland uplifts and basin partitioning during flat-slab subduction in western Argentina

Tomas Capaldi
Capaldi, T., Department of Geological Sciences, Jackson School of Geosciences, University of Texas at Austin, TX, USA
Horton, B., Institute for Geophysics and Department of Geological Sciences, Jackson School of Geosciences, University of Texas at Austin, TX, USA
Stockli, D., Department of Geological Sciences, Jackson School of Geosciences, University of Texas at Austin, TX, USA
Helper, M., Department of Geological Sciences, Jackson School of Geosciences, University of Texas at Austin, TX, USA
Odlum, M., Department of Geological Sciences, Jackson School of Geosciences, University of Texas at Austin, TX, USA
Mackaman-Lofland, C., Department of Geological Sciences, Jackson School of Geosciences, University of Texas at Austin, TX, USA
Ortiz, G., CONICET and Universidad Nacional de San Juan (CIGEOBIO), Departmento de Geofísica y Astronomía, FCEFN-UNSJ, San Juan, Argentina
Alvarado, P., CONICET and Universidad Nacional de San Juan (CIGEOBIO), Departmento de Geofísica y Astronomía, FCEFN-UNSJ, San Juan, Argentina

In the Andes of Argentina (27-33°S), the major cities of Mendoza and San Juan have been repeatedly damaged by large-magnitude earthquakes (e.g., M 7-8 events in 1977, 1952, 1944, 1927, 1894, 1861, 1782) generated by stresses related to flat-slab subduction and associated crustal shortening expressed along the Eastern Precordillera (EP) thrust system. The EP is a North-trending, west-directed backthrust system, forming a frontal triangle zone with respect to the oppositely verging, east-directed Central Precordilleran (CP) thrust system in the orogenic hinterland to the west. Ramp-flat structures of the EP has been linked to west-directed, basement-involved reverse faults of the Sierras Pampeanas (SP) to the east that have broken the once-contiguous foreland basin. Reconstructions of the CP, EP, and SP tectonic histories show large uncertainties in timing of thrust-front propagation and kinematic links between thin- and thick-skin structures. Previous studies have interpreted initial shortening at 5-2 Ma in the CP-EP and 2.6 Ma in the SP, largely on the basis of inferred links with Cenozoic volcanic arc migration.

Andean shortening and erosion along the CP, EP, and SP produces distinguishable sedimentological trends that are recorded in the adjacent foreland basin system. Newly generated fluvial-alluvial stratigraphic sections along EP and SP structures are coupled with paleoflow measurements, sediment composition data, and detrital zircon geochronology to resolve the sequence of uplift along the tectonic provinces. Our results display 1) 18–10 Ma: initial Andean arc and igneous hinterland sediment sources, 2) 12 – 5 Ma: introduction of CP metasedimentary source, 3) 5 Ma-recent shut off of Andean arc and CP sources and synchronous introduction of EP and SP sediments. Compiling preliminary mapping and field observations with historical earthquake focal mechanisms establishes new constraints on structural geometry and kinematic links across the EP and SP transect. The SP structure is interpreted to be an east verging basement involved reverse fault with a nearly horizontal detachment at mid-crustal depth ~25-30 km. Shortening along SP temporally overlaps with movement along the EP west-directed thrust belt with an upper, shallow (<10 km) detachment that potentially links to a deeper basement involved structure. The kinematic association of contrasting EP and SP structures suggest flat-slab slab subduction (initiated at 12 Ma) has driven strain >350 km towards the craton, shifting shortening from purely thin-skinned to a deep rooted hybrid thin-thick skinned system by 5 Ma. New structural and temporal reconstructions of these Andean ranges is critical for evaluating not only the long-term interactions of frontal thrust structures with foreland-basin sedimentation but also assessing Andean earthquake hazards that will impact human populations and infrastructure in western South America.

Keywords: Andes, fluvial stratigraphy, thrust-belts, basement uplifts, U-Pb detrital zircon geochronology, flat-slab subduction, Argentina

SETP
LCPHD

Defining conditions of garnet growth across the central and southern Menderes Massif

Thomas Etzel
Etzel, T., The University of Texas at Austin
Catlos, E., The University of Texas at Austin
Kelly, E., The University of Texas at Austin
Cemen, I., University of Alabama
Ozerdem, C., Gamma Construction
Atakurk, K., Independent Researcher

Here we apply thermodynamic modeling using Theriak-Domino to garnet-bearing rocks from the central and southern portions of the Menderes Massif to gain insight into the dynamics of western Turkey as the region experienced a transition from collisional to extensional tectonics. To this end, we report new pressure-temperature (P-T) paths from garnet-bearing rocks collected along the Alasehir detachment fault, a prominent exhumation structure in the central portion of the Menderes Massif in western Turkey, constituting southern margin of the Alasehir Graben. These paths are compared to those from the Selimiye shear zone in the southern (Cine) Massif. Two Alasehir garnets collected from the same outcrop record two P-T paths: 1) a prograde path beginning at ~565^{o}C and ~6.4 kbar increasing to ~592 ^{o}C and ~7.5 kbar; and 2) near isobaric growth initiating at ~531^{o}C and ~7.1 kbar and terminating at ~571^{o}C and ~7.3 kbar. High-resolution P-T paths could not be modeled for the majority of Alasehir samples due to diffusional modification of garnet. However, conditions were estimated by garnet isopleth thermobarometry at the point of highest spessartine content for each crystal. Calculated P-T values for this subset of samples range between 566-651^{o}C and 6.2-6.8 kbar. Despite this broad range, these P-T conditions are consistent with what is observed in the modeled paths. Th-Pb ages of matrix monazite range from 35.8±3.0 to 20.6±2.4 Ma, suggesting metamorphism in the central Menderes Massif occurred over a 15 m.y. period. Selimiye shear zone rocks show distinct N-shaped P-T paths, suggesting garnets in the central and southern portion of the Menderes Massif record distinctly different tectonic histories.

Keywords: Menderes Massif, Turkey, Garnet P-T paths, thermobarometry

SETP
LCPHD

Testing Models of Orogenic Development in Ecuador: Multi-proxy Provenance Analysis of the Hinterland Cuenca Basin

Sarah George
George, S., Department of Geological Sciences, Jackson School of Geosciences, University of Texas at Austin, TX, USA
Horton, B., Department of Geological Sciences and Institute for Geophysics, Jackson School of Geosciences, University of Texas at Austin, TX, USA
Breecker, D., Department of Geological Sciences, Jackson School of Geosciences, University of Texas at Austin, TX, USA

The Miocene Cuenca Basin sits between the Eastern and Western Cordilleras of Ecuador. The current model for basin formation suggests that the Cuenca Basin formed at sea level, and was connected to the Pacific Ocean until ~10 Ma, when it was uplifted to the current elevation of ~2800 m. Diagnostic source regions allow for a straightforward test of this model. Potential sources include: (1) the Western Cordillera which constitutes the magmatic arc with 100-0 Ma zircons, (2) the Eastern Cordillera which is a retroarc fold-thrust belt comprised of Paleozoic-Mesozoic metamorphic and igneous rocks with 1300-100 Ma zircons, and (3) cratonic provinces which have zircons older than ~1.3 Ga. Six new detrital zircon samples throughout the basin fill contain only zircons <50 Ma, suggesting exclusive derivation from the Western Cordillera. All detrital zircon samples yield robust depositional ages, which young up-section, and document basin opening at ~15 Ma. In addition to detrital zircon geochronology, we present a new measured section of the Miocene siliciclastic basin fill, supplemented by clast counts, subsidence curves, and paleocurrent measurements. Paleocurrents suggest a dominant flow to the north and to the west, and clasts counts show primary derivation from volcanic sources. Together, these data suggest an axial filling of the Cuenca Basin from south to north. At the top of the uppermost fluvial formation (Mangán Formation), we document growth strata, which can be used to constrain intra-basin deformation to ~10 Ma. Finally, oxygen isotopes from pedogenic carbonate nodules in the Cuenca Basin fill have ~2‰ lower values than Eocene nodules in the nearby Quingeo Basin, which could be a signal of uplift, or the formation of an orographic barrier.

Keywords: Andes, uplift, provenance, detrital zircon geochronology, basin analysis, isotopes, pedogenic carbonates

SETP
LCPHD

Quaternary Slip History for the Agua Blanca Fault, northern Baja California, Mexico

Peter Gold
Gold, P., Department of Geological Sciences, University of Austin, Texas
Behr, W., Department of Geological Sciences, University of Austin, Texas
Rockwell, T., Department of Geological Sciences, San Diego State University
Fletcher, J., Centro de Investigación Científica y de Educación Superior de Ensenada (CICESE)

The Agua Blanca Fault (ABF) is the primary structure accommodating San Andreas-related right-lateral slip across the Peninsular Ranges of northern Baja California. Activity on this fault influences offshore faults that parallel the Pacific coast from Ensenada to Los Angeles and is a potential threat to communities in northern Mexico and southern California. We present a detailed Quaternary slip history for the ABF, including new quantitative constraints on geologic slip rates, slip-per-event, the timing of most recent earthquake, and the earthquake recurrence interval. Cosmogenic ^{10}Be exposure dating of clasts from offset fluvial geomorphic surfaces at 2 sites located along the western, and most active, section of the ABF yield preliminary slip rate estimates of 2-4 mm/yr and ~3 mm/yr since ~20 ka and ~2 ka, respectively. Fault zone geomorphology preserved at the younger site provides evidence for right-lateral surface displacements measuring ~2.5 m in the past two ruptures. Luminescence dating of an offset alluvial fan at a third site is in progress, but is expected to yield a slip rate relevant to the past ~10 kyr. Adjacent to this third site, we excavated 2 paleoseismic trenches across a sag pond formed by a right step in the fault. Preliminary radiocarbon dates indicate that the 4 surface ruptures identified in the trenches occurred in the past 6 kyr, although additional dating should clarify earthquake timing and the mid-Holocene to present earthquake recurrence interval, as well as the likely date of the most recent earthquake. Our new slip rate estimates are somewhat lower than, but comparable within error to, previous geologic estimates based on soil morphology and geodetic estimates from GPS, but the new record of surface ruptures exposed in the trenches is the most complete and comprehensively dated earthquake history yet determined for this fault. Together with new and existing mapping of tectonically generated geomorphology along the ABF, our constraints show that contrary to some theories of fault interaction and activity for this section of the San Andreas system, the Agua Blanca Fault has been active over the late Holocene, and should be considered as a potential source of seismic hazard.

Keywords: earthquake hazard, Quaternary geochronology, slip rate, earthquake recurrence, Agua Blanca Fault

LCPHD-27

SETP
LCPHD

Tectonomorphic Influence on Late Cretaceous-Paleogene Sediment Provenance and Dispersal Through West and South Texas From Detrital Zircon Geochronology

Cullen Kortyna
Kortyna, C., Department of Geological Sciences, The University of Texas at Austin, Austin, TX
Corchado Albelo, J., Departamento de Geología, Universidad de Puerto Rico, San Juan, PR
Stockli, D., Department of Geological Sciences, The University of Texas at Austin, Austin, TX
Sharman, G., Department of Geosciences, The University of Arkansas, Fayetteville, AR
Covault, J., Bureau of Economic Geology, The University of Texas at Austin, Austin, TX

Spatiotemporal variations in tectonic style, as expressed by evolving topography, exert a primary control on how sediment is generated and transported from source to sink in terrestrial systems and can influence basin-fill architecture, reservoir presence, and quality. During Late Cretaceous-Paleogene time, Texas was situated in a transitional tectonomorphic landscape between nascent Laramide topography and the Mexican Cordillera. There is considerable uncertainty surrounding the Cretaceous-Paleogene sediment routing systems that dissected this region, including dispersal pathways, catchment extent, and debouchment locations. A robust sediment-routing framework is vital to estimating sediment delivery to the Gulf of Mexico, and, broadly, understanding source-to-sink sediment transfer in systems defined by distinct, evolving tectonomorphic provinces.

We present new, depth-profiled LA-ICP-MS detrital zircon (DZ) U-Pb ages (7119 ages from 52 samples) from Cretaceous-Paleogene fluvial-deltaic sediments in south Texas and the Tornillo Basin of west Texas that offer new insights into the stratigraphic and sediment-dispersal evolution of the Texas source-to-sink system. DZ U-Pb age spectra are characterized by dominant Paleogene-Late Cretaceous age modes, subordinate Jurassic, 1.1, 1.4, and 1.7 Ga and minor Permo-Triassic, Silurian-Ordovician, and Neoproterozoic age modes, and a scarcity of Early Cretaceous DZ ages, typical of sources from the Western U.S. but not from western Mexico. DZ core and rim age relationships show three main clusters: Jurassic cores with Late Cretaceous rims, 1.1 Ga cores with Ediacaran-Ordovician rims, and 1.4-1.7 Ga cores with Late Cretaceous-Paleocene rims. Detrital zircon U-Pb ages, including core and rim relationships, suggest that south Texas rivers received sediment from a mixture of recycled sedimentary, volcanic, and basement source terranes in Arizona (e.g., K-Pg volcanic centers), northeastern Mexico (Chihuahua Trough and Sabinas Uplift), southern Colorado/New Mexico (e.g., Colorado Mineral Belt and basement uplifts), and west Texas (Trans-Pecos volcanic field). This interpreted catchment area is extensive, incorporating large portions of the southwestern U.S. and northeastern Mexico where it drained a tectonically active hinterland characterized by first-cycle magmatic input and sedimentary recycling of Laramide inversion structures. We interpret a three-stage tectonic evolution of the paleo-catchment area: incipient Laramide volcanism and rift inversion in the late Cretaceous followed by a period of relative sediment source and catchment area stability during the Paleocene-Eocene which is then interrupted by the onset of Trans-Pecos volcanism during the Eocene-Oligocene. This study demonstrates the control a dynamic, evolving tectonomorphic landscape exhibits on the sediment-dispersal evolution of long-lived, major river systems.

Keywords: Texas, Provenance, Detrital Zircon Geochronology, Sediment Routing, Cordillera, Laramide

LCPHD-28

SETP
LCPHD

Length scales and types of heterogeneities along the deep subduction interface: Insights from an exhumed subduction complex on Syros Island, Greece

Alissa Kotowski
Kotowski, A., The University of Texas at Austin, Austin, TX
Behr, W., The University of Texas at Austin, Austin, TX
Ashley, K., The University of Pittsburgh, Pittsburgh, PA
Tong, X., The University of Texas at Austin, Austin, TX
Lavier, L., The University of Texas at Austin, Austin, TX

The rheology of the deep subduction interface strongly influences the occurrence, recurrence, and migration of episodic tremor and slow slip (ETS) events. To better understand the environment of deep ETS, we characterize the length scales and types of rheological heterogeneities that decorate the deep interface using an exhumed subduction complex. The Cycladic Blueschist Unit on Syros, Greece, records Eocene subduction to ~60 km, partial exhumation along the top of the slab, and final exhumation along Miocene detachment faults. The CBU reached 450-580?C and 14-16 kbar, PT conditions similar to where ETS occurs in several modern subduction zones.

Rheological heterogeneity is preserved in a range of rock types on Syros, with the most prominent type being brittle pods embedded within a viscous matrix. Prograde, blueschist-facies metabasalts show strong deformation fabrics characteristic of viscous flow; cm- to m-scale eclogitic lenses are embedded within them as massive, veined pods, foliated pods rotated with respect to the blueschist fabric, and attenuated, foliation-parallel lenses. Similar relationships are observed in blueschist-facies metasediments interpreted to have deformed during early exhumation. In these rocks, metabasalts form lenses ranging in size from m- to 10s of m and are distributed at the m-scale throughout the metasedimentary matrix. Several of the metamafic lenses, and the matrix rocks immediately adjacent to them, preserve multiple generations of dilational veins and shear fractures filled with quartz and high pressure minerals.

These observations suggest that coupled brittle-viscous deformation under high fluid pressures may characterize the subduction interface in the deep tremor source region. To test this further, we modeled the behavior of an elasto-plastic pod in a viscous shear zone under high fluid pressures. Our models show that local stress concentrations around the pod are large enough to generate transient dilational shear at seismic strain rates. Scaling the model up to a typical source area for deep tremor suggests these heterogeneities may yield a seismic moment similar to those calculated for tremor bursts in modern subduction zones.

Keywords: subduction, Episodic Tremor and Slow Slip, blueschist, eclogite

LCPHD-29

SETP
LCPHD

High Andean deformation, exhumation, and foreland basin deposition during Neogene changes in subduction zone geometry (32°S)

Chelsea Mackaman-Lofland
Mackaman-Lofland, C., University of Texas at Austin
Horton, B., University of Texas at Austin
Stockli, D., University of Texas at Austin
Capaldi, T., University of Texas at Austin
Orozco, P., Universidad Nacional de San Juan
Alvarado, P., Universidad Nacional de San Juan
Fuentes, F., YPF
Constenius, K., University of Arizona

The southern Central Andes at 27°00'S to 33°30'S represent a premier modern example of flat-slab subduction, high-magnitude thrust belt shortening, and basement-involved deformation in the foreland. Thin- and thick-skinned shortening and uplift of the Andean Cordillera at ~32°S, which locally reaches elevations >6000 m, has been variably associated with Miocene flattening of the subducting Nazca plate, maintenance of retroarc thrust-belt critical wedge taper, and/or reactivation of inherited structures. We present new detrital zircon U-Pb age distributions for synorogenic clastic fill of the Manantiales Basin and apatite (U-Th)/He (AHe) cooling ages for Andean fault blocks to pinpoint the retroarc time-space deformation record and resolve the contrasting kinematic histories and mechanical models proposed for the region. Detrital zircon U-Pb age distributions for the Manantiales deposits constrain foreland basin accumulation from at least 18.6 ± 1.1 to 14.9 ± 3.2 Ma, and show early inversion and sediment contributions from the thin-skinned western Andean cordillera followed by unroofing of the fold-thrust belt in the central and eastern cordillera, consistent with predicted thrust-belt critical wedge deformation patterns. AHe cooling ages constrain thick-skinned uplift and exhumation along the eastern Andean front to ~5-14 Ma. These cooling ages overlap the timing of wholesale shortening and exhumation in the Precordillera structural province to the east, suggesting a regional mid- to late Miocene pulse of thin- and thick-skinned deformation. At 32°S, the deformation pulse coincides temporally with Juan Fernandez Ridge collision, slab flattening, and the resulting inboard sweep of volcanism ca. 9-12 Ma, and may reflect either increased plate coupling or thermal weakening of the upper plate associated with the change in subduction geometry and arc volcanism. Finally, we interpret late Miocene–Pliocene (~2-5 Ma) AHe cooling ages in the hinterland cordillera to reflect passive uplift along reactivated west-vergent structures during the most recent stage of Andean orogenesis.

Keywords: Andes; Argentina; flat-slab subduction; fold-thrust belt; foreland basin; provenance; U-Pb geochronology; apatite (U-Th)/He thermochronology

LCPHD-30

SETP
LCPHD

Thermotectonic evolution of rifting to collision of the central to eastern Iberian-European margin using multi-mineral U-Pb and (U-Th)/He thermochronometery

Margaret Odlum
ODLUM, M., Dept. of Geological Sciences, Jackson School of Geosciences, Austin TX
STOCKLI, D., Dept. of Geological Sciences, Jackson School of Geosciences, Austin TX

The Pyrenees mountains are the result of inversion of the Early Cretaceous rift during the Late Cretaceous-Oligocene collision between the Iberian and European continental margins. Lower to upper crustal rocks exposed in the North Pyrenean Zone (NPZ) preserve the geological and tectonic record of Early Cretaceous rifting, Late Cretaceous inversion, and Cenozoic shortening associated with the Pyrenean orogeny. Basement massifs in the NPZ represent tilted crustal sections, exposing upper to lower crustal metamorphic and magmatic rocks. The highest-grade granulitic gneisses are found at the southern parts of the massif along the suture, with decreasing metamorphic grade toward the north. Samples collected along a crustal transects across the Agly (eastern NPZ) and Saint Barthelemy (central NPZ) massifs were analyzed using zircon, rutile, and apatite (high T: >800-450°C) U-Pb and zircon (U-Th)/He thermochronometry (low-T: ~210-180°C) to constrain the thermo-tectonic history of the central and eastern Iberian-European margin during extension, inversion, and crustal shortening.

Zircon U-Pb ages record the crystallization ages of the granites and metamorphism of the gneisses during the Late Paleozoic Variscan orogeny (~300 Ma). Apatite U-Pb ages from the northern parts of the massifs show similar Late Carboniferous crystallization ages. Rutile and apatite U-Pb ages from structurally deeper granulites in the southern part of the massifs exhibit Aptian-Albian ages cooling ages (~125-100 Ma), suggesting that these lower structural levels of the massifs were rapidly exhumed from lower crustal levels during large magnitude extension and continental break-up. These data are interpreted to document rapid cooling during crustal thinning and synrift exhumation of middle-lower crust. While high-temperature U-Pb thermochronometers document the late Variscan and early Cretaceous tectonic phases, low-temperature zircon (U-Th)/He ages (ZHe) record the inversion and orogenic exhumation of the margin. In the Agly massif, ZHe ages are Late Cretaceous (Coniacian-Maastrichtian (~90-66 Ma)). These ages are interpreted to record cooling associated with underthrusting of the Iberian margin beneath Europe, and exhumation related to earliest Pyrenean orogenic inversion/shortening. In the Saint Barthelemy massif, ZHe ages range from Santonian to Eocene (~83-50 Ma), record Late Cretaceous inversion and synorogenic exhumation during the Eocene.

These new high-temperature thermochronometric data record a period rapid syn-rift exhumation of the basement massifs related to extreme crustal attenuation and hyperextension in the Aptian-Albian. The low-temperature thermochronometers record the earliest orogenic related cooling in the east beginning in the and how the exhumation related cooling propagated westwards through time as the V-shaped rift domain closed and the rift inverted. Integrated, these ages from the Agly and Saint Barthelemy massifs reveal the tectonic evolution of Early Cretaceous extension followed by Late Cretaceous inversion and Cenozoic orogenesis along central and eastern Iberian-European margin, and highlight the along strike variation in rifting and how the inherited rift architecture controlled the inversion and orogenic evolution.

Keywords: Pyrenees, thermochronometry, tectonic inversion, hyperextension

LCPHD-31

SETP
LCPHD

Rates of Olivine Grain Growth in 'Damp' Natural Dunites During Dynamic Recrystallization and Post-deformation Annealing

Pamela Speciale
Speciale, P., Jackson School of Geosciences, The University of Texas at Austin, Austin, TX
Behr, W., Jackson School of Geosciences, The University of Texas at Austin, Austin, TX
Hirth, G., Earth, Environment and Planetary Sciences, Brown University, Providence, RI
Tokle, L., Earth, Environment and Planetary Sciences, Brown University, Providence, RI

The rate of olivine grain growth has profound implications for the strength of rocks in the upper mantle and the timescales over which plate boundary shear zones persist in the mantle lithosphere. Current grain growth laws are based on static annealing experiments on synthetic olivine aggregates under a limited range of conditions. Experiments under water-saturated conditions at relatively low pressure (300 MPa) yield high growth rates, whereas those on dry Forsterite sol-gel at high pressure (1200 MPa) predict significantly slower growth rates. Here we investigate olivine grain growth rates during and after deformation through high pressure, axial compression experiments on 'damp' (~160 H/10^6Si), natural dunites. We conducted four types of experiments at 1000-1200°C, 10^{-4}-10^{-6} s^{-1}, and 1300 MPa confining pressure: 1) constant strain rate, 2) strain rate stepping, with decreased strain rate, 3) post-deformation stress relaxation, and 4) hydrostatic annealing. We compared our results with similar stress relaxation tests performed by van der Wal (1993) on the Anita Bay and Åheim dunites (1200-1300°C). Growth rates are in good agreement with the relation d_f^p-d_0^p=Kt, with grain size (d) in meters, a growth exponent (p) of 3, time (t) in seconds, and a growth rate (K) composed of $K=k_0[\exp(-Q/R/T)]$, with an activation enthalpy (Q) of 527 kJ/mol and pre-exponential term (k_0) of 2.5 m^3s^{-1}. This results in a grain growth rate substantially slower than that predicted by existing grain growth laws for water-saturated olivine, but faster than predicted for dry olivine. These results are most applicable to ambient mantle lithosphere in orogenic environments, whereas the water-saturated and dry olivine grain growth laws are more applicable to the mantle wedge above active subduction zones, and melt-depleted cratonic lithosphere, respectively.

Keywords: experimental deformation, olivine, grain size evolution, stress relaxation, strain localization

LCPHD-32

SETP
LCPHD

Correlating Submarine Fan Complexes using Detrital Zircon Geochronometry

Kelly Thomson
Thomson, K., Department of Geological Sciences, Jackson School of Geosciences, The University of Texas at Austin, Austin, TX
Stockli, D., Department of Geological Sciences, Jackson School of Geosciences, The University of Texas at Austin, Austin, TX
Clark, J., Statoil Research Center, Austin TX
Fildani, A., Statoil Research Center, Austin TX

Early-Middle Eocene turbidite deposits of the Hecho Group in the Ainsa – Jaca Basins in the south central Pyrenees (Spain) preserve the detrital erosional record from the main phase of Pyrenean mountain building. The Hecho Group turbidites have been studied by academic and industry researchers and aided in developing fundamental concepts of turbidite and submarine fan deposition in foreland basin depositional systems. Stratigraphic correlations across the sections of the Ainsa Basin channelized turbidite complexes and the Jaca basin submarine fan complexes are hindered and obscured by discontinuous lateral exposures and syn-depositional structural partitioning. Even after decades of research intra-basin stratigraphic correlations based on field mapping, detailed stratigraphic measurements, magnetostratigraphy, biostratigraphy, sequence stratigraphy, and statistical comparison of framework petrography are still debated. Differences among these models have major implications for interpretations of stratigraphic scaling relationships, reservoir connectivity, and for mass balance reconstructions.

This study proposes a new statistic approach to test the robustness of different stratigraphic correlations through statistical comparison of detrital zircon U-Pb (DZ) age distributions from key stratigraphic horizons in the Ainsa-Jaca basins deep marine sediment routing system. Vertical stratigraphic transects from the Ainsa and Jaca basins were analyzed for DZ U-Pb signatures to fingerprint provenance of siliciclastic input entering the basin and to examine how these provenance signatures change/evolve through time. This study assumes that the DZ age spectra are stable and consistent across laterally correlatable units and that the presence and proportion of specific age components are indistinguishable in the downstream axial direction for a given stratal horizon. This study utilizes established and recently developed statistical methods for the comparison of DZ distributions, such as the Kolmogorov-Smirnov (K-S) test, Kuiper test, and R^2 cross correlation coefficient. Preliminary results indicate that while several correlation models provide “good fits” in comparing DZ distributions at specific horizons, none of the proposed models provide “good fits” across the entire Hecho Group stratigraphic basin sequence. This discrepancy is interpreted to reflect additional processes that modify the DZ age distributions, such as additional transverse sediment input downstream from the Ainsa Basin, fractionation of specific age component by hydraulic sorting and selective deposition, autogenic variability in the proportion of age components within a single system, or statistical and analytical uncertainty introduced through inadequate single grain analysis. This study also has regional implications for the provenance evolution of the Pyrenean orogeny as well as broad implications for the downstream modification of provenance signals via fractionation and mixing processes, source-to-sink scaling relationships, basin scale mass balance calculations, and constraining reservoir connectivity in basin floor fans.

Keywords: Pyrenees, Detrital Zircon Geochronometry, Submarine Fans, Stratigraphy, Foreland Basin, Ainsa Basin, Tectonics & Sedimentation

SETP
LCPHD

A Plastic Formulation of Rate and State Dependent Friction: Emergence of Slip Transient and Earthquakes

Xinyue Tong
Tong, X., Jackson School of Geoscience
Lavier, L., Jackson School of Geoscience

We develop a numerical model for lithospheric deformation that can simulate both long term tectonic (LTT) behavior as well as the seismic cycle. The implementation is a finite element model with a Mohr-Coulomb elastic plastic formulation of rate-and-state dependent friction which can simulate the deformation processes from milliseconds to 100k years. The model takes into account the velocity weakening and strengthening effects by using a rate dependent friction law that is a function of <a-b>. The state variable is the result of plastic weakening or strengthening that decrease or increase the maximum shear stress as a function of the rate dependent frictional effects. We test our formulation on a simple stick-slip experiment at the tectonic scale. The model consists of a single fault of finite thickness with uniform friction properties. By varying both the width of the fault zone and <a-b> we can reproduce fast and slow earthquakes that follow both theoretical and observational scaling relationships. In addition, the model suggests that slow transients differ from earthquakes because most of the mechanical work is spend accumulating inelastic strain while earthquakes use the mechanical work to slip frictionally over the fault interface.

Keywords: Long Term Tectonic, Geodynamics, Seismic Cycle, Numerical Modeling, Earthquakes, Slow Slip Events

SHP
LCPHD

Topographic Control on the Subsurface Heat Budget of Ice Wedge Polygons

Charles Abolt
Abolt, C., Department of Geological Sciences, The University of Texas at Austin, Austin, TX
Young, M., Bureau of Economic Geology, The University of Texas at Austin, Austin, TX
Atchley, A., Earth and Environmental Sciences Division, Los Alamos National Laboratory, Los Alamos, NM
Harp, D., Earth and Environmental Sciences Division, Los Alamos National Laboratory, Los Alamos, NM

Permafrost degradation in ice wedge polygon terrain has accelerated in the last three decades, resulting in drastic changes to tundra hydrology which may impact rates of soil organic carbon mobilization. The goal of this research is to determine to what extent the near surface thermal regime, and hence the vulnerability of the upper permafrost, is controlled by surface topography in ice wedge polygons. The central hypothesis is that energy is preferentially transferred into the polygon subsurface in summer at low, wet zones (such as low-centered polygon centers and troughs), then released to the atmosphere in winter through elevated zones (such as rims) that are less insulated by snowpack. Disturbance to the approximate balance between these seasonal energy fluxes may help explain the onset and development of thermokarst. In this work, we present a numerical model of thermal hydrology in a low-centered polygon near Prudhoe Bay, Alaska, constructed within the Advanced Terrestrial Simulator, a state of the art code that couples a meteorologically driven surface energy balance with equations for surface and subsurface conservation of mass and energy. The model is calibrated against a year of daily ground temperature observations throughout the polygon and used to quantify meter-scale zonation in the subsurface thermal budget. The amount of relief in the rims and the trough of the simulated polygon is then manipulated, and simulations are repeated including a pulse of one warm year, to explore the extent to which topography may influence the response of permafrost to increased air temperatures. Results suggest that up to 80% of energy entering the ground at the polygon trough during summer is released back to the atmosphere through the rims in winter, enhancing cooling of the ice wedge and producing a modest effect on active layer thickness. Simulated polygons with deeper, wetter troughs can sustain thicker active layers than other polygons in average years, but ice wedges in all polygons are most vulnerable to thaw during sporadic warm summers. The results quantify current understanding of positive feedbacks during thermokarst development, and are compatible with historical observations indicating that ice wedge degradation tends to occur in discrete pulses, rather than as a gradual process.

Keywords: permafrost, thermokarst, Arctic, climate change, numerical modeling

SHP
LCPHD

Coupling Aeolian Stratigraphic Architecture to Paleo-Boundary Conditions: The Scour-Fill Dominated Jurassic Page Sandstone

Benjamin Cardenas
Kocurek, G., Jackson School of Geosciences, The University of Texas at Austin, Austin, TX
Mohrig, D., Jackson School of Geosciences, The University of Texas at Austin, Austin, TX
Swanson, T., Department of Earth Science, Rice University, Houston, TX
Hughes, C., Jackson School of Geosciences, The University of Texas at Austin, Austin, TX
Brothers, S., National Academies Space Studies Board, Washington, D.C.

The stratigraphic architecture of aeolian sandstones is a function of dune autogenics and allogenic boundary conditions within which the dune field evolves. Mapping of outcrop-scale bounding surfaces and sets of cross-strata between these surfaces for the Jurassic Page Sandstone near Page, AZ, USA, demonstrates that dune autogenics were dominated by variable dune scour depth, whereas the dominant allogenic boundary conditions were antecedent topography and water-table position. At the study area, the Page Sandstone is ~ 60 m thick and is separated from the underlying Navajo Sandstone by the J-2 regional unconformity, which shows meters of topographic relief. Filling J-2 depressions are thin sets of cross-strata showing climbing architectures. In contrast, the overlying Page consists of packages of one to a few, meter-scale sets of cross-strata between the outcrop-scale bounding surfaces. These surfaces, marked by polygonal fractures and local overlying sabkha deposits, are regional in scale and correlated to high stands of the adjacent Carmel sea. Over the km-scale outcrop, the surfaces show erosional relief and packages of cross-strata are locally truncated (Figure 1). Absent within the packages of cross-strata are early dune-field accumulations, interdune deposits, and apparent dune-climbing. These strata are interpreted to represent a scour-fill architecture created by migrating large dunes within a mature dry aeolian system, in which early phases of dune-field construction have been cannibalized and dune fill of the deepest scours is recorded. At low angles of climb, set thickness is dominated by the component of scour-depth variation over the component resulting from the angle of climb. After filling of J-2 depressions, the Page consists of scour-fill accumulations formed during low stands. Carmel transgressions limited sediment availability, causing deflation to the water table and development of the regional bounding surfaces. Each subsequent fall of the water table with Carmel regressions renewed sediment availability, including local breaching of the resistant surfaces and cannibalization of Page accumulations. The Page record exists because of preservation associated with Carmel transgressions and subsidence, without which the Page would be represented by an erosional surface.

Keywords: sedimentology, aeolian

SHP
LCPHD

Influence of Waves and Tides on Delta-Front and Upper Slope Turbidity Currents and their Deposits: An Outcrop and Laboratory Study

Max Daniller-Varghese
Daniller-Varghese, M., University of Texas at Austin
Smith, E., Colorado College
Mohrig, D., University of Texas at Austin
Myrow, P., Colorado College
Goudge, T., University of Texas at Austin
Hassenruck-Gudipati, H., University of Texas at Austin
Koo, W., University of Texas at Austin
Mason, J., University of Texas at Austin
Swartz, J., University of Texas at Austin
Kim, J., University of Texas at Austin

Recent research on interactions of turbidity currents with waves and tides highlight both their importance and complexity. The Elkton Siltstone at Cape Arago, Oregon, USA, preserves a rhythmically bedded deposit that we interpret as the product of tidally modified hyperpycnal flows under the influence of water-surface waves. Evidence for this is taken from couplet thickness measurements consistent with semidiurnal flood and ebb tides arranged into monthly cycles. These deposits were likely sourced from a suspended sediment-laden river plume; thin, fine beds represent deposition during flood tide, and thick, coarse beds represent deposition during ebb tide. Sedimentary structures within the rhythmites change within a proximal and distal section, but both sections preserve combined-flow bedforms within the thin beds. Our paleo-topographic reconstruction has the proximal deposits located immediately down-dip of the shelf slope-break and the distal deposits located ~1.5km further offshore in ~125m greater water depth. We present experimental results from wave-influenced turbidity currents calling into question the interpretation that combined-flow bedforms necessarily represent deposition at or above paleo-wave base. Turbidity currents composed of quartz silt and very fine sand were released into a 10m long, 1.2m deep tank. Currents ran down a 9-degree ramp with a motor driven wave-maker positioned at the distal end. The currents interacted with the wave field as they travelled downslope into deeper water. While oscillatory velocities measured within wave-influenced turbidity currents decreased with distance downslope, the maximum oscillatory velocities measured in the combined-flow currents at depth were five to six times larger than those measured under a wave field without turbidity currents. These results suggest that combined-flow turbidity currents can transmit oscillating-flow signals beneath the effective wave base. Bed thicknesses, grain-size data and sedimentary structures measured in the rhythmically bedded, combined-flow turbidites of the Elkton Siltstone will be interpreted in the context of these experiments.

Keywords: Turbidity Currents, Experimental Sedimentology, Oregon, Signal Processing

SHP
LCPHD

Groundwater-Surface Water Interactions in a Dam-Regulated River: Hydrologic Processes and Water Quality Implications

Stephen Ferencz
Ferencz, S., Jackson School of Geosciences, University of Texas at Austin, Austin, TX
Cardenas, M., Jackson School of Geosciences, University of Texas at Austin, Austin, TX
Nielson, B., Utah Water Resource Laboratory, Utah State University, Logan, UT
Watson, J., Jackson School of Geosciences, University of Texas at Austin, Austin, TX

A majority of the world's largest river systems are regulated by dams. In addition to being used for water resources management and flood prevention, many large dams are also used for hydroelectric power generation. In the United States, dams account for 7% of domestic electricity, and hydropower accounts for 16% of worldwide electricity production. To help meet electricity demand during peak usage times, hydropower utilities often increase their releases of water during high demand periods. This practice, termed hydropeaking, can cause large transient flow changes downstream of hydroelectric dams. These transient flow increases can result in order of magnitude daily fluctuations in discharge, and the released water can have different thermal and chemical properties than ambient river water. As hydropeaking releases travel downstream, the temporary rise in stage and increase in discharge can enhance surface water-groundwater (SW-GW) exchange between the river and its alluvial aquifer. This dam-induced SW-GW exchange, combined with hydrodynamic attenuation and heat exchange processes, result in complex behavior as a hydropeaking release travels downstream.

The dam-regulated Lower Colorado River downstream of Austin, TX was used as a natural laboratory to observe SW-GW interactions and downstream transport of water, heat, and solutes under hydropeaking conditions. To characterize SW-GW interactions, well transects were installed in the banks of the river to observe exchanges between the river and alluvial aquifer. The well transects were installed at three different distances from the dam (15km, 35km, and 80km). At each well transect conductivity, temperature, and pressure sensors were deployed in the monitoring wells and in the channel. Additional conductivity and temperature sensors were deployed along the study reach to provide a more detailed record of heat and solute transport during hydropeaking releases. The field data spans over two months of daily dam releases that were punctuated by two large natural storm events. To our knowledge, this study is the first to use multiple downstream field sites to characterize how dam-induced SW-GW interactions and in-stream temperature and solute transport behave under hydropeaking conditions.

Keywords: surface water-groundwater interactions, hyporheic, heat, hydropeaking, dam regulation

SHP
LCPHD

Detrital zircon U-Pb geochronology of modern river sands in the Ecuadorian Andes: implications for tectonic history and sediment recycling

Lily Jackson
Jackson, L., Jackson School of Geosciences, University of Texas at Austin
Horton, B., Jackson School of Geosciences, University of Texas at Austin
Vallejo, C., Escuela Politécnica Nacional, Quito, Ecuador

Proposed reconstructions of the Ecuadorian Andes involve contrasting estimates of the timing and style of key orogenic events. U-Pb detrital zircon geochronology of unconsolidated sands from modern rivers with catchment areas spanning different morphotectonic regions yield diagnostic U-Pb age spectra for those regions. Thus, detrital zircon age spectra provide insight into tectonic history by means of elucidating sediment provenance and recycling. We present 1700 new detrital zircon U-Pb ages from 15 samples of unconsolidated sands from 11 rivers in Ecuador that show distinct U-Pb age spectra for various morphotectonic regions. (1) The Oriente Basin is a Cretaceous–Quaternary retroarc foreland basin that is flat-lying in the east (Oriente) with localized uplifts in the west (Subandean Zone). Jurassic arc rocks are restricted to the Subandean Zone, and together with Cretaceous-Neogene sediments make up the dominant surface exposures. River sands in the Oriente-Subandean Zone show a distinctive Jurassic U-Pb age peak, as well as Triassic and Cretaceous age peaks. (2) The Eastern Cordillera contains metamorphosed Paleozoic-Mesozoic rocks and non-metamorphosed Triassic to Jurassic igneous intrusions. Sands from rivers in the Eastern Cordillera have substantial U-Pb age populations of Proterozoic and Paleozoic ages, representing recycled cratonic material. Paleogene-Neogene populations also appear in Eastern Cordillera samples. (3) The Western Cordillera contains Late Cretaceous basement rocks of oceanic plateau origin and intraoceanic island arc sequences, together with Upper Cretaceous-Paleogene sedimentary rocks and Neogene-Quaternary volcanic cover. River sands from the Western Cordillera contain Neogene-Quaternary age populations with minor Triassic and Cretaceous ages. River samples draining Paleogene units in the easternmost Western Cordillera show Proterozoic and Paleozoic ages indicative of exhumation, erosion, and westward transport of detritus from the Eastern Cordillera. Furthermore, the dominant Proterozoic and Paleozoic ages that characterize the Eastern Cordillera rivers provide support for multiple recycling events prior to the current tectonic configuration of the Ecuadorian Andes.

Keywords: Detrital zircon, U-Pb geochronology, Ecuador, modern rivers, tectonics

SHP
LCPHD

MATLAB geoChemistry: An open source geochemistry solver based on MRST

Colin McNeece
McNeece, C., Department of Geoscience, The University of Texas at Austin
Raynaud, X., SINTEF - Mathematics and Cybernetics
Hesse, M., Department of Geoscience, The University of Texas at Austin
Nilsen, H., SINTEF - Mathematics and Cybernetics

The solution of complex geochemical systems is necessary to study many geologically relevant phenomena. To address this need we have incorporated a geochemical system solver into the open source Matlab Reservoir Simulation Toolbox (MRST). The implementation supports equilibrium aqueous speciation, surface complexation (including the CD-MUSIC model), ion exchange, dissolution/precipitation, and redox chemistry. The suite of tools available in MRST makes batch and transport simulations seamless allowing for rapid model development, in particular the ability to explore different domain geometries and transport physics. The solver leverages the automatic differentiation tools available in MRST to solve arbitrarily complex geochemical systems with any choice of species or element concentration as input. Three novel mathematical approaches improve the convergence of the solver 1) the choice of elements as the basis components makes all entries in the composition matrix positive, 2) log variables are used which transfers the nonlinearity to the composition matrix, 3) a priori bounds on variables are calculated from the structure of the problem including species concentrations, element concentrations, and electrostatic terms.

Keywords: geochemistry, scientific computing, reservoir simulation

SHP
LCPHD

Groundwater Dynamics and Export from Active Layer Aquifers Overlying Permafrost

Michael O'connor
O'Connor, M., Department of Geological Sciences, The University of Texas at Austin, Austin, TX
Nicholaides, K., Department of Geological Sciences, The University of Texas at Austin, Austin, TX
Cardenas, M., Department of Geological Sciences, The University of Texas at Austin, Austin, TX
Neilson, B., Utah Water Research Lab, Utah State University, Logan, UT
Kling, G., Department of Ecology and Environmental Biology, The University of Michigan, Ann Arbor, MI

Vast reservoirs of organic matter become accessible each summer when Arctic soils thaw. Groundwater transports this organic matter into streams, where it can be respired into CO2. Many have speculated that groundwater volumes might increase as the climate warms; however, such speculation requires a robust characterization of the hydraulic properties and geometries of the temporary aquifer through which this groundwater flows. Here we present observations and model results describing how groundwater fluxes evolve seasonally and spatially in the temporary ‘aquifers’ underlying the Alaskan North Slope. Saturated and unsaturated permeability and porosity exhibited extreme vertical variability but maintained lateral consistency at different depths. Aquifer saturated thicknesses were controlled by sub-meter topographic features rather than regional topographic gradients. Such variation creates a fluctuating ice table, developing groundwater flow paths that mimic surface topography and skew residence time distributions. We used observed hydraulic properties and aquifer geometries to calculate how groundwater export evolves during a wet year between early and late summer. Despite a deepening of the saturated zone, resulting in large decreases in permeability and groundwater velocity, groundwater fluxes were larger in August than June because the saturated zone expanded sufficiently. However, historical data suggests the opposite could be true under dry conditions where minor fluctuations in the water table elevation could switch the active layer from an effective to ineffective transmitter of groundwater. The significant effects exerted by microtopography and soil property variability on groundwater flow underscore the need for them to be accurately represented within any future groundwater flow predictions.

Keywords: groundwater, permafrost, active layer, climate change

LCPHD-41

SHP
LCPHD

Identification and preliminary characterization of the Lycium Member bed features in the Fish Creek-Vallecito Basin: Antidunes, cyclic steps, and more from a proto-Gulf of California deepwater supercritical fan

Logan West
West, L., Dept of Geosciences, The University of Texas at Austin, Austin, TX
Steel, R., Dept of Geosciences, The University of Texas at Austin, Austin, TX
Olariu, C., Dept of Geosciences, The University of Texas at Austin, Austin, TX
Mohrig, D., Dept of Geosciences, The University of Texas at Austin, Austin, TX
Covault, J., Bureau of Economic Geology, The University of Texas at Austin, Austin, TX

Study of seafloor bathymetry, numerical and physical modeling, and direct observation of turbidity currents increasingly suggests that sediment gravity flows over moderately steep basin slopes commonly reach Froude supercritical states. However, interpretation of supercritical features in deepwater outcrops remains limited in both quantity and scope, leaving stratigraphic qualities of supercritical deposits poorly understood. Slope turbidites on along steep margins of the early Gulf of California are exposed in seismic scale outcrops of the Late Miocene (~6.3-5.3 Ma) Lycium Member in the Fish Creek-Vallecito Basin of south-central California. In this work, we analyze the 100+ m-thick, strongly aggradational slope deposits containing 10-15 bedsets that do not fit well into classical models of deepwater depositional architecture.

Measured sections, bedding orientation, and facies descriptions collected both for strike- and dip-oriented sections are combined with photogrammetry to characterize selected bedsets in three-dimensions. Stacks of 10s of multiple turbidite sandstone beds intercalated with mudstones – all accreting opposite to paleoflow indicators – build into bedsets thought to represent the preserved stratigraphic record of different potential supercritical bedforms, including antidunes and cyclic steps.

Bedset geometries show wavelengths and widths of tens to hundreds of meters and heights of 5-15 m. Bedsets are separated along broader bounding surfaces where bed attitudes change significantly. Bounding surfaces can be erosional with 1-3 m incision or "conformable" with either a similar facies below and above and/or no incision into underlying strata. Bounding surfaces show some lateral variability, suggesting 3D bedforms with some crest-trough sinuosity.

Within the bedsets, individual beds have low-angle sinusoidal to sigmoidal down dip (paleoflow) geometries and lensoidal strike geometries. Bedding facies are dominated by 5-50 cm thick, normally graded, laminated sandstones capped by 1-3 cm bioturbated muds. Sandstones transition into interbedded sandstones and silty mudstones or 1-2 m thick silty mudstones. Present also are incisional, steeply dipping backsets of 0.5-3 m-thick boulder-rich, amalgamated, structureless sandstones with abundant soft sediment deformation that can transition downflow into arching, thinning, normally-graded sandstones.

Lycium slope deposits are here interpreted as having been built by successive Froude supercritical sediment gravity flows in the lower slope of a steep, narrow, and relatively shallow margin in the proto-Gulf of California.

Keywords: Deepwater, Gulf of California, Froude supercritical, FishCreek-Vallecito, antidune, cyclic step

SHP
LCPHD

Weighing controls on shoreline and shelf-margin growth: Insights from Wilcox Group, Gulf of Mexico and numerical models

Jinyu Zhang
Zhang, J., JSG, UT-Austin

This research investigates the relative importance of sediment supply, accommodation, and a series of morphological parameters in controlling shoreline migration, the fundamental process and building block during the accretion of entire shelf-margin sedimentary prism. A better understanding of these controls provides insights on different source-to-sink systems and on the evaluating hydrocarbon potential of frontier basins. These studies were carried out in Wilcox Group, Gulf of Mexico and include two numerical modeling studies.

The greenhouse Wilcox shoreline shows repeated long-distance shoreline regression and retreat, in fact about 37 times during building of Wilcox Group, a stratigraphic scenario a bit different from previous hypotheses that the shoreline movement in low-amplitude, low-frequency greenhouse conditions should be limited. We therefore, suggest that the Wilcox shoreline was controlled by both greenhouse eustasy and variable sediment supply, likely the latter caused by Paleogene hyperthermals. Furthermore, integrated analysis on the paleohydrology of feeder channels, shelf-edge trajectory, and published eustatic curve indicates that a decreasing sediment supply and increasing accommodation control the transition of Lower Wilcox shelf margin from being progradation-dominated to aggradation-dominated.

BQART model, a widely accepted method of reconstructing sediment load, and Monte Carlo simulation are used for reconstructing the Paleogene Wilcox sediment supply. By comparing with the downstream sediment record, this method shows reliable accuracy and precision. The downstream sediment records are mostly within P10-P90 reconstructed sediment load. This study also shows various tectonic, climatic, and geologic factors controlling the sediment supply.

A geometric model of shoreline regression is integrated with sensitivity analysis to understand the relative importance of controls on the formation of highstand shelf-edge deltas. The result indicates the formation of highstand shelf-edge deltas is controlled by multiple accommodation and morphological parameters. Among them, the shelf width is the most important control, whereas subsidence and eustasy are much less important than previous literature implied.

This dissertation emphasizes that there are multiple factors that control the shoreline and shelf-margin growth. It is important for future researches to develop and assess multiple hypotheses for evaluating combinations of controls including sediment supply, relative sea level, and morphological parameters

Keywords: Shoreline, Shelf margin, GoM, Wilcox

U

Pyroclastic Flows from Mount St. Helens: The Effects of Topography on Flow Behavior and Deposition on the Leeward Slope

Elizabeth Davis
Davis, E., The University of Texas at Austin, Austin, TX

Pyroclastic flows are high temperature mass flows that contain volcanic debris mobilized by gas. Topography has been seen to have large effects on the flow paths of pyroclastic flows. These flow paths can be determined by examining trees and other scorched vegetation. Trees in pyroclastic flow paths often appear to be bent or toppled in the direction of flow; however, at Mount St. Helens, there are patches of trees that remain upright in the middle of the surge zone. These upright trees are all located on the lee side, or downwind side, of a topographic ridge. The behavior of pyroclastic flows on the leeside of ridges is not well understood and the factors that determine how the flow will react to the presence of a ridge are unknown. This work is one of the first to directly examine how pyroclastic flows respond to partial blocking and traverse the lee side of a ridge. Laboratory experiments were used to model the effects of topography on flow behavior. These experiments were conducted at the Smithsonian Institution and utilized heated talc powder in air to simulate dilute pyroclastic flows. Thermocouples were evenly distributed along the flow path, providing detailed temperature data. High definition cameras at three strategic locations were used to film each experiment. Topographic barriers were constructed and placed at different distances along the flow path. The heights, widths, and slopes of the barriers were also varied. Flows that interacted with a barrier were observed to lift off sooner than those with no obstruction in every case. Barriers of greater height and width were seen to have more drastic effects on liftoff, with the flow becoming buoyant at or near the obstacle. Barriers with a height approximately equal to 30% of the total flow height resulted in immediate liftoff of the flow and the generation of a buoyant plume. Barriers with a height of 10% of the total flow height were seen to have variable effects depending on barrier width. Those with a width approximate to the total flow width exhibited nearly immediate liftoff, while those with a width of 15% of total flow width had more nominal effects. Furthermore, the barriers placed closer to the vent were seen to induce greater shortening of liftoff distance. The proposed mechanisms for earlier liftoff are increased air entrainment and sedimentation created by the topographic obstacles. The increased air entrainment and sedimentation decrease the density of the flow, thereby allowing them to loft. This allows for greater detachment on the lee side of the barrier and serves as a possible explanation for the standing trees at Mount St. Helens. This research provides greater understanding of flow behavior across topography, which can result in the more accurate assessment of volcanic hazards and the potential sparing of lives.

Keywords: pyroclastic flows, Mount St. Helens, labratory experiments, liftoff distance

U

Isotopic compositions of meteoric water across an elevation gradient in Southern Peru

Derry Xu
Xu, D., University of Texas at Austin, Austin, TX
White, E., University of Idaho, Moscow, ID
Cassel, E., University of Idaho, Moscow, ID
Lynch, B., Indiana University Bloomington, Bloomington, IN
Yanites, B., Indiana University Bloomington, Bloomington, IN
Breecker, D., University of Texas at Austin, Austin, TX

The Central Andes is a prime example of elevated topography generated by oceanic plate subduction. Whereas previous stable isotope studies have investigated the paleoelevation of the Andean Eastern Cordillera, little is known about the paleoelevation of the Western Cordillera, where arc volcanism now occurs. As a first step towards studying the paleoelevation of this region, we investigated the change in $\delta^{18}O$ values of modern soil waters across an elevation gradient from sea level to about 4725 meters in southern Peru. We sampled soil profiles from 5 to 80 cm in 15-20cm increments, and we sampled water from flowing natural streams at various elevations. We used cryogenic vacuum extraction to quantitatively remove non-structural water from soil samples. The $\delta^{18}O$ values of water extracted from soil samples varies with the depth in the soil due to the diminishing effect of seasonality and evaporation. Every high elevation (>3500m) soil profile we measured had nearly constant $\delta^{18}O$ values below 5cm and a total range of $\delta^{18}O$ values between -12.8‰ and -17.1‰, apart from the Cusco profile. In the Cusco profile, the $\delta^{18}O$ values ranged from -7.2 ‰ at 5 cm to -21.8 ‰ at 60 cm, defining a strong monotonic decrease not seen in other soil profiles. The $\delta^{18}O$ trend in the Cusco profile may be different due to the impact of evaporation, soil hydrology, and/or seasonality in the $\delta^{18}O$ values of precipitation. Further spatial analysis must be conducted to pinpoint a specific cause. Considering only the samples collected below 40cm, which are likely the best estimate of mean annual precipitation, the $\delta^{18}O$ values decrease with increasing elevation at a rate higher than the global mean, suggesting that oxygen isotope paleoaltimetry can work in this study region.

Keywords: water isotopes, soil, streams, paleoaltimetry, fractionation, Andes, Peru, cryogenic vacuum extraction

CCG
U

Evidence of Possible Ocean Acidification at the Paleocene-Early Eocene Boundary Recorded in the Adriatic Carbonate Platform

Jordan Oefinger
Oefinger, J., Jackson School of Geosciences, The University of Texas at Austin, Austin, TX
Weiss, A., Jackson School of Geosciences, The University of Texas at Austin, Austin, TX
Košir, A., Institute of Paleontology ZRC SAZU, Slovenia
Martindale, R., Jackson School of Geosciences, The University of Texas at Austin, Austin, TX

The Paleocene-Eocene Thermal Maximum (PETM), a period of abrupt global warming events, is linked to a rapid release of large amounts of carbon into the Earth system. This sudden influx is hypothesized to have caused a mass acidification of surface ocean waters and a decrease in carbonate deposition in shallow water ramps and carbonate platforms. While rapid ocean acidification has the potential to devastate marine ecosystems, evidence of abrupt changes in pH and saturation have only been reported from deep-sea records. A well-preserved shallow carbonate platform from the Kras region of Slovenia records, continuous exposures of long term deposition, including the Paleocene-Eocene boundary, which manifests as a dissolution horizon. Through the analysis of dissolution surfaces found in this region, shallow platform ocean acidification is considered as a possible cause for the horizons. We analyze boundary samples to determine if the surfaces formed in an acidified ocean, subaerially, or are due to erosion diagenesis (i.e. stylolitic) using petrography and elemental mapping of the boundary. These surfaces have been analyzed using the Environmental Scanning Electron Microscope (ESEM) Energy Dispersive Spectra (EDS) to create a preliminary elemental map of the focus area. Then, samples will be mapped on the Electron Microprobe (EPMA) to gather more detailed data on the boundary composition to further explain the preserved surface of the PETM. The analyses of these dissolution surfaces in the Kras region will be used to determine whether ocean acidification occurred in this region during the PETM .

Keywords: Carbonates, PETM, ocean acidification

CCG
U

The Control of Grain Size on Carbon Dioxide Dissolution into Water

Esben Pedersen
Pedersen, E., Jackson School of Geosciences, The University of Texas at Austin, Austin, TX
Larson, T., Bureau of Economic Geology, The University of Texas at Austin, Austin, TX
Hesse, M., Jackson School of Geosciences, The University of Texas at Austin, Austin, TX
Wen, B., Institute for Computational Engineering and Sciences, The University of Texas at Austin, Austin, TX

Carbon sequestration is a method of mitigating anthropogenic carbon emissions. Sequestration is accomplished by dissolution of large volumes of CO_2 into a brine saturated reservoir. There are two mechanisms driving the dissolution: convection and diffusion. The onset of convection is determined by density-driven flow associated with the increase of water density with CO_2 saturation. It is important to understand the rate of CO_2 dissolution in these systems because the longer the time scale of dissolution, the greater time that free phase CO_2 gas could leak out of the domain. Convection dominated systems can store CO_2 much more efficiently than diffusion dominated systems, and so ensuring the incidence of convective dissolution could play a key role in enhancing CO_2 storage security. A suite of laboratory experiments conducted with water-saturated packings of spherical beads across a range of grain sizes show a strong stepwise correlation between effective permeability and the resultant dominant dissolution mechanism. Higher permeability packings experience more vigorous convection while low permeability packings lead to more pure diffusion cases. The analysis of these experiments will be used to predict the characteristic dissolution regime associated with porous media of varying permeability.

Keywords: Carbon sequestration, Porous Media, Convection, Diffusion

EG
U

Cement Stratigraphy in Solution-Collapse Breccias, Lower Ordovician Knox Group, Tennessee-Kentucky

Raeann Garcia
Garcia, R., The University of Texas at Austin, Austin, TX
Kyle, J., The University of Texas at Austin, Austin, TX
Miller, N., The University of Texas at Austin, Austin, TX

Diagenetic effects initiated by a 10-My period of subaerial exposure following deposition of the Lower Ordovician Knox Group carbonates are common features extending throughout the Appalachians and into the continental interior of North America. The breccia bodies are broadly similar over a >50,000 km^2 area, including cementation dominantly by coarse hydrothermal dolomite and calcite. The upper part of the late breccia systems had high interblock and fracture porosity that was partially filled with carbonate, sulfide, and related minerals. From the economic perspective, the major features are extensive solution-collapse breccia networks that locally serve as petroleum reservoirs and host strata-bound zinc and related MVT mineralization precipitated from basinal brines generally interpreted to be driven by late Paleozoic orogenic events. However, the cement assemblage, sequence of pore filling, and remaining porosity vary considerably, suggesting spatial and temporal variation in basinal brine systems and cementation histories.

Microstratigraphic studies of carbonate cements provide greater insights into the development, cementation, and porosity preservation in these areally extensive breccia systems. Cathodoluminescence variation in dolomite cements has been used to define local or regional cement microstratigraphy. These studies have shown that CL response is largely due to trace element variation, particularly the Mn and Fe contents. CL variation in dolomite cements has been used to define local or regional cement microstratigraphy. Breccia characterization enhanced by X-ray computed tomography and regional cement microstratigraphy, quantified by LA-ICP-MS geochemistry, are in progress to constrain the history of breccia formation and cementation, with attendant multi-scale effects on porosity. Initial results of LA-ICP-MS analysis show the potential to examine a diverse group of trace elements that may be useful to define detailed microstratigraphy without the limitations of CL techniques.

Keywords: microstratigraphy, dolomite, Tennessee, breccia, cathodoluminescence

EG
U

Migration deconvolution using non-stationary matching operators

Sarah Greer
Greer, S., Bureau of Economic Geology, The University of Texas at Austin, Austin, TX
Fomel, S., Bureau of Economic Geology, The University of Texas at Austin, Austin, TX

Least squares migration is more computationally expensive than conventional migration, but it produces a more accurate image of the subsurface—conventional migrated images generally exhibit less correct amplitude and frequency content. Migration deconvolution attempts to correct these differences by applying a filter to a conventional migrated image to produce a more accurate image with less computational cost than least-squares migration. This filter approximates the inverse Hessian operator, and can be approximated by solving a data matching problem between two conventionally migrated images. Previously, this has been done using non-stationary, or spatially and temporally variant, matching filters in a sliding-window approach. However, we propose using two separate non-stationary operators—one to account for amplitude variations, and the other to account for frequency variations. Successful results were achieved on synthetic data.

Keywords: migration deconvolution

EG
U

Characterization of gas hydrate-bearing sediments from Green Canyon 955, Gulf of Mexico, using Raman spectroscopy

Jesse Gu
Gu, J., Department of Geological Sciences, The University of Texas at Austin, Austin, TX
Dong, T., Department of Geological Sciences and Institute for Geophysics, The University of Texas at Austin, Austin, TX
Lin, J., Department of Geological Sciences, The University of Texas at Austin, Austin, TX
Flemings, P., Department of Geological Sciences and Institute for Geophysics, The University of Texas at Austin, Austin, TX

We employ micro-Raman spectroscopy to characterize unpressurized sediments from gas hydrate-bearing intervals. These sediments were cored from Green Canyon 955 in the northern Gulf of Mexico in May 2017 during the UT-GOM2-1 expedition. We use micro-Raman spectroscopy, which has a spatial resolution of 1 μm, to identify minerals and assess gas hydrate reservoir geochemical conditions. Micro-Raman spectroscopy allows us to identify mineral phases and mineral chemistry that can be challenging to classify either optically or with x-ray diffraction (XRD). Small mineral grains can be difficult to analyze optically, and minor minerals can be challenging and time-consuming to classify using XRD. These minor minerals and organic constituents provide insight into sediment provenance. Understanding sediment provenance allows us to constrain sediment transport and depositional processes during the Pleistocene, when the gas hydrate-bearing sediments were deposited. Furthermore, Raman spectra can reveal the chemistry of organic matter within sediments, which is important for the study of ecosystem evolution and paleoclimate. Preliminary XRD results show a composition of mainly quartz with minor amounts of alkali feldspar, amphibole, muscovite, dolomite, calcite, and clays, including potential kaolinite and chlorite. We separate grains based on their density and grain size by sieving and centrifuging. We then gather Raman spectra on at least 100 grains on grain mounts for each group of grains. After the Raman spectra are analyzed, bulk-sediment composition can be recalculated as the weighted average of integrated modes of each size class. Combining Raman spectroscopy with optical observations and XRD allows us to gain a more comprehensive understanding of the gas hydrate-bearing sediments and their origins.

Keywords: Raman spectroscopy, Green Canyon 955, sediment characterization, gas hydrates

SETP
U

Detrital Zircon Signal Migration in Eolian Systems: Investigating a Modern Foreland Dune Field in Argentina

Jaime Hirtz
Hirtz, J., Department of Geological Sciences, Jackson School of Geosciences, University of Texas at Austin, TX, USA
Capaldi, T., Department of Geological Sciences, Jackson School of Geosciences, University of Texas at Austin, TX, USA
George, S., Department of Geological Sciences, Jackson School of Geosciences, University of Texas at Austin, TX, USA
Stockli, D., Department of Geological Sciences, Jackson School of Geosciences, University of Texas at Austin, TX, USA
Horton, B., Institute for Geophysics and Department of Geological Sciences, Jackson School of Geosciences, University of Texas at Austin, TX, USA
Mohrig, D., Department of Geological Sciences, Jackson School of Geosciences, University of Texas at Austin, TX, USA

The use of detrital zircons (DZ) has become increasingly popular in paleotectonic reconstructions. However, few existing studies demonstrate how DZ migration histories apply to modern eolian environments, which is crucial to understanding how sediment provenance in ancient eolian deposits relate to paleotectonic settings. Our experiment will investigate the DZ signal propagation and migration from source-to-sink of Medanos Grandes. Medanos Grandes is a broad dune field located in the broken foreland basin of west-central Argentina, and is one of Argentina's largest and driest eolian systems. Through mineral separation and laser ablation inductively coupled plasma mass spectrometry (LA-ICP-MS), we collected the age of 140 zircon grains by measuring U-Pb ages from six various locations. Diagnostic age distributions are characterized by (1) 1400-1300 Ma Laurentian aged sediments; (2) 1200-1000 Ma Cuyania basement and Sunsas magmatic arc sediments; (3) 725-550 Ma Sierras Pampeanas uplift sediments; (4) 550-450 Ma Famatinian and Pampean arc sediments; (5) 440-300 Ma Carboniferous arc sediments; (6) 300-240 Ma Choiyoi igneous arc sediments; (7) 175-145 Ma Jurassic intrusion sediments; and (8) 50-0 Ma Andean magmatic arc sediments. This quantitative analysis of DZ U-Pb age distributions allow us to interpret information about source-to-sink processes by tracking zircon propagation and migration through modern eolian environments in contractional orogens.

Keywords: Detrital Zircons, U-Pb Geochronology, Sediment Provenance, Source to Sink, Eolian, Argentina.

SETP
U

Thermal Evolution of a Distal Hyperextended Margin - a Case Study of Zabargad Island, Red Sea

Samantha Robbins
Robbins, S., Dept. of Geological Sciences, Jackson School of Geosciences, University of Texas at Austin
Stockli, D., Dept. of Geological Sciences, Jackson School of Geosciences, University of Texas at Austin

Thermal evolution of a distal hyperextended margin – A case study of Zabargad Island, Red Sea

Samuel Robbins and Daniel F. Stockli

Dept. of Geological Sciences, Jackson School of Geosciences, University of Texas at Austin

Dramatic advances in our understanding in how to break-up continents in the absence of a hot spot or abundant magmatism have taken place over the past decades. Geophysical data have elucidated the structural and stratigraphic evolution of these magma-poor hyperextended continental rifted margins. These magma-poor margins share overall geometric and evolutionary similarities which have been used to define general architectural characteristics of these types of margins. The broad architectural zones commonly interpreted in magma-poor rift margins through geophysical data and geological observations are the proximal margin, preserving normal faulting associated with diffuse initial extension and stretching, a necking domain, a highly attenuated or hyperextended distal margin, and an exhumed mantle. However, beyond fossil continental margins caught up in orogenic systems, such as in the Alps, only few exposed examples of hyperextended distal margins exist in rift systems in the world. One of these examples is Zabargad Island, Egypt, in the central Red Sea – a section of the distal rifted margin uplifted and subaerially exposed along an oceanic fracture zone. Zabargad Island exposes a hyperextended slice of lower continental crusts, sandwiched between exhumed subcontinental mantle peridodite and syn- and post-rift sedimentary strata. The subcontinental mantle consists of three bodies of peridotite and a highly deformed lower crustal basement complex consisting of granulites, gneisses interlayed with amphibolites, gabbros, and pyroxenites. Studies in the past have focused on the tectonothermal and geochemical history of the island, but the timing and magnitude of exhumation during hyperextension within the context of the Red Sea distal rift margin is still poorly understood. This study employs multiple U-Pb and (U-Th)/He thermochronometric techniques to investigate the thermal and tectonic evolution of the lower crust during hyperextension and lithospheric break-up. In particular, we are looking to determine whether the lower crust experienced any reheating in response to juxtaposition with the mantle during exhumation and the structural kinematics of the lower crust during rifting. Preliminary data show that the basement material is a fragment of the Nubian Shield with zircon U-Pb ages ranging from 559 +/- 12 Ma to 588 +/- 14 Ma. The granulites/peridotites also appear to have been cross-cut by 8.1 +/- 0.2 Ma felsic dikes that likely formed during rifting. Apatite (~450°C) and rutile (550°C) U-Pb thermochronometry will be applied to constrain the thermal evolution in the lower crust during rifting. Finally, (U-Th)/He low-temperature thermochronometry will constrain the thermal evolution during final exhumation. Overall, this project aims to reconstruct the continuous time-temperature history of the distal magma-poor Red Sea hyperextended margin exposed on Zabargad Island, which will allow for a better understanding of the structural, thermal, and hydrothermal processes operating during continental break-up. These new results will also provide new constraints for the timing of extreme crustal thinning during Red Sea rifting and help better understand the mechanisms of lower crustal/mantle exhumation during hyperextension.

Keywords: Zabargad, Red Sea, thermochronology, rifted margins, mantle exhumation

SHP
U

Calculating the Volume of Late Quaternary Mississippi River Off Shelf Deposits

Ryan Herring
Herring, R., Department of Geological Sciences, The University of Texas at Austin, Austin, TX
Olariu, C., Department of Geological Sciences, The University of Texas at Austin, Austin, TX

In order to achieve a greater understanding of sediment dispersal during transgression and regression associated with river deltas, the last such cycle of the Mississippi River delta is studied herein. The primary focus of this project is to reconstitute the Mississippi Valley shape and filling deposits, and to estimate the quantity of sediment which “escaped” from the valley onto the shelf.

Upon the inception of the Late Wisconsin glacial stage, while the eustatic sea level was falling, the Mississippi River was well entrenched and its deltas extended onto the continental shelf. Following the Late Wisconsin glacial maximum, as the glaciers melted, the sea level rose rapidly and, consequentially, the river sediments filled the valleys in its ensuing retrogradation. Eventually as the sea level steadied upon the conclusion of the glacial stage, the Mississippi alluvial system’s deltas prograded back outside its valley, towards the sea.

Employing maps and borehole data from the Lower Mississippi River Valley and Delta, previously collected and published by Fisk (1944), Saucier (1994), Dunbar (1984, 1994, 1995), and Kulp (2000), the sediment deposited in the valley and delta by the Mississippi River since the Last Glacial Maximum has been mapped and the volume quantified. This volume encompasses the initial sediment deposited during retrogradation and that which was later deposited during progradation of the alluvial system. The calculated sediment volume according to different authors can then be subtracted from the predicted volume of sediment transported by the river during this time in order to deduce the volume of the off shelf deposits.

Keywords: Mississippi, shelf, delta, river, glacial maximum, valley, deposits, volume, mapping, borehole, logs

SHP
U

Heat Transport in the Streambed of a Large Regulated River

Sebastian Munoz
Munoz, S., Department of Geologic Sciences, The University of Texas at Austin, Austin,TX
Ferencz, S., Department of Geologic Sciences, The University of Texas at Austin, Austin, TX
Neilson, B., Utah Water Research Laboratory, Utah State University, Logan, UT
Cardenas, M., Department of Geologic Sciences, The University of Texas at Austin, Austin, TX

Dams affect over half of the Earth's large river systems. In large river systems, river regulation such as hydropeaking may have more obvious and profound effects than global warming. The downstream effects of dams are not limited only to the fluvial system but also propagate into aquifers and hyporheic zones. However, very little is known about how dams affect temperatures of downstream subsurface temperatures. This study investigates surface and groundwater interactions in the thermal regime of a 5th order dam-regulated river on several spatial scales. Two transects of thermistors recorded temperature gradients in the riverbed over the course of several flood pulses at 5 minute intervals. One transect was perpendicular to the river flow spanning the 68 m from bank to bank with sensors spaced every 2.75 m at depths of 0.1, 0.2, 0.3 and 0.5 m in the river bed. The other one was parallel to the bank with 72 thermistors spaced every meter and at the same depths as the perpendicular transect. The cross channel transect additionally had 5 piezometers installed at 0.5 m depth at regular intervals across half the channel with instruments collecting temperature, pressure and conductivity. The banks and the channel respond differently to flood pulses. At the bank the river fluctuates between gaining and losing on hour timescales. When the stage increases, warmer surface water penetrates into the subsurface and during the receding limb, cooler groundwater upwells as the river returns to base flow conditions. This activity is limited to the bank, which sees a larger range of temperatures than the channel, and is influenced by both surface and groundwater while the channel is primarily influenced by surface water. In the channel of the river, temperature does not change dramatically with change in stage. Overall, with increasing depth surface water influence decreases, and with proximity to bank the magnitude of temperature diminishes. The implications of this study suggest that the temperature regime of hydropeaked rivers vary drastically from banks to channel in a large regulated river.

Keywords: Surface Water, Groundwater, Dam regulation, Hyporheic Zone

SHP
U

Groundwater Model Using Variable Transmissivities Matches Observed Flows

Kindra Nicholaides
Nicholaides, K., The University of Texas at Austin
O'Connor, M., The University of Texas at Austin
Cardenas, M., The University of Texas at Austin
Neilson, B., Utah State University
Kling, G., University of Michigan

As global warming continues, arctic permafrost is degrading. Soil organic carbon stored in permafrost may potentially be broken down in-situ or be leached by shallow groundwater and enter surface water bodies. One possible outcome is CO_2 and methane enter the atmosphere as greenhouse gases and exacerbate climate change. To understand this process, we need to study the way in which groundwater flows through thin, shallow active layer aquifers. Because surface water is often thought to dominate arctic hydrology systems, active layer flow has been largely ignored in hydrological models. Here we develop a 2-D vertically integrated numerical groundwater flow model informed by direct measurements to account for groundwater discharge into an arctic stream. Imnavait is a first-order watershed on the North Slope of the Brooks Range in Alaska. Measurements of water table depth and ice table depth were taken on a hillslope at Imnavait at 80 points. Hydraulic conductivity was determined from extracted soil core samples. These measurements were extrapolated from the hillslope-scale to the watershed-scale and used to parameterize the model. Total active layer groundwater flow into the stream from the watershed was calculated with this model. We found the model results closely match the observed stream flows from a downstream hydrograph.

Keywords: active layer, arctic, groundwater flow model

SHP
U

Investigating fluvial pattern and delta-planform geometry based on varying intervals of flood and interflood

Jacqueline Rambo
Kim, W., Advisor

Physical modeling of a delta's evolution can represent how changing the intervals of flood and interflood can alter a delta's fluvial pattern and geometry. Here we present a set of six experimental runs in which sediment and water were discharged at constant rates over each experiment. During the "flood" period, both sediment and water were discharged at rates of 0.25 cm3/s and 15 ml/s respectively, and during the "interflood" period, only water was discharged at 7.5 ml/s. The flood periods were only run for 30 minutes to keep the total volume of sediment constant. Run 0 did not have an interflood period and therefore ran with constant sediment and water discharge for the duration of the experiment.The other five runs had either 5, 10, or 15-min intervals of flood with 5, 10, or 15-min intervals of interflood. The experimental results show that Run 0 had the smallest topset area. This is due to a lack of surface reworking that takes place during interflood periods. Run 1 had 15-minute intervals of flood and 15-minute intervals of interflood, and it had the largest topset area. Additionally, the experiments that had longer intervals of interflood than flood had more elongated delta geometries. Wetted fraction color maps were also created to plot channel locations during each run. The maps show that the runs with longer interflood durations had channels occurring predominantly down the middle with stronger incisions; these runs produced deltas with more elongated geometries. When the interflood duration was even longer, however, strong channels started to occur at multiple locations. This increased interflood period allowed for the entire area over the delta's surface to be reworked, thus reducing the downstream slope and allowing channels to be more mobile laterally. Physical modeling of a delta allows us to predict a delta's resulting geometry given a set of conditions. This insight is needed especially with delta's being the home to many populations of people and a habitat for various other species.

Keywords: delta, flood, interflood, topset, channel

Thank You

to our Sponsors, Volunteers & Participants

ConocoPhillips

TEXAS Geosciences

The University of Texas at Austin

Jackson School of Geosciences

Jackson School of Geosciences

GSEC

Graduate Student Executive Committee